# DEVELOPMENT OF A FRAMEWORK FOR AUTONOMOUS 3-DIMENSIONAL CRANIOFACIAL ANTHROPOMETRIC DATA ACQUISITION

**SALINA BINTI MOHD ASI**

**FACULTY OF DENTISTRY**
**UNIVERSITY OF MALAYA**
**KUALA LUMPUR**

**2018**

# DEVELOPMENT OF A FRAMEWORK FOR AUTONOMOUS 3-DIMENSIONAL CRANIOFACIAL ANTHROPOMETRIC DATA ACQUISITION

SALINA BINTI MOHD ASI

THESIS SUBMITTED IN FULFILMENT OF THE REQUIREMENTS FOR THE DEGREE OF DOCTOR OF PHILOSOPHY

FACULTY OF DENTISTRY
UNIVERSITY OF MALAYA
KUALA LUMPUR

2018

UNIVERSITI MALAYA

ORIGINAL LITERARY WORK DECLARATION

Name of Candidate: **SALINA BINTI MOHD ASI**

Registration/Matrix No.: **DHA 090001**

Name of Degree: **DOCTOR OF PHILOSOPHY**

Title of Project Paper/Research Report/Thesis ("this Work"):

**DEVELOPMENT OF A FRAMEWORK FOR AUTONOMOUS 3-DIMENSIONAL CRANIOFACIAL ANTHROPOMETRIC DATA ACQUISITION**

Field of Study: **COMPUTERISED ANTHROPOMETRY**

I do solemnly and sincerely declare that:

(1) I am the sole author/writer of this work;
(2) This work is original;
(3) Any use of any work in which copyright exist from, or reference to or reproduction of any copyright work has been disclosed expressly and sufficiently and the title of the Work and its authorship have been acknowledged in this Work;
(4) I do not have any actual knowledge nor do I ought reasonably to know that the making of this work constitutes and infringement of any copyright work;
(5) I hereby assign all and every right in the copyright to do this Work to the University of Malaya ("UM"), who henceforth shall be owner of the copyright in this Work and that any reproduction or use in any form or by any means whatsoever is prohibited without the written consent of UM having been first had and obtained;
(6) I am fully aware that if in the course of making this Work I have infringed any copyright whether intentionally or otherwise, I may be subject to legal action or any other action as may be determined by UM.

Candidate's Signature Date: 17-7-18

Subscribed and solemnly declared before,

Witness's Signature Date: 17-7-18

Name: PROF. DATO' DR. ZAINAL ARIFF
ABDUL RAHMAN
Designation: DEKAN
FAKULTI PERGIGIAN
UNIVERSITI MALAYA
KUALA LUMPUR

**DEVELOPMENT OF A FRAMEWORK FOR AUTONOMOUS 3-DIMENSIONAL CRANIOFACIAL ANTHROPOMETRIC DATA ACQUISITION**

## ABSTRACT

Craniofacial anthropometry (CFA) is the study that measures the human face and head to supports visual description. It describes the craniofacial complex in exact measurements instead of subjective assessment. Researchers and medical professionals use craniofacial anthropometry as a tool to study facial morphology. Many abnormal faces had been quantified against the normal face measurements. This helps the medical professional in understanding various facial syndromes and enable them to plan surgeries for these patients. Conventionally, the measurement is taken directly on the patient's face and human errors could be introduced, besides the need for a well-trained examiner to perform it. Methods of taking facial measurement have evolved and are influenced by the development of the computer hardware and software, and imaging technologies. Nowadays, 3-D images are obtained using stereo-photogrammetry camera system but still needs human input and is susceptible to the human errors. The main objective of this research is to propose for an automated CFA system with expert knowledge embed in it, so that it can simulate the capability of a human expert. The objectives of the project are 1) to determine inter- and intra-examiner errors, 2) to evaluate the reliability and validity of the VECTRA-3D, for further use, 3) to develop an expert system, the craniofacial anthropometry expert system (CFA-ES), 4) to evaluate the reproducibility of CFA-ES anthropometric landmarks localization and the reliability and validity of the CFA-ES against Vectra-3D. Methods: 19 measurements from 30 respondents were directly measured by a well-trained dentist. Then, 100 sets of 19 CFA measurements were acquired indirectly using Vectra-3D from 100 3D facial images. Of these images 30 would be the testing images and 70 would be the training images for the CFA-ES

development. Then, the 3D images were pre-processed into 2.5D images and intelligent shape model for normal CFA was constructed. Correlation regression was used to build a mathematical equation to convert pixel unit into millimetre. CFA-ES produced 18 measurements except the tip of nasal protrusion. Paired t-test was performed on 18 measurements to evaluate the accuracy of CFA-ES and ICC was used to analysed the reliability of the measurement. Results: For Vectra-3D, 3 measurements (ex-ex, ex-enL, ex-enR) were not clinically significant where systemic bias was observed. For reliability, 1 measurement was not reproducible, 3 were moderate while 15 were good to excellent. For CFA-ES, all landmark positions were reproducible. The reliability for the positions were good to excellent. For the accuracies of the measurements, a systemic bias was observed at orbital and orolabial. Seven measurements were significant, however, the mean differences were less than 2 mm.

Keywords: Craniofacial Anthropometry, Reliability, Validity, Active Shape Model and Expert System

***DEVELOPMENT OF A FRAMEWORK FOR AUTONOMOUS 3-DIMENSIONAL CRANIOFACIAL ANTHROPOMETRIC DATA ACQUISITION***

**ABSTRAK**

Antropometri kraniofacial (CFA) adalah satu kaedah untuk mengukur wajah manusia dan memberi deskripsi wajah dalam ukuran yang tepat. Penyelidik dan profesional perubatan menggunakannya sebagai alat untuk mengkaji morfologi muka manusia. Sehubungan dengan itu, beberapa bentuk muka yang abnormal juga dikenalpasti. Ini membolehkan doktor memahami pelbagai sindrom muka dan membantu merancang pembedahan untuk pesakit terlibat. Secara konvensional, pengukuran ini dilakukan secara terus ke atas muka pesakit, tetapi proses ini tidak begitu tepat kerana biasanya terdapat kesilapan manusia semasa proses pengukuran. Pada kebiasaannya, pengukuran secara begini perlu dilaksanakan oleh doktor yang berpengalaman. Walau bagaimanapn, kaedah ini telah berkembang dan dipengaruhi oleh pembangunan perkakasan dan perisian komputer, Pada masakini, pengukuran diambil dari imej-imej 3D tetapi masih memerlukan bantuan manusia, jadi ianya juga terjejas dengan kesilapan manusia. Objektif: Objektif utama kajian ini adalah untuk mencadangkan satu sistem pengukuran antropometri automatic yang menggunakan pengetahuan pakar supaya ia dapat mensimulasikan kepakaran manusia semasa pengukuran. Sistem ini mestilah dapat mengesan tanda antropometri dan menghasilkan ukuran antropometri yang tepat. Oleh itu, objektif kajian ini adalah, 1) menilai ralat di antara 2 pemeriksa dan pada diri pemeriksa 2) menilai kebolehpercaya dan kesahihan Vectra-3D 3) membangunkan sistem pakar kraniofasial antropometri (CFA-ES), 4) menilai kebolehan CFA-ES mengenai keberkesanannya mengesan tanda antropometri dan menilai kebolehanpercaya dan kesahihan CFA-ES. Tatacara kerja: Sebanyak 19 ukuran antropometri daripada 30 responden diukur secara langsung oleh doktor gigi yang terlatih. Kemudian, 100 set ukuran dari responden diambil dengan

menggunakan Vectra-3D dari 100 3D imej. Daripada 100 imej ini, 30 imej akan digunakan sebagai ujian dan 70 akan digunakan untuk membina pangkalan pengetahuan. Kemudian, imej 3D ini diekspot kepada 2.5D, seterusnya model bentuk aktif (ASM) untuk CFA dibina. *Correlation regression* digunakan bagi membangunkan persamaan matematik untuk menukar jarak unit piksel kepada unit milimeter. CFA-ES menghasilkan 18 ukuran. Ujian statistik t-berpasangan dilakukan untuk menganalisa ketepatan pengukuran Vectra-3D dan CFA-ES. Ujian *Intraclass Correlation Coeficient (1CC)* digunakan untuk mengukur kebolehharapan bagi Vectra-3D dan CFA-ES. Keputusan: Vectra-3D, dari 13 ukuran yang tidak signifikasi, hanya 3 secara klinikal tidak signifikasi (ex-ex, ex-enL, ex-enR), di mana kesalahan sistem dijumpai. Bagi kebolehharapan, 1 ukuran adalah tidak kebolehjana semula, 3 daripadanya adalah keboleharapan pertengahan manakala 15 adalah bagus ke sangat bagus. Bagi CFA-ES, kesamua 23 tanda adalah kebolehjana semula dan keboleharapan adalah bagus ke sangat bagus. Ralat sistem boleh didapati di kawasan mata dan mulut. Tujuh ukuran adalah signifikan, walaubagaimanapun perbezaan mereka adalah kurang dari 2 mm.

Katakunci: *Craniofacial Anthropometry, Reliability, Validity, Active Shape Model and Expert System*

## ACKNOWLEDGEMENTS

I would like to thank Allah, for blessing me with everything; in whatever I do throughout my life and for giving me guidance and strength to see me through this study. I would like to express my sincere gratitude to those who had helped me to achieve success in this study. I extend my apologies to anyone whom I may have failed to mention.

First of all, I wish to express my heart felt appreciation to my supervisors, Professor Dato' Dr Zainal Ariff Bin Abdul Rahman and Dr Effirul Ikhwan Bin Ramlan, for their invaluable support, guidance and advice throughout this study and the support given to complete this thesis.

Secondly, to my husband Mr Johari Bin Din, my children, thank you for your understanding, overwhelming support and motivation. To my late parents, Mr Mohd Asi bin Sarim and Mrs Rokibah binti Siran, without their constant love, care and support, I would not have been who I am today. I am greatly indebted to them and thank them for everything.

Thirdly, I am very grateful to the Ministry of Higher Education, Malaysia for the financial support under the Skim Latihan Akademik Bumiputra (SLAB) scholarship. I am also very grateful to the University Malaya for the Universiti of Malaya's Postgraduate Research Fund (PS168/2010B) that supported this study.

Finally, I would like to extend my sincere thanks to my friends and colleagues, especially to Mrs Nor Hidayah Ismail and Mrs Roshahida Ahmad for enormous help in the data collection process and in technical aspect of VECTRA-3D throughout the project, Dr Saravanan who had helped me at the early stage of manual data acquisition and Prof. Dr Puteh Saad for her encouragement and motivation. To Assoc. Professor Dr Siti Adibah Othman who runs the 3D Imaging Laboratory, I owe her a lot for the help and effort. Lastly, many thanks to the staff at Department of Oral &Maxillofacial Clinical Sciences, Faculty of Dentistry. Thank you for all your support.

**SALINA BINTI MOHD ASI**
**2018**

## TABLE OF CONTENTS


**ABSTRACT** iii

**ABSTRAK** v

**ACKNOWLEDGEMENTS** vii

**TABLE OF CONTENTS** viii

**LIST OF FIGURES** xi

**LIST OF TABLES** xiv

**LIST OF ABBREVIATIONS** xv

**LIST OF APPENDICES** xvi

**CHAPTER 1: INTRODUCTION** 1

1.1 Research Background 1

1.1.1 Methods of Craniofacial Anthropometry 3

1.1.2 Accuracy of Craniofacial Anthropometry 5

1.2 Research Problem 6

1.3 Research Objectives 7

1.4 Research Scope 8

1.5 Thesis Organization 9

**CHAPTER 2: LITERATURE REVIEW** 11

2.1 Historical perspective of facial measurement 11

2.1.1 Principle of human body canon (Pre-Renaissance) 11

2.1.2 Towards Ideal Facial Proportion ($14^{th}$ – $17^{th}$ Century) 12

2.1.3 Physical Anthropology ($18^{th}$ – $19^{th}$ Century) 13

2.1.4 Objective Measurement an Proportion ($20^{th}$ Century) 13

2.2 Application of Craniofacial Anthropometry 15

2.2.1 Analysis of facial morphology 15

2.2.2 Forensic 21

2.2.3 Facial Correction and Surgery 22

2.2.4 Nutritional and Growth 26

2.3 Craniofacial Anthropometry 27

2.3.1 Craniofacial Anthropometry Landmarks and Measurement 27

2.3.2 Factors affecting accuracy and reliability of anthropometric measurements 28
2.3.3 Intra- and Inter-Examiner Errors 29
2.4 Methods of Craniofacial Anthropometry 30
2.4.1 Direct Method 31
2.4.2 Indirect Method 32
2.5 Validity and reliability of craniofacial anthropometry 33
2.6 Facial feature extraction 36
2.7 Automatic Craniofacial Anthropometry 38
2.8 Active Shape Model 40
2.8.1 A Shape Model 40
2.8.2 The feature model 42
2.8.3 Active Shape Model 43

**CHAPTER 3: RESEARCH METHODOLOGY**

3.1 Problem Definition 44
3.2 The Proposed Solution 45
3.2.1 The User Requirement 45
3.2.2 Craniofacial Anthropometry Expert System (CFA-ES) 46
3.2.3 Research questions 47
3.3 Material and Method 48
3.4 Preliminary Phase 49
3.4.1 Ethic Approval 50
3.4.2 Craniofacial Anthropometry landmarks and measurements 50
3.4.3 Self-Calibration and Inter-Calibration 51
3.5 CFA Data Acquisition 51
3.5.1 Research Materials 53
3.5.2 CFA data acquisition by Direct Method 55
3.5.3 CFA data acquisition by VECTRA-3D 58
3.5.4 CFA data acquisition by CFA-ES 66
3.5.5 The Framework of CFA-ES 67
3.5.6 Image preparation and exportation 68
3.5.7 Training CFA Shape Model 69
3.5.8 Calibration 74

3.6 Inter- and Intra-Examiner Assessment 80
3.7 Facial feature extraction using local method 81
3.7.1 The training dataset 82
3.7.2 Landmark detection and auto measurement 83
3.8 Statistical Analysis 84

**CHAPTER 4: RESULTS AND DISCUSSION** 86
4.1 Introduction 86
4.2 Inter- and Intra-examiner error assessment 86
4.3 Reliability and Validity of VECTRA-3D 86
4.3.1 Accuracy of Vectra-3D 88
4.2.2 Reliability of Vectra-3D 89
4.4 Reproducibility of Anthropometric landmarks localization by CFA-ES 93
4.4.1 Reliability of landmarks position produced by CFA-ES 94
4.4.2 Accuracy of the landmark positions produced by CFA-ES 97
4.5 Validity and Reliability of CFA-ES against Vectra-3D 97
4.5.1 Accuracy of the CFA-ES 98
4.5.2 Reliability of the CFA-ES 99

4.6 Local landmarks detection using Haar Cascade Classifier and Viola and Jones object detection framework 103
4.6.1 Haar Cascade Classifier 104

**CHAPTER 5: CONCLUSION**
5.1 Research Summary 106
5.2 Research Finding 108
5.3 Future Enhancement 109

**REFERENCES** 111

**APPENDIX** 123

## LIST OF FIGURES


| | | |
|---|---|---|
| Figure 2.1: | First 3 shapes variation of a face model (Cootes, 2007) | 41 |
| Figure 2.2: | Figure 2.2: The selected feature points for constructing the grayscale profile (Cootes, 2000) | 42 |
| Figure 3.1: | The Automatic Craniofacial Anthropometry Framework. The red path is the training path to establish the expert knowledge. The black path is the front-end system. The blue processes are the preparation process, the green processes are the back-end module and the white process is the front-end module. | 48 |
| Figure 3.2: | Methodology Process Flow | 52 |
| Figure 3.3: | Direct Method of Craniofacial Anthropometry: An examiner performs direct facial surface anthropometry on a respondent. | 56 |
| Figure 3.4: | A Digital Caliper | 58 |
| Figure 3.5: | Spread Caliper | 58 |
| Figure 3.6: | The measurement of Face Region (a) maximum face width (zy-zy), (b) upper face height (n-sto), (c) lower face height (sn – gn), (d) face height (n-gn) | 59 |
| Figure 3.7: | The measurement of the Orbit Region (a) endocation width (en-en), (b) exocathion width (ex-ex), (c) inter pupilary length (d) eye fissure length (en - ex), (e) eye fissure height (ps-pi) | 60 |
| Figure 3.8: | The measurement of Nose Region (a) the nose height (n-sn), (b) the nose width (al-al) (c) tip of nose protrusion (sn-prn) | 60 |
| Figure 3.9: | The measurement of the Orolabial Region (a) labial fissure width (ch-ch), (b) Cutaneous upper lip height, (c) upper vermilion height (d) lower vermilion height | 61 |
| Figure3.10: | The VECTRA-3D Stereo-photogrammetry System: An examiner acquired the 3D facial image of a respondent and performed the anthropometric measurement on the 3D facial image using the Mirror ® Software. | 63 |
| Figure 3.11: | Facial image capture scheme for VECTRA-3D Stereo-photogrammetry System. View from x and y planes | 63 |
| Figure 3.12: | VECTRA 3D Stereo-photogrammetry System | 64 |

| | | |
|---|---|---|
| Figure3.13: | The VECTRA-3D Calibration Panel. | 64 |
| Figure3.14: | Detail methodology process flow for the development of automatic system module: Image preparation, Exportation of 2.5D facial image, CFA Shape Model Training, Measurement calibration and CFA data acquisition on testing facial images. | 68 |
| Figure3.15: | Example of 2.5-Dimensional Frontal Face Training Images. | 70 |
| Figure3.16: | An example of training image that made up the shape of frontal face. These 77 landmarks include the craniofacial landmarks, used to construct the face shape for this project. | 71 |
| Figure3.17: | The face shape landmarks with numbering in order to check the sequence is in correct position. | 72 |
| Figure 3.18: | The mean shape aligned on a training image. | 72 |
| Figure 3.19: | The whole process of training and detecting. | 74 |
| Figure 3.20: | The geometry of a pinhole camera. (Image from: opticsphysics.weebly.com/pinholers) | 75 |
| Figure 3.21: | The geometry of a pinhole camera as seen from X2 axis. (Image from: opticsphysics.weebly.com/pinholers) | 76 |
| Figure 3.22: | Example of Calibration Image. | 78 |
| Figure 3.23: | Example of training data set: above the inner eye-corner *(en)* and below the external eye-corner *(ex)*. | 82 |
| Figure 3.24: | The landmarks position in the training data set. On the left is inner eye-corner and on the right, is external eye-corner. | 82 |
| Figure 3.25: | The algorithm used to remove the false positive detections | 83 |
| Figure 3.26: | A sample of the thirty (30) testing images used for the validation of VECTRA-3D. | 85 |
| Figure 4.1: | Systematic bias: for intercanthal *(en-en)* and biocula *(ex-ex)* the blue line was measurements obtained by direct method and the red lines were by Vectra-3D i.e. Vectra-3D measurement for biocula always smaller than direct method and for intercanthal vice versa. | 92 |

| | | |
|---|---|---|
| Figure 4.2: | The CFA Mean Shape aligned and position itself on the facial image. | 94 |
| Figure 4.3: | 23 CFA landmarks are extracted and localized | 95 |
| Figure 4.4: | Some of the example results of landmark localization for 23 CFA landmarks on several facial images. | 97 |
| Figure 4.5: | Samples of successful cases in obtaining the eye fissure length for right eye | 104 |
| Figure 4.6: | Samples of successful cases in obtaining the eye fissure length for left eye. | 105 |
| Figure 4.7: | A miss detection of endocathion (en) | 105 |

## LIST OF TABLES


| | | |
|---|---|---|
| Table 3.1: | Craniofacial Landmarks description for the face | 54 |
| Table 3.2: | Craniofacial Measurements description for the face. | 55 |
| Table 3.3: | The example of calculated distances in pixel in VECTRA-3D environment | 79 |
| Table 3.4: | The ICC Index Categories (Koo & Li, 2016) | 85 |
| Table 4.1: | ICC test result for Intra- and inter-examiner analysis | 87 |
| Table 4.2: | Paired t-test and ICC results of measurements obtained by Direct Method and Vectra-3D. | 90 |
| Table 4.3: | The mean difference from comparing between anthropometric measurement obtained by direct method and VECTRA-3D. | 92 |
| Table 4.4: | Reliability of Ground Truth and CFA-ES anthropometric landmarks localization. | 96 |
| Table 4.5: | Paired t-test: Accuracy of anthropometric landmark produced by CFA-ES against ground truth marking | 99 |
| Table 4.6: | Paired t-test and ICC results for validity and reliability CFA-ES against Vectra-3D. | 101 |
| Table 4.7: | Results of paired t-test and ICC between measurement by HAAR classifier and byVectra-3D | 105 |

## LIST OF ABBREVIATIONS

| | |
|---|---|
| 3DFN | 3D Facial Norm |
| 2.5D | 2.5-dimensional |
| 3D | 3-dimensional |
| AAM | Active Appearance Model |
| ASM | Active shape model |
| ASD | Autism spectral disorder |
| CFA | Craniofacial Anthropometry |
| CFA-ES | Craniofacial Anthropometry Expert System |
| CFR | Craniofacial reconstruction |
| CFNS | Cranio-frontonasal Syndrome |
| COM Port | Communication Port |
| CBCT | cone-beam computed tomography |
| FASD | Foetal alcohol spectrum disorders |
| FAS | Foetal Alcoholic Syndrome |
| GA | Genetic Algorithm |
| GIMP | GNU Image Processing |
| HED | Hypohidrosis ectodermal dysplasia |
| ICP | Iterative Closest Point |
| ICC | Intra-class Coeffcient Correlation |
| MEC | Medical Ethic Committee |
| NS | Noonan syndrome |
| PCA | Principal Component Analysis |
| MRI | Magnetic Resonance Imaging |
| ROI | Region of Interest |
| RTA | Road Traffic Accident |
| STASM | Search Active Shape Model |
| TASM | Training Active Shape Model |
| TCS | Treacher Collins syndrome |
| UMMC | University Malaya Medical Centre |
| VAM | Visualizing and Measuring |
| VCFS | Velo-cranio-facial syndrome |

## LIST OF APPENDICES


Appendix A: Ethical Approval Letter

Appendix B: Patient Information Sheet

Appendix C: Consent Form

Appendix D: Data Acquisition Form

Appendix E: Sample of Data Acquisition Direct Method and Vectra-3D

Appendix F: Sample Output Craniofacial Measurements from Automatic Method

# CHAPTER 1: INTRODUCTION

## 1.1 Research Background

Craniofacial anthropometry (CFA) is becoming an important tool for taking measurements on face and head since it was introduced in the field of physical anthropology by Ales Hrdlička, who was the pioneer in medical anthropometry (Farkas, 1996). He introduces fourteen craniofacial measurements together with other human body measurements to be used in the anthropology department to measure the human body for industrial purposes, such as art, military selection, body correction in gymnastic, medical and dental purposes, criminal and other identification and scientific investigation (Hrdlička, 1920). When craniofacial anthropometry was used in the study of facial morphology, more craniofacial measurements and facial landmarks were identified and described (Kolar & Salter,1997; and Farkas1994a). Doctors used to describe dysmorphic characters with the terms such as "wide-set eyes", "broad nose", and "large mouth" which are very subjective. These visual descriptions known as anthroposcopy is one of the oldest examination methods but is still being used in the medical field today (Farkas,1994a). However, the descriptions are very subjective and anthropometric measurements can overcome this subjectivity.

These facial measurements are extensively used in many research fields and have many applications, for example anthropology, anatomical and anthropometry description, growth study, malformation diagnosis, facial reconstruction in forensic, orthodontic, surgical planning and evaluation, and maxilofacial and plastic surgery (Sforza, de Menezes & Ferrario, 2013; Katic & forrest, 2005; Li et al., 2013; Claes et al., 2010; Dias Beaini & Melani, 2013; Farkas, 1994a; and Popat et al., 2012). In medical and dental practices, craniofacial measurements help doctors in the planning of treatments for

patients needing corrective surgery. For example, precise facial measurements in cleft palate patients will enable doctors to plan treatments and corrective surgery for this group of patients (Cevidanes et al., 2010; Farkas, Forrest & Phillips, 2000; and Othman et al, 2013). In orthognathic surgery facial deformities are corrected by repositioning bone segment. Evaluation of the craniofacial region and soft tissue profile help doctors to plan facial correction and perform the surgery proper (Hajeer, Ayoub & Millet, 2002; Marchetti et al., 2011; Ferrario et al., 1993; and Popat, Richmond & Drage, 2010).

Many diagnose of dysmorphic syndromes are confirmed based on the recognition of subtle morphological anomalies in the craniofacial region. Clinically to identify the genetic causes of human diseases, highly precise measurements of phenotypes will increase our understanding on the translation of genotype to phenotype (Farkas, 1996). For example, high variability in head circumference, head length and biocular distance can be observed in Down's syndrome patients (Bagić & Verzak, 2003). In patients with Noonan syndrome, higher faces were observed (Nagle, Teibe & Kapoka, 2005). Quantitative analysis by Aldridge (2011) observed that patients with autism spectrum disorder (ASD) display facial distinct phenotype compared to normal boys. Studies on prenatal alcohol exposure showed that children with foetal alcoholic syndrome (FAS) and partial foetal alcoholic syndrome have a distinctive facial phenotype that can be characterized anthropometrically (Moore et al., 2002; Douglas et al., 2003; and Mutsvangwa et al., 2010).

Studies on facial trauma in Malaysia showed that facial trauma is common cause of head injuries and commonly results from road traffic accident (RTA), especially among motorcycle accident (Hussaini et al., 2007; Yasir, 2014). Three broad divisions of maxilofacial injuries can be observed: facial bone fractures, soft tissue injuries, and dento-

alveolar injuries (Hashim & Iqbal, 2011). It is consistently reported that motorcycle accident is the main cause for facial injuries and the majority involves young adult male below the aged of 30 years old (Hussaini et al., 2007; Hashim & Iqbal, 2011 and Yasir, 2014). The face is vital to human appearance and function, and injuries to the facial skeleton are rarely fatal but pose numerous long-term consequences physiologically, functionally and aesthetically (Yasir, 2014 and Nordin et al., 2014). Plastic surgery is vital to help these young patients who can be successfully treated if the surgeons have access the craniofacial normative data of Malaysian young adult group.

Normative databases on accurate anthropometric measurements are indispensable to determine the degree of deviations of abnormal facial morphology from the normal population (Farkas, 1996; Farkas et al., 2005; and Cheung et al., 2011). Congenital and post-traumatic facial correction surgery can be successfully done when the normal references are made available to the surgeons (Farkas et al., 2005). Therefore, it is important for standard anthropometric database to be established. With this, the measurements taken from a patient can be compared with the values obtained in the normal population and deviations from normative values can be evaluated. This can be used in the treatment planning of congenital and post-traumatic, facial disfigurement, to established common facial dysmorphic syndrome profile for early diagnosis of common syndromes and for facial corrective surgery (Farkas et al., 2005 and Nagle et al., 2005).

### 1.1.1 Methods for Craniofacial Anthropometry

Craniofacial anthropometry has been done by several common methods including craniometry, radiography cephalometry, computer tomography, 2D and 3D photogrammetry and laser scanning (Douglas, 2004 and Al-Khatib, 2010). However, different methods serve different needs. Craniometry enables measurements of facial and

cranial bones while cephalometry and computer tomography enable researchers/examiners to obtain measurements of hard and soft tissue from living subjects. Facial soft tissue measurements can be measured by photogrammetry and laser scanning techniques (Al-Khatib, 2010). This project is interested in obtaining the craniofacial soft-tissue measurements.

Traditionally, facial soft tissue measurements have been obtained directly on living subjects using traditional callipers or digital ones. Craniofacial anthropometry in 3-dimensional photogrammetry (stereo-photogrammetry) and laser scanning enable measurement on 3-dimesional image or 3-dimensional points of cloud data. The 3D image and 3D cloud point data produced by a computer system reflects true form of facial complex. The advantages of these methods are that there is no direct engagement between examiner and respondent or patient and image and cloud point data can be archived with no radiography involved.

Current computerized anthropometric system still need human interaction with the system before one can obtain facial measurements. In essence, the examiners need to mark the craniofacial landmarks on the 3D images photographed by the system. Then, the examiners need to select two points of the landmarks to generate the measurement needed (Aynechi et al., 2011; Asi, Ismail & Rahman, 2012; and Fagertun et al., 2014).

The use of image processing technique with automatic detection of facial landmarks is important in many applications in the field of computer vision such as face recognition and detection. In craniofacial anthropometry automatic extraction of facial features and landmarks would enable automatic measurement in relevant clinical distance and angle (Douglas, 2004). The application of automatic facial landmarks recognition related to

foetal alcoholic syndrome (FAS) has led to improvements in our ability to recognize and diagnose cases of FAS; this success can be extended to other syndromes (Meintjes et al., 2002; Mutsvangwa et al., 2010; and Moore & Ward, 2012a).

### 1.1.2 Accuracy of Craniofacial Anthropometry

Accuracy of measurements is very important as the data obtained will reflect the true results of our studies. There are few ways where errors are introduced in the measurement process during direct measurement. A well-trained examiner is highly recommended to perform the measurement (Kolar & Salter, 1997 and Farkas, 1996). The examiner must be able to identify the craniofacial landmarks correctly with the use of good instruments to perform the relevant measurement (Farkas,1996 and Hrdlička,1920). The long hour interaction might reduce the quality of the measurement, because the examiner and respondent might get tired. For children and patient with involuntary movement the examiner will experience difficulties during the measurement process. Furthermore, any mood change in the examiners will also affect the measurement process. The determination of the anthropometry landmarks may be different by different examiners. Moreover, some landmarks will be referred to many times in the measurement process and this might affect the reading when the examiners identify the location differently for the first reading and subsequent reading.

The used of computerized anthropometry system would overcome human related errors associated with direct method (Wong et al., 2008; Weinberg et al., 2004; Liang et al., 2013 and Ozsoy et al., 2009). However, the examiner need to mark the facial landmarks before they can get any measurement. Different examiner might mark the landmarks differently and the same examiner might mark the facial landmarks differently at different times (Fagertun et al., 2014). Furthermore, anthropometric landmarks may be variable.

Some landmarks have prominent features but some other landmarks do not, because of the associate bony feature underneath. Example of the landmarks are the nasion, gnanthion, zygions and subnasion.

### 1.2 Research Problem

Studies on normal craniofacial measurements were usually carried out for a certain group in the population and were limited to certain age groups, certain sets of craniofacial measurements and used different craniofacial anthropometry methods. To develop normal reference facial measurements, a large set of data was needed to represent the population. There are studies that reported the Malaysian normal craniofacial anthropometry comprising three major ethnic groups, namely the Malay, Chinese and Indian (Ngeow & Aljunid, 2009b; Shaheera et al., 2014; Purmal & Alam, 2013; Abdullah et al., 2006). But the studies were limited to two major age group (children and adult) with different sets of craniofacial measurements obtained and with the use of different methods. Therefore, to establish a normative database, the researcher need to acquire data in a large scale and it is time consuming by the current method available as discussed in the previous section. Due to this, there are less work being done on the normative database.

In 3D-stereophotogrammetry, for example using the VECTRA-3D method, there is no engagement between examiner and respondent. Even though this is an indirect method using computer technology where the measurement is done on the 3D images, the process of marking the appropriate landmarks is still tiring as it involves a large scale of data; for examples in this study there are twenty-three landmarks to be marked on one 3D image. Landmarks that need to palpate due to the bony structure underneath are difficult to identify.

This research proposes to develop an expert system for craniofacial anthropometry. This system shall locate the craniofacial landmarks and produce craniofacial measurements automatically. The system is to be embedded with the expert knowledge of craniofacial anthropometry. All problems and errors presented in direct and indirect methods shall be removed to enable the system to produce more reliable measurements consistently. The new method will consist of a craniofacial expert knowledge base and this knowledge will guide the system in producing good measurements.

### 1.3 Research Objectives

The goal of this study is to propose a framework for automatic craniofacial anthropometric landmarks detection and measurement. This automatic system uses digital image of front face captured by the VECTRA-3D stereo-photogrammetry system. In the proposed system framework, few processes in the direct method and Vectra-3D will be removed and optimized. The proposed system automatically annotates craniofacial landmarks and then performs the craniofacial measurement. All the measurements will be generated electronically. The system is pre-trained with a proven set of craniofacial measurements data which is produced by a craniofacial anthropometric expert.

In order to achieve the goal, there are four (4) objectives being defined for this study.

1. To determine inter- and intra-examiner errors in craniofacial anthropometry when using the VECTRA-3D Stereo-photogrammetry System.
2. To investigate the reliability and validity of the craniofacial anthropometric measurements (in millimetre) taken between VECTRA-3D stereo-photogrammetry system and direct method.
3. To develop craniofacial anthropometry shape model which is used to automatically detect and locate twenty-three (23) craniofacial anthropometry

landmarks on digital images of the front face and analyse the reproducibility of the landmarks localization in comparison to the ground truth data.

4. To compare the mean difference of craniofacial anthropometric measurements (in millimetre) obtained between automatic craniofacial system and stereo-photogrammetric anthropometry system (Vectra-3D). The comparison is to validate the automatic system against Vectra-3D and shall give us knowledge on how far the output from automatic system deviates from Vectra-3D.

### 1.4 Research Scope

In this study, normal respondents were needed as volunteer to participate. Twenty-three (23) selected craniofacial anthropometric landmarks and nineteen (19) measurements are used.

VECTRA-3D stereo-photogrammetry system with dual module system for full-face imaging from Canfield Scientific Inc., Fairfield, NJ, USA was used to capture 3-dimensional frontal images. A proprietary 3D Mirror Software was used to display and analyse the scanned 3-dimensional images. All 3-dimensional images from VECTRA-3D are used in this study to achieve the first and the second objectives. However, to achieve the other two objectives, we need to build our own software framework to automatically locate the 23 anthropometric landmarks. Due to this, all 3-dimensional images from VECTRA-3D system shall be exported and used in the new framework. The exported images are not in 3-dimension but are in 2-dimension in portable network graphic (PNG) image format. However, the images preserved the look of 3-dimensional effect and termed as 2.5-dimensional image.

The selected craniofacial landmarks and measurements used in this study were obtained from four regions of the face namely, the face, orbit, nose and orolabial regions. The facial images must be obtained in natural pose, not wearing spectacles and for the male respondents they need to shave to remove beard or moustache. This is because the VECTRA-3D camera system can only photograph the human skin and this is important to ensure the accuracy of the measurements perform on the digital image.

The study involves two examiners. The first examiner is a dentist and has been well-trained with craniofacial anthropometry. He is responsible in the direct measurement as specified by Farkas, (1996). The other examiner is a computer scientist researcher who is responsible for acquiring measurements from VECTRA-3D and from the proposed method. She has been trained with craniofacial anthropometry using VECTRA-3D for three months.

### 1.5 Thesis Organization

This thesis is divided into 5 chapters. Chapter 1 gives introduction and background of the study. It also described the problem statements and objective of the project.

Chapter 2 provides the literature review of the research project. It summarises previous related work and the results from the fact-finding of current existing systems, current technologies and other related and relevant matters pertaining to the craniofacial anthropometry as well as image processing techniques especially on the facial landmarks detection.

Chapter 3 is the methodology of the project describing the research problems and the requirements. It explains the proposed solution and describes the procedures and all related experiments of the project.

Chapter 4 describes and analyses all the results obtained. It also discusses research findings from this study.

Chapter 5 concludes the whole research project and suggestions for future enhancements.

# CHAPTER 2: LITERATURE REVIEW

## 2.1 The historical perspective of facial measurement

Finlay, in 1980 nominated Hippocrates (460-357 BC) as a pioneer in physical anthropology because Hippocrates had described the variety of skull though he did not use measurements to distinguish the variation he discovered (Finlay, 1980).

Vegter & Hage, 2000, described four stages of the development towards modern facial measurement. The first was the pre-renaissance era where the principle of human body canons was the main discussion. Second, the renaissance era where many works discussed the ideal facial proportion measurements and third, the post-renaissance era (during the eighteenth and nineteenth century) which discussed mainly on physical anthropology. Lastly was the twentieth century when doctors and researchers acquired facial measurements objectively (Vegter & Hage, 2000).

### 2.1.1 Principle of human body canons (Pre-Renaissance)

The Egyptians were believed to be the first to define a principal for the canons of the human body where they divided the human body from top to bottom in 22.25 like parts to make up a human figure and described the middle finger to be one-nineteenth of the adult height (Vegter & Hage, 2000). But Sneijder, 1928 denied the existence of any standards in Egyptian art because the Egyptian descriptions lacked important human body landmarks such as the nipples, umbilicus, and knees (Vegter & Hage, 2000). However, the principal of human body canons had influenced the Greek and Roman artists who used numerous canon rules to describe the ideal form of the human figure in term of anatomy (Vegter & Hage, 2000 and Kolar & Salter, 1997).

The earliest record of facial proportional analysis was the Greek neoclassical canons which was used to describe the facial morphology (Toma, 2014). A Greek sculptor Polycleitus (450-420 BC) reported the height of the face to be one-tenth of the length of the body and the whole head was one-eighth of it while head and neck together were one-sixth of the total body length (Vegter & Hage, 2000 and Kolar & Salter, 1997). Aristotle (384-322 BC) emphasized the proportion of human body and face on aesthetics and formulated the relationship between body features and human character (Vegter & Hage, 2000).

### 2.1.2 Toward Ideal Facial Proportion (14th–17th Century)

The so-called ideal facial proportion was introduced by Leonardo da Vinci (1452-1519) to describe an ideal face (Finlay, 1980 and Vegter & Hage, 2000). He used lines to relate specific structure of the face and head, and segmented it into small units to be able to produce a different scale. He extensively described the proportion of how the body and face should ideally be shaped. He translated it in his drawings to formulate an ideal proportion for a face for example the size of the mouth equals the distance between the parting of the lips and the edge of the chin, whereas the distance from chin to nostrils, from nostrils to eyebrows, and from eyebrows to hairline are all equal, and the height of the ear equals the length of the nose (Vegter & Hage, 2000).

Albrecht Dűrer (1471–1528) extended Leonardo da Vinci's ideal facial proportion by further dividing the face into three equal lengths, the forehead, the nose, mouth and chin and further divided the mouth and chin into smaller parts (Finlay, 1980 and Vegter & Hage, 2000).

### 2.1.3 Physical Anthropology (18th - 19th Century)

In the 18th century, Pieter Camper (1722-1789) had introduced the first numerical measurement of facial angle and did measurement of a lot of men and apes skull. He found that apes have larger facial angles while men have smaller facial angle. He was also countered that black men did not originate from the apes (Vegter & Hage, 2000). The dimension assessment of skulls in this era had led some investigators to discriminate certain races regarding to intelligence and other qualities. Blumenbach (1776) had established the way to analyse the skulls by introducing the system of craniometry. He divided the human species into five races: Caucasian or white race, Mongolian or yellow race, Malayan or brown race, Negroid or black race, and American or red race (Farkas,1994a and Toma, 2014).

### 2.14 Objective Measurement and Proportion (20th Century)

In the twentieth century, Jacques Joseph (1865-1934) who is the father of modern rhinoplasty emphasised on the important of nasal profile for cosmesis, and studied the aesthetics of various inclination of nasal bridge. He divided the nose into three parts, the bony, the septal cartilaginous and the cartilaginous and soft-tissue tip (Farkas, 1994 and Vegter & Hage, 2000).

Ales Hrdlička, 1920, who is the pioneer in modern anthropometry had introduced fourteen (14) measurements of the head and face and described the instruments used in the craniofacial anthropometry at the Department of Anthropology. The purpose of the measurement was to study the facial morphology, focusing on diagnostic and treatment in facial defect (Farkas, 1996). He also described the methods to perform these measurements and method to identify the landmarks precisely (Hrdlička, 1920; Kolar &

Salter, 1997 and Farkas1996). The first fourteen (14) craniofacial measurements that were introduced were from the head, face, nose and ear regions (Hrdlička, 1920).

In 1931, B. Holly Broadbent, Sr. (1894-1977) introduced the basic technique of cephalometric assessment of living subject that records the shadow images of both hard and soft tissue (Vegter & Hage, 2000). Cephalometry is the first indirect form of facial anthropometry (Vegter & Hage, 2000). In the next year Milo Hellman (1872-1947) popularized the application of anthropometry and facial analysis in orthodontic (Farkas1, 996).

Over two decades, Leslie G. Farkas had undertaken an extensive work on facial measurements by measuring and comparing more than 100 dimensions. He defined standard for almost every soft-tissue measurement of the head, had described facial syndrome morphology such as cleft lip and palate and lateral dysplasia, and defined role of anthropometry in the evaluation of many disorders (Farkas & James, 1977 and Farkas, Posnick & Hreczko, 1991).

To summarize, earlier measurements and proportion were obtained to understand the human body and face proportion. The human beauty was translated in term of facial proportion and had described the perfect facial proportion. In the next era, the skull dimensions assessment had provided information on human race and was used to discriminate human race with different values and qualities. In the last century until recently, the objectives of the facial soft and hard tissues assessment are for the evaluations of facial disorder and facial correction, industrial purposes and other medical reasons.

## 2.2 Application of Craniofacial Anthropometry

### 2.2.1 Analysis of facial morphology

Facial morphology is the study of facial structures, form and shape. Analysis of the human face has a long tradition, as discuss earlier. There are many different techniques that have been applied to analyse facial morphology and assess growth of the head and face for the purposes of determining aetiology, diagnosis, treatment planning and clinical outcome assessment of different kinds of malocclusion, facial asymmetry and dysmorphology.

**Normative Database**

When anthropometric methods were introduced into clinical practice to quantify changes in the craniofacial framework, features distinguishing various races/ethnic groups were discovered. Facial disorder includes congenital disorder, facial dysmorphism and facial trauma. To treat these facial disfigurements successfully in members of specific ethnic groups, surgeons require access to normal craniofacial databases based on accurate anthropometric measurements. These normal facial feature assessments can be archived in databases known as normative data of normal facial measurements and this data is indispensable for precise determination of the degree of deviations from the normal (Farkas et al., 2005).

Farkas and his international team had established a normative database on several continents (Farkas et al., 2005). Their study group consisted of 1470 healthy subjects with aged between 18 to 30 years old which consisted 750 males and 720 females. From this 780 were from Europe and all of them were Caucasians, which comprised 53.1% of the group. 180 subjects were from the Middle-East which comprised of 12.2% of the total study group. There were five Asian groups with a total of 300 subjects which comprised

about 20.4% and four groups of people of African origin with a total of 210 subjects which comprised of 14.3%.

Recently there are many efforts to establish normative databases but the coverages were still limited to some races and certain age groups, for example, Ngeow & Aljunid (2009) only described the Malays normative data for young adult aged between 18 and 25 years old (Ngeow & Aljunid, 2009a, 2009b). Arslan (2008) defined the prevalence of three different groups of Turkish young adult with regards to their face types of euryprosopic, metoprosopic or leptoproposic based on facial indices derived from by assessing their vertical and horizontal facial dimensions (Arslan, Genc, Odaba & Kama, 2008). Cheung (2011) developed a normative database of 3D cephalometric measurements based on CBCT and 3D photogrammetry of Chinese adults in Hong Kong and this was the first normative database based on CBCT and 3D photogrammetry of the Chinese population in that region. The results were comparable with those reported in the literature for conventional 2D cephalometric analysis and established the unique features of Chinese faces (Cheung et al., 2011).

A 3D facial norm (3DFN) project by researchers from the University of Pittsburgh, is an interactive, web base repository of 3D facial image and its measurements (Weinberg et al., 2015). The system allows user access to statistics and individual anthropometric data, including 3D facial landmark coordinates, 3D-derived anthropometric measurements, 3D facial surface images, and genotypes from every individual in the dataset. The database currently consists of 2454 male and female participants ranging in age from 3 to 40 years from four United State states.

**Facial Anomalies**

The unique facial morphology is made from separate cartilaginous, osseous, dental and soft-tissue elements, where their coordinated pattern of growth, development and ageing produces a non-static outline that can be modelled and varied by the combined action of internal (genetic and epigenetic) and external (environmental) factors (Sforza et al., 2013).

The used of craniofacial anthropometry in the studies of craniofacial anomalies enable researchers to define the facial morphology of several craniofacial dysmorphism. It also enables one to establish the relationship of the phenotype and genotype. By understanding how far the measurements of the anomalies deviate from the normal measurements, it is very helpful in soft tissue correction, especially in the patient with cleft (Vegter & Hage, 2001). Realizing the presence of morphology anomalies at the early age for example in the foetal alcoholic syndrome (FAS) and autism (ASD) enable early precaution steps to be taken by the family and the medical professionals (Douglas, 2004; Moore et al., 2002; Moore & Ward, 2012b and Aldridge et al., 2011).

Experienced geneticists often make immediate diagnosis by recognizing characteristic facial features of a syndrome while inexperienced clinicians may struggle to make such a Gestalt diagnosis, e.g., in very young children or when they have had limited exposure to certain syndromes or to affected individuals of the same age or ethnicity. Thus, objective analysis of dysmorphic facial growth is potentially useful in training clinical geneticists and in assisting clinical diagnosis (Vegter & Hage, 2001 and Meintjes et al., 2002).

The studies of cleft palate based on the facial surface measurement only began in the twentieth century when Peyton published his first anthropometric measurements on cleft

in 1931. The cleft's soft tissue facial appearance had been studied and evaluated by means of anthropometric and cephalometric technique at that time and most studies demonstrated the deficient growth of the maxilla and the deformities of facial profile (Vegter & Hage, 2001). Further contribution by Farkas, on facial surface measurements of patients with unilateral form of lateral facial dysplasia had defined the morphology characteristic of cleft's face in children by calculating proportion indices (Farkas et al., 2000 and Farkas & James, 1977).

Kolar (1985) described the craniofacial anthropometric of patient with Treacher Collins syndrome (TCS). The most defective and frequent findings were the subnormal facial depth measurements which disproportionately increase toward the mandible and affected the width of the face frequently and severely compared to the mandible. Other characteristics are, the orbits to be hyperteloric with disproportionately short eye fissures microtip ear, "parrot-beak" nose, character hypoplastic receding chin and supernormal nose defects (Kolar & Salter, 1985).

A diagnosis of a foetal alcoholic syndrome (FAS) is given only to individuals who are most severely affected (Moore et al., 2002). However, a group of FAS with less severe or with incomplete manifestations of FAS need to be given attention, as diagnosis at an early stage of life would able to cure them (Douglas et al., 2003). Anthropometric assessment of FAS facial phenotype is able to identify this group of FAS (Moore et al., 2002). Due to a high prevalence of FAS being reported in South Africa, a large scale of scanning method for FAS using cost-effective screening method is needed. Preferably less expert is needed in FAS diagnosis in the screening program. (Meintjes et al., 2002 and Douglas, 2011).

Other important facial syndrome studies are, abnormal growth in Crouzon syndrome (Richtsmeier & Lele, 1990) and the establishment of anthropometric data in a patient with microdeletions of 22q11 (Guyot et al., 2001). Studies on Down syndrome patients enable one to classify the trait of the syndrome, hence helping in the diagnosis of the syndrome (Bagic and Verzak, 2003 and Asha et al., 2011). A significant difference in facial morphology in boys with autism spectral disorder (ASD) has also been observed (Aldridge et al., 2011). Another genotype and phenotype related study were the Craniofrontonasal syndrome (CFNS), conducted by van den Elzen et al. (2014). On the other side of growth spectrum, Wagenmakers et. al. (2014) quantified the craniofacial characteristics of patients with acromegaly. A 3D cephalometry was used to analyse craniofacial disproportions in patients with long-term remission of acromegaly Wagenmakers et. al. (2014). On the other hand, anthropometric assessments of Noonan syndrome (NS) able one to classify the velo-cranio-facial syndrome (VCFS) using five pattern recognition algorithms; the nearest mean, decision trees, neural networks, logistic regression, and support vector machines are able to achieve high identification rate for both syndromes. This will assist the inexperienced clinician to diagnose particular syndrome especially in very young children (Hammond et al., 2004).

Various uses of craniofacial measurement on a dysmorphic face from the previous studies have been presented. The use of 3D facial morphology analysis had given more opportunity describing an improved description of most genetic causal diseases. This is because of the ease of craniofacial data acquisition and assessment by using computer and imaging technology. Also, using mathematical analysis and new intelligent computer algorithm would help in developing of a new technology of screening method in craniofacial syndrome. Thus, the analysis of the craniofacial morphology data can become more sophisticated but also accurate and fast.

**Morphometry**

Morphometrics is the quantitative analysis of shape and is used by craniofacial researchers to study variation of facial shape geometric models in normal or abnormal human face shapes (Hammond et al., 2004; Mutsvangwa et al., 2010; Douglas, 2011). Most studies of facial morphology have concentrated on the delineation of characteristic features and not on the construction of computational models of face-shape variation. These models are used to visualize and discriminate facial differences between or within syndromes, or between groups with specific syndromes and the general population (Hammond et al, 2004). The concept of variation in facial geometric model had been studied by DeCarlo, Metaxas & Stone, (1998). They automatically generate variations of human face geometric models by generating a collection of random measurements according to anthropometric statistics for likely face measurements in a population (DeCarlo, Metaxas and Stone, 1998)

.

A dense surface model of 3D digital image can be used to analyse 3D facial morphology by establishing a correspondence of the dense points across each 3D face image. The model will provide dramatic visualizations of 3D face-shape variation. (Hammond et al., 2004). These facial shape variations have potential use for training physicians to recognize the key components of particular syndromes.

Clinically, morphometric studies on FAS were aimed to generate various geometrical face models which can be useful in the diagnosis of different type of FAS (Mutsvangwa & Douglas, 2007; Mutsvangwa et al., 2010 and Douglas, 2011). Several researchers used generalised Procrustes analysis and principal component analysis and applied these to facial landmarks obtained from stereo-photogrammetry. Geometric morphometric analysis of stereo-photogrammetrically derived 3D facial landmarks allows visualization

of the facial anomalies associated with FAS, as well as classification of facial shapes. It is able to identify the four facial shapes of FAS.

### 2.2.2 Forensic

In forensic anthropology, average measures across a population may inform the likely appearance of victims from their remains (Farkas, 1994); and in the recovery of missing children, by ageing their appearance taken from photographs (Farkas, 1994 and DeCarlo et al., 1998).

One important contribution of anthropometry is in aiding facial restoration leading to recognition of a missing child. This can be achieved by using reliable measurements obtained from the measurement of the photograph (photogrammetry) and facial anthropometric of population norm, that enable one to produce objective parameters for facial reconstruction. Anthropometric data is used to convert a snap-short picture into a life-sized photograph, which will help to obtain objective data from the face of the person at the time of disappearance (Farkas, 1994).

In the case of missing child, the knowledge of age-related changes in the head and face between birth and young adulthood could assist in adjusting the size and facial framework to the current date (Farkas, 1994). However, most children's photographs are found to be not ideal for used in the procedure of ageing as the child is usually smiling. To overcome this limitation, the proportion of the face is retained in harmony with the real child to avoid perpetuating any facial expression which distorts appearance. Proportion indices will show the main proportion quantities in face quality. The harmonies and disproportion would influence the selection of the new measurements for the face. The calculated measurement and with the skill of an artist will complete the new face (Farkas, 1994).

Photographic reconstruction of the skull of an unknown victim will depend on the pathologist's report and police investigation routine. The forensic artist will need to weigh the importance of the collected data and together with the skills, awareness of the surface measurement of the head and face, and understanding the nature of developmental changes affecting the face will create the desired results (Farkas, 1994).

A corpse may not be recognisable due to its state of decomposition, soft tissue mutilation or incineration. Craniofacial reconstruction (CFR) can be very useful to identify the body if there were no other identification evidence available (Claes et al., 2010).

Forensic Facial Reconstruction is a branch of Forensic Anthropology that attempts to approximate the appearance of an unknown individual through soft tissue reconstruction after anthropological craniofacial analysis is carried out. The reconstruction publicized in the media aims at a recognition, which can trigger formal human identification (Dias et al., 2013).

### 2.2.3 Facial Correction and surgery

Progress in facial correction and surgery for the last 2 decades had increased rapidly. The understanding of facial morphology and measurement area have played an important role for this. The facial defects can be categorised as congenital, physically damage such as accident or syndromic facial defect. To treat these facial disfigurements in any population successfully, surgeons require access to craniofacial databases based on accurate anthropometric measurements of the population (Farkas et el., 2005). Normative database and anomaly description or quantification in the dysmorphic face had helped the

clinicians and surgeon in making decision and in planning surgery on patients to treat congenital or post-traumatic facial disfigurements (Farkas et al., 2005).

Posnick and Farkas (1994), had presented seven successful clinical cases for facial reconstruction namely, unilateral coronal synostosis, trigonocephaly, sagittal suture synostosis, Crouzon's syndrome, Apert's syndrome with total cranial vault dysplasia and hypoplasia, isolated cleft palate and the deformity with malocclusion (Posnick & Farkas, 1994).

They had derived and discussed anthropometric measurements that are clinically important for facial reconstruction for the above cases. In the head region there are five measurements particularly effective in the clinical practice, the head width (eu-eu), forehead width (ft-ft), the head height (v-n), head length (g-op) and head circumference (on g-op plane). In the face region, there are seven key anthropometric surface measurements which provide useful clinical information, namely the facial height (n-gn), upper face height (n-sto), mandibular height (sto-gn), face width (zy-zy) and the mandible width (go-go). There are at least two measurements in the orbital region, the intercanthal width (en-en) and the biocular width (ex-ex). At the nasolabial region, six facial measurements are most useful, i.e. nose height (n-sn), nose width (al-al), nasal tip protrusion (sn-prn), cutaneous upper lip height (sn-ls), vermilion upper lip height (ls-sto) and lower lip height (sto-li). Finally, there are two measurements in the ear region, the ear width (pro-pa) and ear length (sa-sba) (Posnick & Farkas, 1994).

Craniofacial measurements are also important in evaluating surgery, besides, a quantitative comparison of anthropometric data before and after surgery to provide an objective assessment of surgical outcomes (Farkas, 1994). Ferrario et al., (1999)

evaluated facial changes occurring after orthognathic surgery in 5 patients using a 3D system with landmarks representation of soft tissue facial surface. Results showed that global asymmetry of facial soft tissues was increased, but asymmetry in the lower facial third was reduced. In this evaluation, the method used in this study proved to be complementing the diagnostic aid, enabling quantitative evaluation of the final soft tissue results of surgery, which were proportional to those expected on the basis of the type of treatment and skeletal data (Ferrario et al., 1999).

A similar study by El-Hakim in 2001 investigated whether surgery on the growing nasal septum had or had not adversely affect nasal and mid-facial dimensions. The study was done to treat patients who had significant nasal obstruction and cosmetic disfigurement secondary to skeletal septal deformities. The treatment involved having the quadrilateral cartilage removed, remodelled, and reinserted as a free graft. Related facial linear measurements and indices of the face and nose were measured pre-operatively and post-operatively. Their results showed that the changes were not considered clinically different relative to age-appropriate norms, the dimensions of the nose and mid-face and their proportionality did not change after surgery (El-Hakim et al, 2001).

Many sophisticated methods of planning and evaluating orthognathic surgery have been invented. A review by Papadopoulos (2002) found that 3D imaging techniques provide extensive possibilities for detailed and precise analysis of the whole craniofacial complex, for virtual (on-screen) simulation and real simulation of orthognathic surgery cases on bio-models before treatment, as well as for the detailed evaluation of the effects of treatment. They found that the laser scanning in combination with the stereolithographic bio-modelling seems to be a very promising combination for three-dimensional imaging,

although there was still a considerable room for improvements (Papadopoulos et al., 2002).

Swennen et. al., (2009) presented an integrated 3D virtual approach toward cone-beam computed tomography-based treatment planning of orthognathic surgery in clinical routine. They described the different stages of the workflow process for routine 3D virtual treatment planning of orthognathic surgery (Swennen Mollemans & Schutyser, 2009). The process included 3D image acquisition, then the construction of 3D virtual augmented model, followed by formulated treatment planning surgery discussion and the manufacture of a 3D splint; next, the 3D virtual treatment planning was transferred to the operating room, and lastly the evaluation of 3D virtual treatment outcome.

Another similar study by Cevidanes et al., (2010) discussed the development of methods for computer-aided jaw surgery, which allows incorporation of a high level of precision which is necessary for transferring virtual plans to be used in the operating room. They also present a complete computer-aided surgery system developed in close collaboration with surgeons for surgery planning and the simulation including the construction of 3D surface models from cone-beam computed tomography (CBCT), dynamic cephalometry, semi-automatic mirroring, interactive cutting of bone, and bone segment repositioning (Cevidanes et al., 2010).

Popat et. al., (2010) reviewed a software package for three-dimensional orthognathic planning, the Maxilim ® by Medicim NV, Belgium. The system familiarised readers with the technique of creating a virtual 3D patient. The software used recent virtual reality technique, augmenting CBCT volumes of the maxilla, mandible and dentition and is able

to produce a virtual 3D patient which allow planning of orthognathic surgery entirely in 3D (Popat et al., 2010).

Plooij et. al. 2001, have done a survey to predict the surgical and orthodontic outcome with a presumption that three important facial tissues should be established based on the integration of the structure of the facial soft tissue, facial skeleton and dentition, and photographic 3D images. However, the complete triad with optimal quality cannot be captured by the craniofacial imaging techniques but can only be achieved by 'image fusion' of different imaging techniques to create a 3D virtual head. Hence, a 3D digital image fusion models of two or more different imaging techniques for orthodontics and orthognathic surgeries was developed by Plooij et al., (2001). They found that image fusion and especially the 3D virtual head is accurate and realistic tools for documentation, analysis, treatment planning and long-term follow-up (Plooij et al., 2011).

In the study of face transplant surgery by Caterson et. al., (2012), the facial landmarks were fixated to the corresponding cephalometric landmarks to restore function and appearance, with emphasis on phonation, mastication, and functional upper airway. Part of these reconstructions procedures involved in the combinations of hard and soft tissues of the mid-face (Caterson et al., 2012).

### 2.2.4 Nutrional and Growth

A study by Dellavia, (2010) on facial structure growth identified the main direction of facial growth in subjects with hypohidrosis ectodermal dysplasia (HED). Electromagnetic digitizer was used to acquire facial linear distances in the upper, middle, and lower third of the face from 4 different age groups and compared with normal data. They found that in the first time span the growth of all facial measurements showed a reduction in HED

subjects compared with control subjects. However, deviation from the normal facial growth of HED subjects tends to lessen with age (Dellavia et al., 2010).

## 2.3 Craniofacial Anthropometry

This project focused on anthropometry of the face, therefore, craniofacial anthropometry term as used in this project refers to the human face measurement.

### 2.3.1 Craniofacial Anthropometry Landmarks and Measurement

This thesis focuses on the craniofacial area of the human body. Therefore, any discussion on the anthropometry are more focused on the craniofacial area of the human body. Earlier part of this section, anthropometry is discussed as a general anthropometry which is more on defining the meaning of anthropometry and the measurement of the body part. Later in this thesis, methods of anthropometry will focus more on the direct, or manual anthropometry, indirect anthropometry, and morphometry. Before further discussing on anthropometry, another important assessment that has been used by the doctors and researchers namely anthroposcopy is highlighted.

**Anthroposcopy (visual assessment)**

Anthroposcopy is one of the oldest methods of examination that is still in use in medicine today and with the observations made relative to a set of reference values or standards but the method is very subjective (Farkas, 1994a). There is a trend toward more objective assessment of some characteristics such as skin colour, hair colour, a certain form, and distribution. To make it less subjective, tools such as colorimetric charts or scales are used as a reference for comparison. The problems with such scales relate to intermediate shades or gradations. The use of photometric devices that identify spectral wavelengths has provided more objective assessment of skin, hair, and eye colour (Toma, 2014).

### 2.3.2 Factors affecting accuracy and reliability of anthropometric measurements

There are three important requirements that affect the accuracy of anthropometric measurements (Farkas, 1996 and Hrdlička, 1920). Firstly, the examiner's skill which is the most important requirement that ensure the accuracy of craniofacial measurements. A skillful examiner is important in taking the measurements whereby the skill in measurement depends more on number of subject examined per year than on years of doing the measurement (Farkas, 1996). The basic skill requirement for the examiners is the ability to locate or identify the craniofacial landmarks correctly. Davenport (1940) had reported there was a problem in examining children with head deformity due to inaccurate identification of fronto-temporale (ft) on the forehead in normal children (Farkas, 1996). Secondly, it is essential to have a set of highly reliable measuring tools (Farkas, 1996 and Hrdlička, 1920). Thirdly, is the cooperation of the patients and the quality of the engagement between the patients and the examiners during the measurement session (Farkas, 1996). Any movement during the measuring process would affect examiner's concentration in performing the measurement. In direct measurement it is very hard to perform measurement on children and patient with involuntary movement. Tiredness, change of mood and lost in concentration would affect the accuracy in the craniofacial anthropometric data acquisition (Farkas, 1996, Ferrario et al., 2003 and Wong et al., 2008).

A study by Jamison and Ward (1991) had highlighted that difficulty in locating the craniofacial landmarks is the major factor affecting the accuracy of anthropometric measurements (Farkas, 1996). They further added that the reliability was positively correlated with the size of the measurements and had suggested that measurement size should be included in the list of factors that affect precision and reliability in

anthropometry other than ease of locating landmarks, measurement technique, and systematic bias in the application of the technique (Jamison & Ward, 1993).

The level of accuracy of the anthropometric data depends on the use of the data. A high or extreme accuracy of the craniofacial anthropometric measurement does not require in some applications but would possibly be expected in other application or studies, for example the level of accuracy for the CFA measurements would possibly high in the normative database but not extremely required for anatomical reference (Farkas, 1996). However, in the study of genetic causal diseases and the phenotype - genotype quantification there is a need for highly accurate anthropometry data (Sforza & Ferrario, 2006 and Aldridge et al., 2005).

### 2.3.3 Intra- and Inter-Examiner Errors

Intra-examiner study evaluation is important to define consistency and detect degree of measuring skill in the craniofacial anthropometry by repeat measurement (Hrdlička,1920 and Farkas, 1996). It can test the examiner's skill measurements. In longitudinal study whereby several examiners are involved, evaluation of inter-examiners measurement is also important to define consistency of the measurement taken between two or more examiners (Farkas, 1996).

Toma et. al. (2009) studied the reproducibility of facial soft tissue landmarks on 3D laser scanned facial image (Toma et al., 2009). They used 63 craniofacial variables where the x, y and z coordinates of facial landmark were identified and recorded by two examiners while one of the examiner repeated the measurement process after two weeks. They found that in intra-examiner evaluation, a total of 7 measurements had more than 1 mm difference. In inter-examiner evaluation, a total of 11 measurements had more than 1 mm

difference. They also found that some landmarks showed greater reproducibility in certain planes of space e.g. subnasale was more often reproduced in Y-axis in males rather than in females. They suggested that the different landmarks reproducibility should be considered when evaluating changes related to growth and healthcare interventions.

Metzler et. al. in 2012 used 3dMDface system to investigate the intra-observer repeatability of 27 craniofacial landmarks in 7 young children between 6 and 18 months of age with a total of 1134 measurements (Metzler et al., 2012). They concluded that, the reliability in craniofacial measurements can be achieved by the 3D soft-tissue imaging techniques such as the 3dMDface System, but the degree of precision is dependent on the landmarks and axis therefore, in any clinical investigations, the degree of reliability for each landmark evaluated must be addressed and take into account.

**2.4 Methods of Craniofacial Anthropometry**

Anthropometry methods has changed rapidly along with the development of computer hardware and software, and imaging technologies (Al-Khatib, 2010 and Douglas, 2004). Conventionally, the standard method of facial surface measurement, the direct or manual facial measurement involves using callipers, ruler and measuring tape which is being practice until recently (Farkas, 1994). Then the indirect measurement using the 2D photographs, 3D facial image from the stereo-photographs generated from Stereo-photogrammetry system, for example C3D by Ayoub (2003) and 3D laser scanner (Kau et al., 2006). In addition, we can analyse facial hard tissue from the Cephalometric, Magnetic Resonance Imaging (MRI) and Cone Beam Computed Tomography (CBCT) (Al-Khatib, 2010; Douglas, 2004, 2011; DeCarlo et al., 1998; Kohno et al., 2005 and Hajeer et al., 2002).

In the last few years, technology has provided new instruments for three-dimensional analysis of human facial morphology (Sforza et al., 2013). Currently, quantitative assessments of dimensions, spatial positions and relative proportions of distinctive facial features can be obtained for both soft and hard tissues. This project however, only concentrates on the measurement of the facial soft tissue. The recent past has seen great advances in three-dimensional imaging which include laser scanning or stereo-hotogrammetry (Al-Khatib, 2010). These technologies allow one to fuse digital data obtained from various image analysers to produce 3D images of the facial surface which can be used to obtain craniofacial measurements (Al-Khatib, 2010). This 3D dense digital data (the 3D image) is able to represent the human face complex accurately.

Basically, there are three methods in acquiring the craniofacial anthropometric data. The direct method, the indirect method and the automatic method.

### 2.4.1 Direct Method

Direct method or manual anthropometry is currently considered as a gold standard for craniofacial assessment, as the method is simple, inexpensive, efficient and non-invasive, very demanding and does not require complex instrument (Farkas, 1994a; Moore & Ward, 2012b; Sforza & Ferrario, 2006 and Douglas et al., 2003). The standard instruments for direct measurement are sliding and spreading calipers which are made of metal, and the metric tape which is made of fabric and has a millimetre scale (Farkas, 1994 and Hrdlička, 1920). The measuring tool must be ideal to enable one to measure correctly and precisely. For example, plastic measuring tape is not suitable taking the measurement because it is not flexible enough to adhere to the skin (Farkas, 1994).

The limitation of this method includes the need for patient cooperation, time consuming, not suitable for children and patients with involuntary movement and necessitates a well-trained examiner (Aldridge et al., 2005; Sforza & Ferrario, 2006 and Guyot et al., 2003). A large anthropometric data acquisition for each individual consume longer time may be prone to error. In addition, manual measurement has no proper and permanent records archived (Farkas, 1996 and Guyot et al., 2003).

### 2.4.2 Indirect Method

There are several techniques that generates 3D image. Only 3D scanning for facial soft-tissue will be described. Laser scanning and stereo-photogrammetry shall be described in this section. Computerised tomography system would provide an output of 3D images for soft and hard facial tissues. However, the use of radiation would not be suitable for such a purpose.

#### 3D Image Scanning Laser Scanning

This technology depends on projecting a known pattern of laser light onto the object of interest which is based on geometric principles to create a 3D model of the object (Majid, Chong & Setan, 2006). Many studies test the accuracy and precision of laser scanner utilizing digital calipers (Kau et al., 2006 and Ozsoy et al., 2009). The results showed that the accuracy of laser scanner was less than 2 mm in the plaster model with a precision of 0.8 - 1 mm on the human face. Laser scanning gives a non-invasive, accurate, and reproducible means for medical applications (Hajeer et al., 2002). However, this technology has a long scan time, making it difficult to apply for children (Ozsoy et al., 2009). The laser scanner is unable to capture soft tissue texture which results in difficulties in identification of certain landmarks. Moreover, the patient's eyes must also be closed for protection and the head must be kept in a fixed position.

**Stereo-photogrammetry**

Stereo-photogrammetry was first proposed by Zeller, 1952 to examine the soft tissues of the face (Meintjes et al., 2002). A stereo pair of facial photographs were recorded in a stereo-metric camera and used to make contour maps of facial morphology.

The basic principle of stereo-photogrammetry is the use of two (2) or more cameras as a stereo pair to capture simultaneous images of the subject (Kau et al., 2006). The cameras are placed apart from each other and the subject's face is enclosed by a calibration frame or placed in a space in which a calibration object was previously imaged (Majid, Chong, & Setan, 2006). The cameras' focal lengths, their exact position to each other and to the object are calculated during the calibration procedures (Majid, Chong, & Setan, 2006). After that, 3D facial image can be captured and displayed on the monitors so that landmarks can be selected either manually or by using image processing algorithms (Hajeer et al., 2002). The acquired 3D coordinates are used to calculate distances between points that allow subsequent 3D reconstruction of the entire face (Kau et al., 2006). There are many 3D stereo-photogrammetric commercial systems that are available in the markets.

## 2.5 Validity and reliability of craniofacial anthropometry

Before any methods of craniofacial anthropometry is being used as standard implementation, accurate determination of the precision and accuracy of each system is mandatory. There are many studies being done to determine the validity and reliability of craniofacial measurements using various methods of the facial measurement acquisition.

Stereo-photogrammetry systems are among the popular system tested. Stereo-photogrammetry system produces three dimensional facial or head surface image and is suitable to acquire facial surface measurement. Moreover, the system used normal camera which capture the images as fast as a few in millisecond. Reliability is the degree to which an assessment tool produces stable and consistent results. There are studies that investigated the reliability and validity of a new technology use in anthropometry. Wong et al. (2008) investigated the validity and reliability of 3dMDface system (3DMD, Atlanta) and recommended its use to overcome the limitation of direct anthropometry.

Kuijpers et. al. (2014) studied soft tissue analysis, evaluation of bone grafting, and changes in the craniofacial skeleton and reported that digital dental casts was able to evaluate the treatments and changes over a period of time (Kuijpers et al., 2014). Li et al., (2013) investigated the used of the structured light scanning system to capture 3D images of cleft lip infants. They studied the accuracy and the precision of the acquired 3D facial data by comparing them with direct measurements. The new method was proven to be a non-invasive, accurate and precise when used in cleft lip anthropometry (Li et al., 2013).

Hajeer et. al., in 2002 studied the reproducibility of facial landmarks identification by C3D, a 3D imaging system developed by Glasgow University and The Turing Institute, funded by the United Kingdom Department of Trade and Industry. The landmark reproducibility by C3D was high for 20 of the chosen points. The system was useful in studying facial soft tissue changes following orthognathic surgery and other types of facial surgery, as well as assessing facial soft tissue growth and development of the craniofacial complex (Hajeer et al., 2002).

Aynechi et. al., (2011) tried to determine the influence of landmark labelling on the accuracy and precision of an indirect facial anthropometric technique. They studied the validity and reliability of 3dMDface with and without landmark labelling. They concluded that soft tissue facial measurement with the 3dMDface system demonstrated similar accuracy and precision with traditional anthropometry, regardless of landmarking before image acquisition. Larger disagreements were found regarding measurements involving ears and soft tissue landmarks without distinct edges. The 3dMDface system demonstrated a high level of precision, especially when facial landmarks were labelled (Aynechi et al., 2011).

Metzler et al., (2013) validated 3D VECTRA five pod (manufacturer: Canfield, Fair- field, NJ) surface-contour mapping on craniofacial region. They compared measurements of distance acquired manually on a mannequin by VECTRA-3D system. Another study by Abdulkareem & Al-Mothaffar, (2012), evaluated 18 facial anthropometric measurements accuracy and reliability obtained from low cost Photomodeler. They concluded that accuracy and precision of photosystem and photomodeler are suitable to be used in taking craniofacial measurements.

Aksu, Kaya & Kocadereli (2010) determined the reliability of the reference distances used for photogrammetric assessment. Five lateral and four frontal parameters were measured directly on 100 subjects' faces. For photogrammetric assessment, two reference distances for the profile view and three reference distances for the frontal view were established. Standardized photographs were taken and all parameters that had been measured directly on the face were measured on the photographs (Aksu, Kaya, & Kocadereli, 2010). They concluded, for profile assessment, the use of T-Ex reference

distance was reliable for Prn-Sn and Sn- Sto in both sexes. For frontal assessment, Ex-Ex and En-En reference distances were reliable for Ch-Ch in male subjects.

### 2.6 Facial feature extraction

Facial feature points are generally referred to as facial salient points such as the corners of the eyes, corners of the eyebrows, corners and outer midpoints of the lips, corners of the nostrils, tip of the nose, and the tip of the chin. In computer vision, facial feature extraction is essential to various facial image analysis such as face recognition, facial expression recognition, lips reading, facial tracking and facial animation. Generally, method used in facial feature extraction can be divided into two categories.

The first, is the local method or bottom-up method. It is used to detect local face components such as eye pupil, eye corner, mouth corner and a tip of the nose. In the local method, the image data is examined at a low level, looking for local structures such as edge, lines and corner or regions, which are assembled into groups to identify the objects of interest (Cootes, 2000). Local feature point can be represented by a complex wavelet such as Haar wavelet and Gabor wavelet. The use of Haar-like-feature that has a similarity with Haar wavelet has been successfully employed to detect a face in real-time application (Viola & Jones, 2001 and Lienhart & Maydt, 2002). Gabor wavelet is favoured by researchers due to its good performance but it is computationally exhaustive. Gabor wavelet has been successfully implemented in computer vision application such as face recognition (Wiskott1 et al., 1997 and Vukadinovic & Pantic, 2005) and facial expression identification (Samad & Sawada, 2011). However, the feature models of facial landmarks are mutually independent, this will easily affect the detection results by the variation of lighting and pose.

The second is the global method or top-bottom method, where the whole geometric structure of face component is used to locate the interested facial landmarks. It uses a set of feature landmarks to form a global facial structure model. It has more ability to endure detection error of individual landmark. Therefore, the global method generally obtains better performance in locating facial landmarks. There are three commonly methods used in the global method: 1) Deformable template (DT), 2) Active shape model (ASM) and 3) Active appearance model (AAM). Both ASM and AAM are provided by (Cootes et al., 1994; Cootes & Taylor, 2004). They iteratively decrease an energy function to obtain the optimized facial landmark locations.

The active shape model has successfully been applied in medical image analysis, such as computed tomography (CT) and it can be applied to locate facial feature landmarks. However, the accuracy of the facial feature localization is still a problem because face images are more complex than medical images. Therefore, researchers keep on proposing new methods to improve its performance. Improvement on original ASM by Milborrow (2007) proposed a new landmark profile model to move the landmark to the position that best matches that landmark's model profile and suggest the tentative new position of a landmark. Several studies proposed a hybrid system which uses the combination technique with wavelet and other local method (Jiao et al., 2003; Zuo & de With, 2004; Huang, Hsu & Cheng 2010 and Cristinacce & Cootes, 2007),

ASM has a high success rate, therefore, it is widely applied and used in many different problems. Moreover, the expert knowledge can be captured in the annotation of the training examples (Cootes, 2000). The models give a compact representation of allowable variation but are specific enough not to allow arbitrary variation different from that seen in the training set.

## 2.7 Automatic Craniofacial Anthropometry

Research in automatic facial feature detection on a 3D facial image has started more than two decades ago when the 3D capture devices start to be more common and when important 3D face databases are available publicly (Creusot, Pears & Austin, 2010). Analysis of the facial complex needs to be done on a 3D image to correctly assess the geometrical shape of a face (Ozsoy et al., 2009). The use of 3D stereo-photogrammetry scanners in indirect anthropometry has overcome problems of taking craniofacial measurements in small children and patients with involuntary movement. However, facial landmarking on the 3D images is still manually determined by the examiner. One of the important rules in craniofacial anthropometry is the ability to locate craniofacial anthropometric landmarks correctly (Farkas, 1996 and Hrdlička, 1920). Automatic landmarking can become an alternative method in taking craniofacial anthropometry to acquire consistent and highly accurate measurements. In the studies that acquire large facial image datasets, the manual approach is very labour intensive.

Currently, there were several researches who had implemented automatic landmarking on 3D images to automatically detect craniofacial anthropometry landmarks. Dauglas et. al. (2003) automatically extract eye features and locate the eye landmarks automatically in her study of Foetal Alcoholic Syndrome (FAS). The approach used genetic algorithm and eye template to fit the cubic splines of the upper and lower eyelids and the mean absolute differences between automatic and manual measurements were less than 1 mm for palpebral fissure length (PFL) and interpupillary distance (IPD) (Douglas et al., 2003).

Ruiz and Illingworth, (2008) who used classical ASM to detect facial landmarks depended on a statistical joint location model for configurations of facial features. Results demonstrate that the automatic procedure successfully and reliably locates landmarks and,

when compared to an Iterative Closest Point (ICP) algorithm, reduces the mean error for location of landmarks by half (Ruiz & Illingworth, 2008).

Gupta, Markey and Bovik (2010), proposed the anthroface 3D to recognize a face. They locally extracted the facial landmarks on 3D facial images to detect and recognize a face (Gupta, Markey & Bovik, 2010). They extracted ten (10) facial anthropometric landmarks. They isolated and employed unique textural and/or structural characteristics of these fiducial points, and established anthropometric facial proportions of the human face for detecting them.

Creusot et. al. (2010), presented a proof-of-concept for a face labelling system, capable of overcoming this problem, as larger number of landmarks are employed. A set of points containing hand-placed landmarks is used as input data. The aim here is to retrieve the landmark's labels when some part of the face is missing. By using graph matching techniques to reduce the number of candidates, and translation and unit-quaternion clustering to determine a final correspondence, evaluation the accuracy at which landmarks can be retrieved under changes in expression, orientation and in the presence of occlusions.

Kohno et. al. (2010), propose some methods to automatically estimate the position of orbitale and tragion from raw 3D scanner data. The 3D scanner captures point cloud and mesh data representing the body surface. To utilize the data, they needed underlying anatomical landmarks. The tragion position is estimated using three methods, by detecting the saddle shaped area, by setting an average position relative to ear lobe, and by 3D template matching. Orbitale position is estimated by regression analysis using the position of eyes and subnasale as independent variables (Kohno et al., 2005).

Liang et. al., in 2013 produced 20 established facial landmarks. They developed a geometric methodology that can automatically locate ten (10) established landmark points and seven (7) other supporting points on human 3D facial scans. Then, a deformable matching procedure establishes a dense correspondence from a template 3D mesh with a full set of twenty (20) landmarks to each individual 3D mesh (Liang et al., 2013).

### 2.8 Active Shape Model (ASM)

An active shape model (ASM) is a method of matching a statistical shape model of a form ASM is a statistical model, which contains a global shape model and a lot of local feature models (Cootes, 2011).

#### 2.8.1 A Shape Model

The shape model is made up of *n* facial feature points and each one is located at obvious face contour. The positions of these *n* points are arranged into a shape vector X that is,

$$X = [x_1, x_2, \ldots x_k, x_n, \ldots y_1, y_2, \ldots y_k \ldots y_n]^T \quad (2.1)$$

Where $x_k$ and $y_k$ are the horizontal and vertical coordinates of the $k^{th}$ feature point respectively (Cootes, 2000, Milborrow, 2007). All the training shapes should be aligned first to obtain the statistic variation of feature-point shapes. The ASM alignment procedure is an iterative process as summarized below:

1) All training sample are normalized according to two-eye positions.
2) Rotate, scale and translate each shape to align with the first shape in the training set.
3) Calculate the mean shape from the aligned shapes.
4) Normalize the mean shape.
5) Realign every shape with the normalized mean shape.
6) If not convergence, return to step 3.

After finishing the alignment procedure, the eigenvectors of the covariance matrix corresponding to main shape variations can be generated by using the Principal Component Analysis (PCA) operation (Cootes, 2011). The shape model can be approximately represented as:

$$x = \bar{X} + Pb \tag{2.2}$$

Where $\bar{X}$ is the mean shape model, $P = [\Phi_1, \Phi_2, \ldots\ldots \Phi_t]$ is the eigenvectors corresponding to the $t$ largest eigenvalues and $b$ is the shape parameter which is the projection coefficient that $X$ projects onto $P$. Figure 2.1 shows the face models of the first three eigenvectors with varying $b_i$ values. Obviously, $b_i$ defines shape variation. In general, the larger $b_i$, the more deviation the face shape will be. Usually, $b_i$ is constrained within the range of $\pm 3\sqrt{\lambda}$ so that a constructed face shape will not degenerate too much.

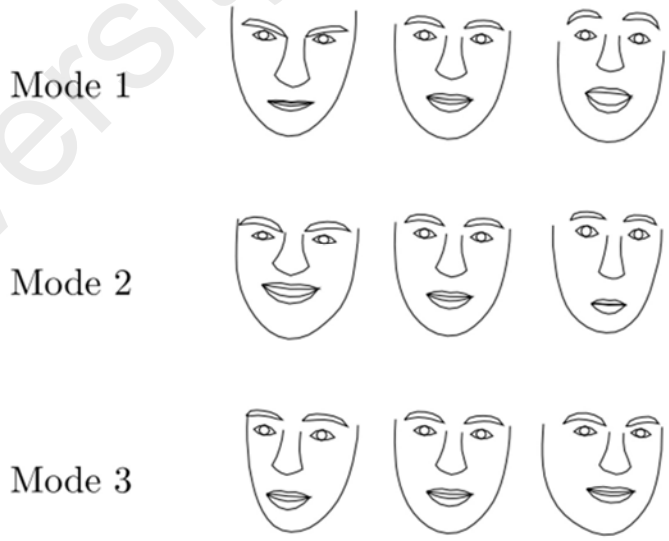


Figure 2.1: First 3 shapes variation of a face model (Cootes, 2007)

### 2.8.2 The feature model

In general, we suppose a landmark is located on a strong edge. According to the normal direction of a landmark, we can get m pixels on both sides Figure 2.2 of this landmark and each pixel has a grey-level value. So, for each landmark, there are in total *2m+1* gray-level values which form a grey-level profile represented as $dg = [g_i0, g_i2, .. , g2m]$, where *i* is the landmark index. In order to capture the frequency information, the first derivative of profile $dg_i$ is calculated as

$$dg_i = [g_i1-g_i0,\ g_i2-gi1,\ ..,\ ,\dots\ ,g2m-(g2m-1)] \tag{2.2}$$

In order to lessen the influence of image illumination and contrast, $dg_i$ is normalized as:

$$y_i = \frac{dg_i}{\sum_{k=0}^{2m-1} |dg_i k\ |} \tag{2.3}$$

The feature vector $y_i$ is called "grey scale profile".

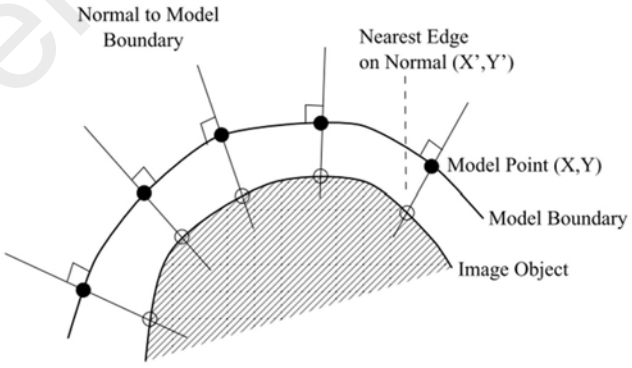


Figure 2.2: The selected feature points for constructing the grayscale profile (Cootes, 2000)

### 2.8.3 Active Shape Model (ASM)

The ASM searching algorithm uses an iteration process to find the best landmarks which can be summarized as follows:

1) Initialize the shape parameters $b$ to zero (the mean shape).

2) Generate the shape model points by using: $x = \bar{X} + Pb$.

3) Find the best landmark, by using the feature model.

4) Calculate the parameters $b'$ as $b' = P^T(z - \bar{X})$.

5) Restrict parameter $b'$ to be within of $\pm 3\sqrt{\lambda}$.

If $|b' - b|$ is less than a threshold, then the iteration process is completed; else $|b = b'|$, and return to step 2.

# CHAPTER 3: RESEARCH METHODOLOGY

## 3.1 Problem Definition

Until recently, accuracy of the anthropometric measurements acquisition is always an issue and any new method used for measurement will need an evaluation of its accuracy and reliability (Farkas, 1996; Aynechi et al., 2011 and Fourie et al., 2011). Human factors were the most important concern in taking accurate measurements (Farkas, 1996; Wong et al., 2008; Toma et al., 2009 and Fagertun et al., 2014). In direct anthropometry, a well-trained examiner was highly recommended to obtain measurements (Farkas, 1996; Hrdlička, 1920; Kolar & Salter, 1997; and Douglas et al., 2003). However, the experts are not always available to take the measurements and expert involvement could impose high cost, for example in screening process (Nagle et al., 2005; and Meintjes et al., 2002).

The most important task during measurement process is the ability to identify the anthropometric landmarks correctly (Hrdlička, 1920). In the situation of taking measurement in children and patients with involuntary movement, to identify the landmarks and measurements acquisition would be difficult. Furthermore, human emotion, tiredness and mood changes during measurements, would affect the process and degrade the quality of the patient and examiner relationship (Farkas, 1996).

Another factor that need to be concerned is the consistency of the measurements produced by examiners. In longitudinal study, subjects are usually examined regularly at certain ages over a period of time. Usually there are several examiners who are involved in taking the anthropometric measurements (Farkas, 1996; and Douglas, 2004). Therefore, consistency in taking the measurements by these examiner over a period of time and the consistency of measurements taken between examiners are important.

A new method such as 3D stereo-photogrammetry system, allowed the process of taking anthropometric measurements to be done on a 3D facial image instead of directly on the patient's face. This method is referred as indirect anthropometry. In this method, the 3D geometry of point cloud images is produced within few milliseconds and is suitable for taking the measurements in children and patients with involuntary movement (Wong et al., 2008). This is because it avoids patient and examiner engagement. The 3D image produced by the system, reflexes the true human geometry facial complex and is suitable to be used in taking the measurement (Ozsoy et al., 2009). However, using 3D facial image, the anthropometric landmarks with less or no prominent features are difficult to identify. These landmarks need to be palpated to confirm their position because the landmarks points were associated with the bony feature under the facial tissue. Example of these landmarks are the zygion, nasion, subnasion and gnanthion. In indirect method, the examiner is not able to perform palpation, however, the system allowed examiner to rotate the 3D facial image to further examine and identify these landmarks.

## 3.2 The Proposed Solution

### 3.2.1 The User Requirements

To address the above problems, there is a need for a system that is able to produce anthropometric measurements automatically. The most important module needed is the identification of the craniofacial anthropometric landmarks. This module must be able to localize the facial landmarks accurately. In order for the proposed system to be able to do its job, an expert way to identify the anthropometric landmarks should be available in the systems. Therefore, there is a need for a system is able to perform measurements like an expert indirectly.

Basically, the system should consist of two important aspects:

1. To detect craniofacial landmarks automatically. This would address the inconsistency of the anthropometric landmarks identification and reduce variability of landmarks localization. In this project, there were 23 craniofacial anthropometric landmarks that need to be located automatically.
2. To produce the craniofacial anthropometric measurements automatically. For the system to be used by the examiners, all measurements produced must down to the nearest millimetres. There are nineteen (19) measurements to be produced.

### 3.2.2. Craniofacial Anthropometry Expert System (CFA-ES)

This research project proposed an expert system which combined the expert skill of locating the anthropometric landmarks and image processing technique, to perform craniofacial anthropometry automatically. The system is known as the craniofacial anthropometry expert system (CFA-ES). The CFA-ES framework is shown in Figure 3.1. There are 3 major modules in the frameworks:

1) The image pre-processing
2) The knowledge base (the back-end)
3) The automatic measurement modules (the front-end).

The back-end module is a training module that generates expert knowledge database which consist of the craniofacial anthropometry shape model (CFA-Shape Model) and the correlation conversion equation. The CFA-Shape Model will perform the automatic localization of anthropometry landmarks and the conversion equation will convert the measurement from pixel to millimetre. The detail of the methodology of system development is discussed in section 3.6.5.

The front-end module is the automatic measurement process that uses the expert knowledge, the active shape model and the conversion equation to execute its tasks. Firstly, the system searches the region of interest (ROI) which is the face. Then the active shape model searches the face shape in the new image and try to fit the shape nicely and accordingly. Then it extracts the x,y coordinates of the twenty three (23) craniofacial landmarks. Next, it calculates the distances of measurements in pixel and lastly it produces eighteen (18) craniofacial measurements in millimetres.

### 3.2.3 Research questions

The Vectra-3D stereo- photogrammetry system is the 3-dimensional (3D) facial scanner used in the current study. A study on the inter- and intra-examiner error when using Vectra-3D needs to be done in order for the examiners to familiarize herself with the system, and to learn and observe for any discrepancy of output measurements between examiners. An advantage of doing so is the examiners can benchmark their anthropometry skill with each other. Therefore, the first research question is, to determine for discrepancies in data acquisition between and within examiners. Any new method used in anthropometry needs to have a determination of its reliability and validity because the 3D images will be used in the CFA-ES study. Any new equipment for use in craniofacial studies such as the 3D images, though validated by the manufacturer need to be reassessed by the end user. Therefore, the second research question is, to determine the validity and reliability of the craniofacial measurements acquired by Vectra-3D is compared to direct method. The third research question is to determine if the CFA landmarks detected by CFA-ES were reproducible. Lastly, the forth research question is, to determine the accuracy and reliability of craniofacial measurements obtained using the automatic craniofacial anthropometry system (the CFA-ES).

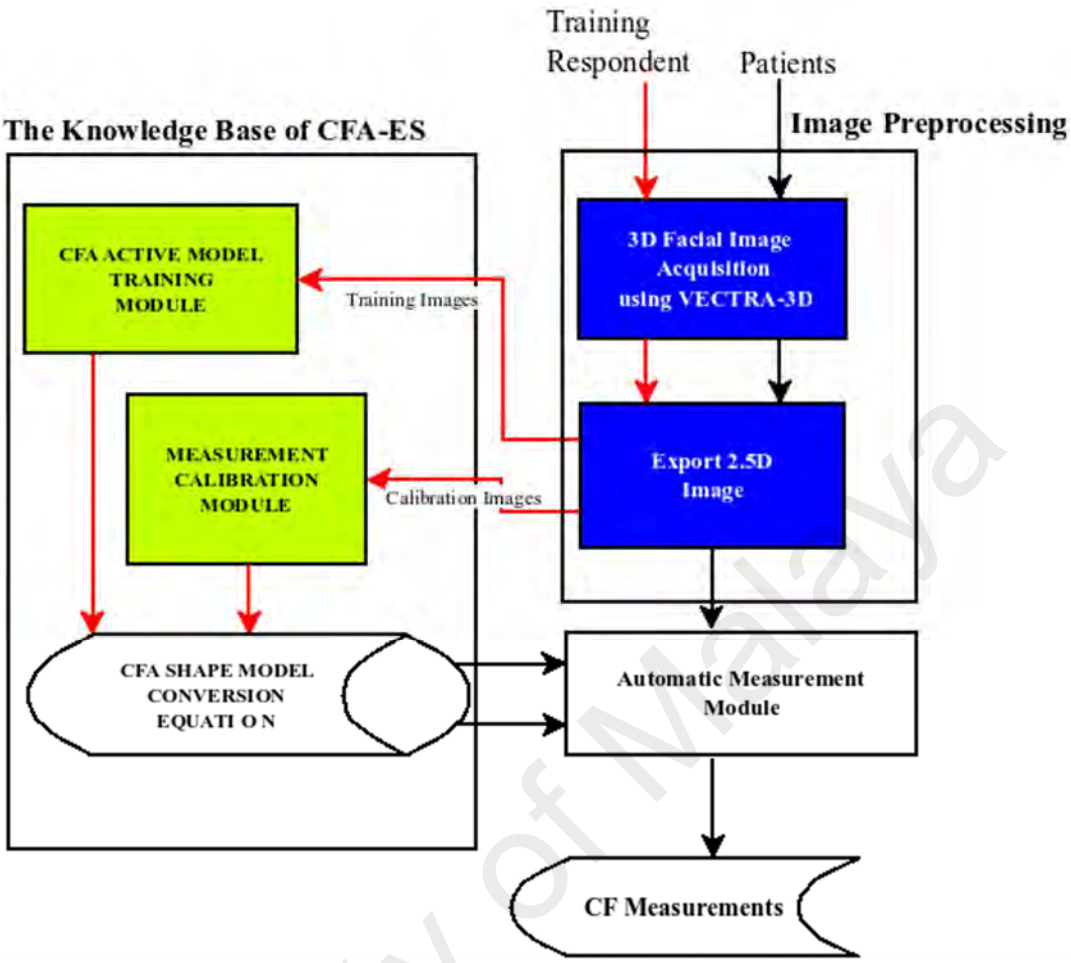


Figure 3.1 The Automatic Craniofacial Anthropometry Framework. The red path is the training path to establish the expert knowledge. The black path is the front-end system. The blue processes are the preparation process, the green processes are the back-end module and the white process is the front-end module.

### 3.3 Materials and Method

The methodology process flow of this project is shown in Figure 3.2. There are four major phases involved, 1) preliminary, 2) CFA measurements acquisition, 3) automatic CFA system development and 4) statistical data analysis.

As for the CFA data acquisition, three methods were performed i.e. the direct method, the semi-automatic method and automatic method. The direct method is a manual measurement whereby the measuring process was done directly on the respondent's face. In the second phase, the semi-automatic method which is also referred as indirect CFA

measurement was performed. The measurement was done on respondent's 3D facial image that was captured. In this project, VECTRA-3D stereo-photogrammetry system was used in the indirect CFA measurement. Later in this thesis this method is referred to as Vectra-3D measurement. Last, which is the automatic method, CFA data acquisition was done by the expert system developed for this project, the CFA-ES. The CFA-ES system locates the anthropometric landmarks automatically without human intervention except for the 3D image pre-processing task, to produce CFA measurements.

Due to the hospital policy at the time where a non-medical staff was not allowed to handle patient or respondent, therefore, two main examiners were needed in the project. One of the examiners is a well-trained dentist, Dr. Saravanan (DS) who specialized in craniofacial measurement and was responsible for the direct measurement. The other examiner is a computer scientist, Salina Asi (SA), who was responsible in the Vectra-3D measurement. Because of this, intensive discussion on craniofacial landmarks identification and measurement processes was carried out to make sure both examiners had consensus understanding on CFA landmarks identification and definition and the measuring process. This was done to reduce the inter- and intra-examiner error during the measurement process.

### 3.4 Preliminary Phase

In the preliminary phase, there were few steps that need to be done before the acquisition of CFA measurements. Firstly, to obtain the appropriate ethics approval from the University Malaya's Ethics Committee. Secondly, to determine a set of CFA landmarks and measurements to be used in the project. Thirdly, both examiners needed to perform self-calibration and inter-calibration process (as describe in section 3.3.5) before performing the measurements.

### 3.4.1 Ethics Approval

To obtain appropriate ethics approval all required forms and documents i.e. project proposal, patient information sheet, consent form and data acquisition form were produced. These documents were submitted for ethics application. The ethical approval was obtained on the 25th May 2010 for the Faculty of Dentistry Medical Ethics Committee (MEC), University of Malaya. The ethical approval letter is attached at Appendix A. The MEC ethics number for this project is DFOS097/0035(P). Beside the use for the ethics application, the data acquisition form was also used to ease the process of CFA data acquisition.

### 3.4.2 Cranio-facial anthropometric landmarks and measurements

The craniofacial anthropometric (CFA) landmarks and measurement for this project are listed and described in Table 3.1 and 3.2. Altogether 23 CFA landmarks and 19 measurements were considered in this research project. The selected landmarks and measurements were obtained from the face, orbit, nose and orolabial region. The landmarks and measurements that were used in this project, are adequate to plan for treatment in the area of craniofacial region and are essential landmarks for the study of facial morphology (Farkas, 1994). Detailed discussion on CFA landmarks definition and identification was carried out intensively by both examiners. The second examiner was exposed to CFA measurement procedures for 6 months.

Both examiners had been trained on the use and handling of VECTRA-3D stereo-photogrammetry system and the Mirror software. VECTRA-3D stereo-photogrammetry system will be discussed in later section. To ensure the consistency of the two examiners

in identifying CFA landmarks, a few steps have been approached, i.e. self-calibration, and inter- and intra-examiners analysis.

### 3.4.3 Self-Calibration and Inter-calibration

Self-calibration was done by each examiner before taking anthropometric measurements. Calibration, was done by measuring repeatedly directly or indirectly on a face or 3D image. The measurement process was performed at least five times and stopped when the difference between the last and the first measurements was not more than two (2) millimetres. The use of two (2) millimetres was agreed after consulting the craniofacial surgeon who was the main supervisor for this project. It was further confirmed by Abdulkareem & Al-Mothaffar, (2012). For inter-calibration, measurements taken by the examiner (SA) calibrated with experience research assistant, Roshahidah Ahmad (RA) by measuring ten (10) images using VECTRA-3D system. The image was picked up randomly.

## 3.5 CFA Data acquisition

The CFA data acquisition begun after ethics approval was obtained. The participants for this project were volunteers from staffs, students, and friends from University of Malaya Medical Centre (UMMC), Faculty of Dentistry, University of Malaya and a private college in Cheras Kuala Lumpur. Initially, there were difficulties in getting the volunteers for the project because some people thought that the procedure might harm them. However, as the project became better known, more were willing to volunteer. Another hurdle that slowed down the process of data acquisition was the fact that direct asurement could only be performed when the examiner and the volunteer were

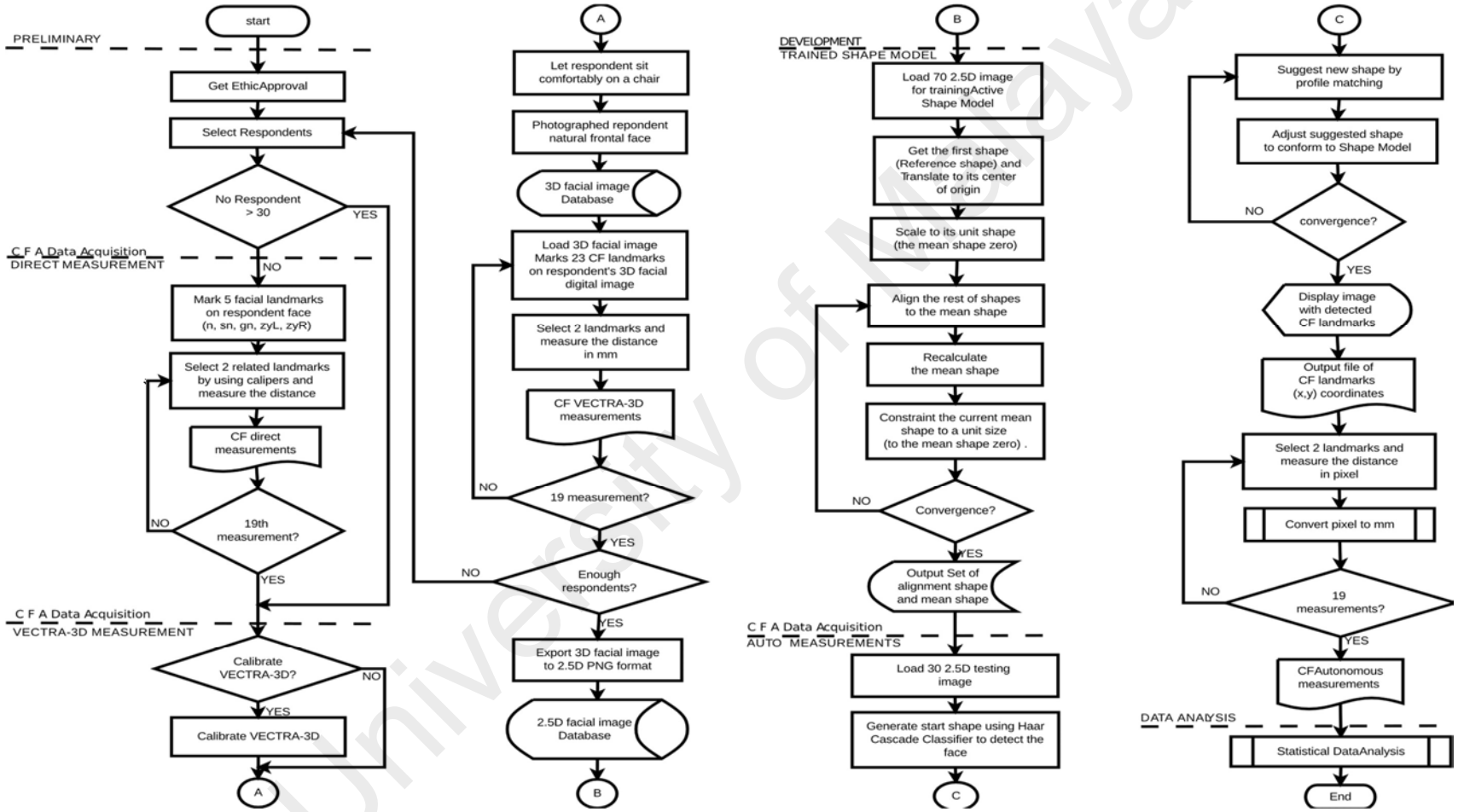


Figure 3.2 Methodology Process Flow

available to do the measurement. This was because the examiner is a dentist and has other work commitment as well as the volunteers.

The measurement process was carried out at the Department of Oral & Maxillofacial Clinical Sciences and the 3D Imaging Laboratory of Dentistry Faculty, University of Malaya, and at a meeting room in Cybernetic College.

### 3.5.1 Research Material

The data sample consisted of 100 normal adult volunteers, aged between 18 to 30 years old. There were equal numbers of men and women respondents. The respondents were Dental Surgery Assistant (DSA) student trainees at the University Malaya Medical Centre (UMMC), staffs from the Department of Oral & Maxillofacial Clinical Sciences, Faculty of Dentistry, under- and post-graduate students from the Dental Faculty, under-graduate students from Cybernetic College, Kuala Lumpur and friends.

Respondents were informed on the research procedures so they understand the whole process involved. They could refer to the patient information sheet and contact the higher authorities from the Dental Faculty for further inquiry. Respondents who agreed to participate in the project needed to fill in a personal information form. Based on the information provided from the volunteers, they were screened before being included in the project following the criteria below:

1. They must have no deformity of either congenital or non-congenital at their craniofacial area.
2. They must not have undergone any facial correction surgery.
3. Their family history must not have any inter-racial marriage for two previous generation.
4. Their age must be between 18 to 30 years old.

Table 3.1: Craniofacial Landmarks description for the face

| No | Landmark | Description |
|---|---|---|
| Face | | |
| 1. | Zygion (zyR) | & The most lateral point on the zygomatic arch, identified by the maximum bizygomatic (facial) breath. |
| 2. | Zygion (zyL) | |
| 3. | Nasion (n) | The midpoint of the nasofrontal suture. |
| 4. | Subnasale (sn) | The midpoint of the angle at the columella base where the lower border of nasal septum and the surface of the upper lip meet. |
| 5. | Gnanthion (gn) or menton | The lowest median landmark on the lower border of the mandible. This is a bony landmark and requires pressing the instrument down to reduce the effect of the soft tissue as much possible. |
| Orbital | | |
| 6. | Endocanthion (enR) | The point at the inner commissure of the eye fissure. |
| 7. | Endocanthion (enL) | |
| 8. | Exocanthion (exR) | The point at the outer commissure of eye fissure. |
| 9. | Exocanthion (exL) | |
| 10. | Palpebrale superius (psR) | The highest point in the midportion of the free margin of each upper eyelid. |
| 11. | Palpebrale superius (psL) | |
| 12. | Palpebrale inferius (piR) | The lowest point in the midportion of the free margin of each lower eyelid. |
| 13. | Palpebrale inferius (piL) | |
| 14. | Interpupilary (ipR) | The center of eye (Left and right 'ip' will be considered as different landmarks) |
| 15. | Interpupilary (ipL) | |
| | | |
| 16. | Alare (alR) | The most lateral point on each alar contour. |
| 17. | Alare (alL) | |
| 18. | Pronasale (prn) | The most protruded point of the nasal tip, identified on the lateral view of the rest position of the head. |
| Orolabial | | |
| 19. | Cheilion (chR) | The point where the outer edges of the upper and lower vermilions meet at the outer corner of the mouth. |
| 20. | Cheilion (chL) | |
| 21. | Stomion (sto) | The midpoint of the labial fissure when the lips are closed and the teeth shut in the natural position. |
| 22. | Labiale (or labrale) superius (ls) | The midpoint of the upper vermillion line. |
| 23. | Labiale (or labrale) Inferius (li) | The midpoint of the lower vermillion line. |

Table 3.2: Craniofacial Measurements description for the face.

| Region | No. | Measurement | Description |
|---|---|---|---|
| Face | 1. | zy-zy | Maximum face width |
| | 2. | n-gn | Face height |
| | 3. | n-sto | Upper face height |
| | 4. | sn-gn | Lower face height |
| Orbit | 5. | en-en | Inter-canthal width |
| | 6. | ex-ex | Biocular width |
| | 7. | ex-en(l) | Eye fissure length (left) |
| | 8. | ex-en(r) | Eye fissure length (right) |
| | 9. | ps-pi(l) | Eye fissure height (left) |
| | 10. | ps-pi(r) | Eye fissure height (right) |
| | 11. | ip-ip | Inter pupillary width |
| Nose | 12. | n-sn | Nose height |
| | 13. | al-al | Nose width |
| | 14. | sn-prn | Nose protrusion |
| Orolabial | 15. | ch-ch | Labial fissure width |
| | 16. | sn-sto | Upper lip height |
| | 17. | sn-ls | Cutaneous upper lip height |
| | 18. | ls-sto | Upper vermilion height |
| | 19. | sto-li | Lower vermilion height |

The selected respondents were required to sign a consent form so that they can make their choice whether to accept or to refuse to be a volunteer in this study. A copy of the form is attached in Appendix C.

### 3.5.2 CFA data acquisition by Direct Method

Figure 3.3 shows an examiner performs direct craniofacial measurement on a respondent. The technique was simple to perform, relatively non-invasive and inexpensive. A respondent was seated at rest position on a dental chair with his/her head at Frankfurt position. The face must be in neutral expression, this was to relax the facial muscles. The process was carried out in a room under a standard clinical lighting which was bright enough to examine the respondent's face. The examiner started taking the measurements when the respondent comfortably at resting position on the dental chair.

Figure 3.3: Direct Method of Craniofacial Anthropometry: An examiner performs direct facial surface anthropometry on a respondent.

***3.5.2(a) Measurement Tools for direct anthropometry***

Anthropometric tools used in direct method were the digital sliding callipers, hand held spreading callipers, ruler and measuring tape. (Figure 3.4 and 3.5) are images of a digital callipers and a spreading calliper. The spreading calliper was used to measure the face breadth *(zy – zy)* because the digital sliding callipers could not spread large enough to cover the facial breadth. Other measurements were obtained by digital sliding callipers. Example on how the measurement should be done in direct measurement for every region are shown by Figure 3.6 until Figure 3.9.

Figure 3.6 shows the measurement at the facial region, i.e. the facial breadth, the facial height, the upper and lower facial height. Figure 3.7 shows the measurement at the orbital region, i.e. the endocanthion width (or inter-canthal), the exocanthion width (or biocular), the eye fissure heights, the eye fissure width and the interpupilary distance. Figure 3.8

shows the measurement at the nose area, i.e. the nasal height, the nasal width and the nasal tip of protrusion. Figure 3.9 shows the measurement process at orolabial region, i.e. the labial fissure width, upper lip height, cutaneous upper lip height, upper vermilion height and lower vermilion height.

### *3.5.2(b) Measurement procedure*

Firstly, the respondent's face was marked with five landmarks (nasion *(n)*, ghanthion *(gn)*, alare *(al)*, subnasion *(sn)* and nasal protrusion *(prn)*) by a water base marker. These landmarks were sometimes hard to determine and need to palpate to correctly locate them (except the prn). This marking will ensure that the examiner would use the same landmarks when measuring other measurements that were based on these landmarks, and hence reduced the intra-examiner error. Other landmarks were easy to identify due to their natural features. Then, to obtain a measurement the examiner would locate two landmarks and placed the calliper on the landmarks. The examiner's assistant recorded the measurement in the data acquisition form. The examiner was just concentrating on placing and adjusting the calliper to get accurate measurements and did not look at the readings. This was done to reduce bias where the examiner might remember the first dataset measurements and this will affect the acquisition of the second dataset measurements. This process was repeated until all nineteen (19) measurements were measured. The final dataset would be the average of the two datasets (Wong, et al., 2008). The examiner will rest for about fifteen (15) to twenty (20) minutes before he obtained the second dataset. The fifteen (15) minutes period of time was recommended by one of the researchers in the faculty and was agreed by the supervisor. Data acquisition form is attached in Appendix D and some sample of the data acquisition are attached in Appendix E. One set of data would take an average of fifteen to twenty minutes to acquire. Both

respondent and examiner needed to be in good mood, relaxed and not feeling tired so that the measurements could be acquired smoothly and accurately.

Figure 3.4 A Digital Caliper

Figure 3.5 Spread Caliper

### 3.5.3 CFA data acquisition by VECTRA-3D

In contrast to the direct method, the semi-automatic or Vectra-3D measurement cannot perform the measurement directly on the respondent's face but does so on the respondent's 3-dimensional frontal facial image. Therefore, the examiner did not engage directly with the respondent. The examiner performed the measurement on the 3D facial images of the same respondents as from the direct method. The Vectra-3D method was non-invasive and simple but need a camera system which can produce 3D images. This 3D camera system used computer technology and is relatively expensive. The VECTRA-3D stereo-photogrammetry system came together with the Miror ® software used to acquire 3D facial images of respondents, construct and display the 3D images. The Mirror ® software helps to measure the soft tissue of craniofacial area. Please refer section 3.5.3(b) for further explanation of the VECTRA-3D system. We will refer the semi-automatic method as VECTRA-3D for the rest of the thesis.

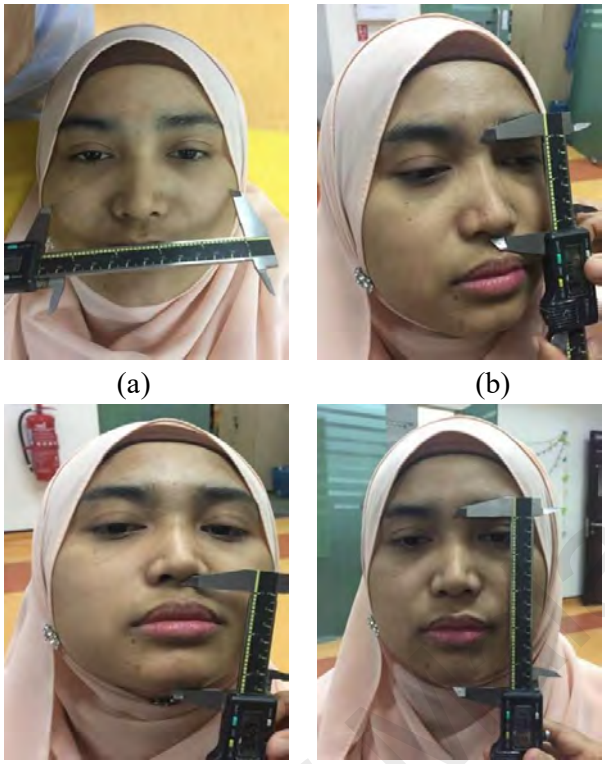

(a) (b)

(e) (d)

Figure 3.6 The measurement of Face Region (a) maximum face width (zy-zy), (b) upper face height (n-sto), (c) lower face height (sn – gn), (d) face height (n-gn)

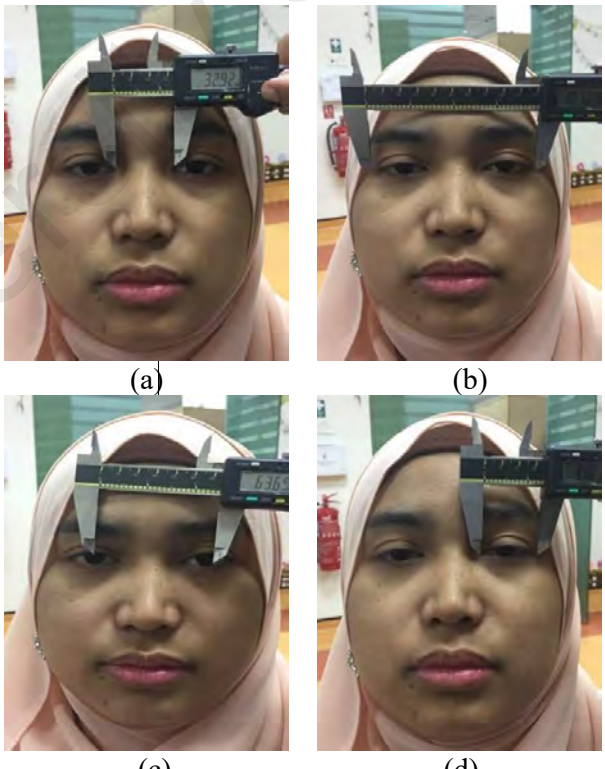

(a) (b)

(c) (d)

(e)

Figure 3.7 The measurement of the Orbit Region (a) endocation width (en-en), (b) exocathion width (ex-ex), (c) inter pupilary length (d) eye fissure length (en - ex), (e) eye fissure height (ps-pi)

(a)

(b)

(c)

Figure 3.8 The measurement of Nose Region (a) the nose width (al-al), (b) the nose height (n-sn), (c) tip of nose protrusion (sn-prn).

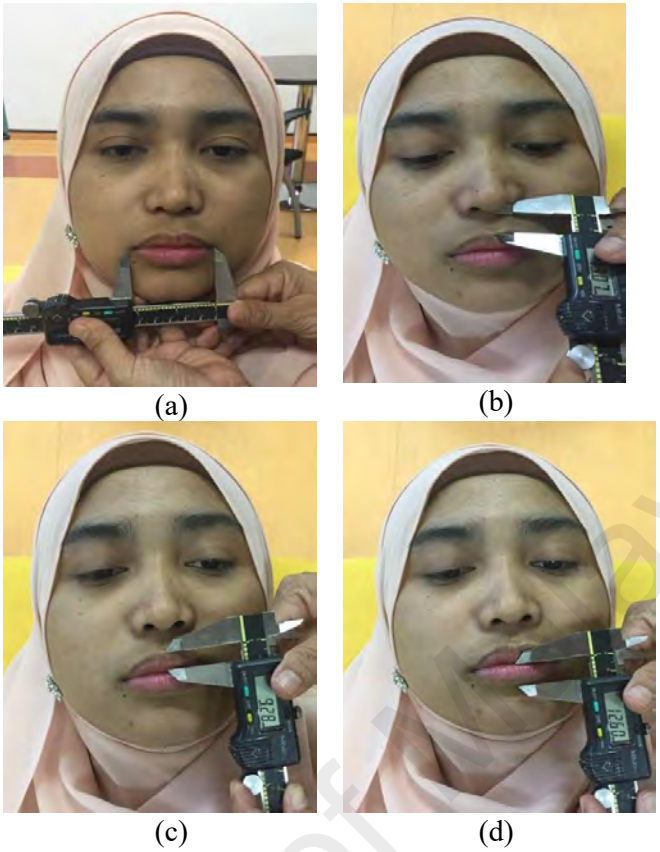

Figure 3.9 The measurement of the Orolabial Region (a) labial fissure width (ch-ch), (b) Cutaneous upper lip height, (c) upper vermilion height (d) lower vermilion height

One hundred (100) 3D frontal facial images were photographed by VECTRA-3D camera system. Out of these, thirty (30) images were 3D facial images of the direct method samples. The photography sessions were done in two different places. Thirty (30) subjects were photographed at the 3D imaging laboratory at Faculty of Dentistry of University of Malaya. Another seventy (70) respondents were photographed at the seminar room at Cybernetic College in Cheras Kuala Lumpur. The photography sessions were done under a standard clinical lighting which has enough lighting to produce a good 3D images. These seventy (70) images were used in the training phase of CFA automatic system framework (CFA-ES).

### *3.5.3(a) VECTRA-3D Stereo-photogrammetry System*

VECTRA 3D Stereo-photogrammetry (VECTRA-3D) system was used to capture 3D facial images of the respondents. The VECTRA-3D camera system was developed by Canfield Imaging System of Canfield Science Inc. The module that was used in this study was a tripod model which is capable to capture image of 180° view. The camera system is capable in taking the 3D images of face, but is not able to take the 3D image of the whole head. Diagram in Figure 3.11 is the schematic illustration of the camera setup.

The VECTRA 3D system is a semi-automatic digital system. This system use stereo-photogrammetric technique to produce 3D images with high-resolution colour surface of the face in two milliseconds (Information from VECTRA-3D technical manual). The system consists of four synchronized digital cameras which were set at fixed angles and there are two cameras on each side. The system consists of five main parts, the tripod, the camera panel, the dongle, the calibration panel and the computer system. The camera panel is connected to the computer through the dongle at a serial communication port (COM port). The tripod holds the camera panel firmly and can be adjustable according to the height preferred. After the system had been assembled and set up, the system needs to be calibrated by using the calibration panel. Figure 3.12 shows the camera system set up and Figure 3.13 shows the calibration panel.

The 3D geometry is captured by projecting a random light pattern onto the surface of an object, while simultaneously obtaining digital images with overlapping views of target. Its geometric accuracy is reported to be less than 0.3 mm (source: VECTRA-3D technical manual). The system software algorithms utilize the four (4) 2-dimensional (2D) images and combine these into a single 3D point cloud. To enhance visualization, points comprising the surface are link by vertices creating a 3D polygonal mesh.

Figure 3.10: The VECTRA-3D Stereo-photogrammetry System: An examiner acquired the 3D facial image of a respondent and performed the anthropometric measurement on the 3D facial image using the Mirror ® Software.

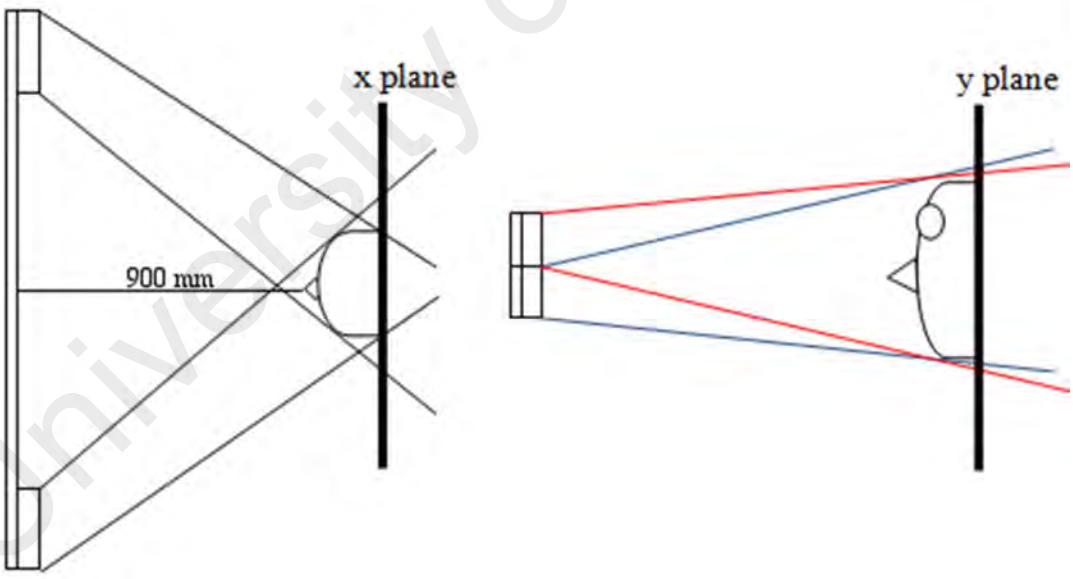


Figure 3.11: Facial image capture scheme for VECTRA-3D Stereo-photogrammetry System. View from x and y planes

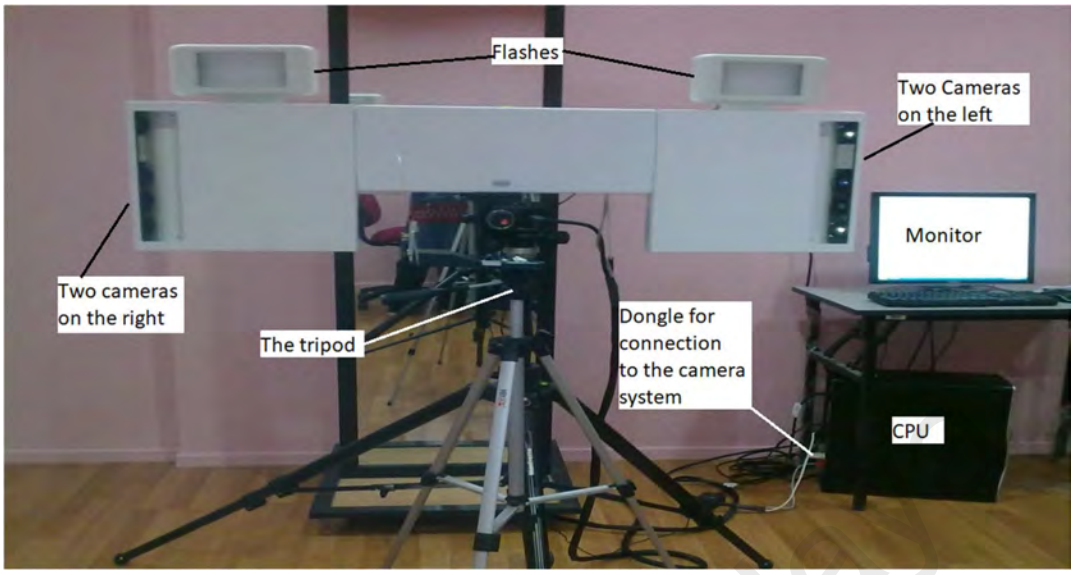


Figure 3.12: VECTRA 3D Stereo-photogrammetry System

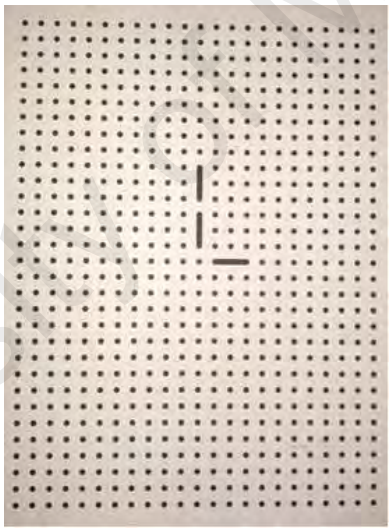

Figure 3.13: The VECTRA-3D Calibration Panel.

The system also comes with a software package the VAM (Visualizing and Measuring) that can measure the distance in millimetre between two selected points on an image separately from the Mirror 3D ® software. VAM enables the examiners to view the captured images in 3D geometry. The software also can be used to measure the anthropometric measurements in linear, as curvature or as volumetric. The examiner

performs the anthropometric measurement on the respondents' 3D images by pointing and clicking. She also could rotate and zoom in the image before marking the landmarks.

### *3.5.3(b) Vectra-3D Measurements Process*

Firstly, after every set up of the VECTRA-3D system, the VECTRA-3D need to be calibrated as per manufacturer protocol and was performed prior to a photography session. This procedure was done to ensure that the camera produced a good and accurate 3D image. At the Cybernetic College photographic session, the calibration process was done every time after the system was set up because it was dissembled at the end of the day. At the imaging lab we calibrated the system at beginning of the data collection session. The system was left in the lab intact. If the camera system did not produce good image, the system was re-calibrated again. Below are the steps of the calibration process for Vectra-3D (from Vectra-3D manual):

1. Click calibrate button (upper left corner of the screen) from the camera and holding the calibration panel
2. A dialog box prompts you to capture images in the first calibration position
    a. Hold the calibration panel/target 900 cm in front of the camera so that the L is upright.
    b. Tilt the top of the calibration panel back about 45 degrees from the pod face.
3. Click button capture images (in the dialog box). The flash will be triggered and the system will capture image. Wait 20 second.
4. Once the flash recharged, the dialog box prompt you to capture images in second calibration position.
    a. Hold calibration panel so that the L is upright.
    b. Tilt top calibration panel forward about 45 degrees toward the camera.

5. Click button capture image (in the dialog box) the flash triggered and the system will capture images. It takes few minutes to process the calibration images.
6. When the message, “Calibration Completed successful” appear, click ok.

Respondents were seated at resting position on a chair which is place 90 cm in front of the cameras. The 3D facial image of the respondent was obtained using Mirror ® software (Figure 3.10). Then, the examiner marked all twenty-three craniofacial landmarks on the 3D facial image. Then, to measure the distance of a measurement the examiner selected two points (landmarks) that represented the measurement by pointing and clicking. Then, the examiner clicked the menu in the system to choose the menu to get the linear distance of the two points. All the measurements were recorded in the data acquisition form.

### 3.5.4 CFA data acquisition by CFA-ES

The automatic CFA measurement was performed by the CFA Expert System (CFA-ES). The development of the CFA-ES will be discussed in detail in the next section. The 3D facial scanner used in this project, the VECTRA-3D photogrammetry system is a proprietary system where the software code was not accessible. Therefore, an automatic module was built and used separately. Due to inability to access 3D image processing libraries for this project, 2D image processing libraries were used to build the automatic framework. Therefore, the automatic module received the input of 2D image. The 2D image does not represent the facial complex and was not suitable to be used in this study. However, VECTRA-3D system has a function to project a 3D image into a 2.5D image or 2D image. A 2D image produced by VECTRA-3D system is a flat 2D image and does not represent facial complex. A 2.5D image projected by VECTRA-3D system is a 2D image that has a 3D-like feature and is able to represent the facial complex which is suitable for use in this project. The automatic module processed the 2.5D images that

were imported from VECTRA-3D and produced 23 anthropometric landmark locations of x and y coordinates. Only 18 CFA linear measurements derived from 23 CFA landmarks were produced by CFA-ES. The linear measure of the tip of nasal protrusion *(sn-prn)* was not measurable in 2.5D image format.

### 3.5.5 The Framework of Craniofacial Anthropometric Expert System

The detailed methodology on the development of CFA-ES and the anthropometric measurements acquisition are shown in Figure 3.14. This figure summarised the project methodology of part b and c in Figure 3.2. There were 4 important sub-modules: the image preparation and exportation, the CFA shape training, the calibration, and the landmark detection and measurement. The image preparation and exportation are the pre-processing image module of the expert system framework. The algorithm for the training module is shown in Figure 3.2. The shape module was kept in the expert knowledge base as shown in Figure 3.1. The calibration process is discussed in section 3.6.8. The landmarks detection and measurement is the front-end module as shown in Figure 3.1. The detail algorithm for this module is shown in Figure 3.2, part c.

**Software Libraries**

There were three (3) main software libraries for use in the development: the OpenCV version 2.9 libraries, openCV face HAAR classifiers and the STASM 4.0. OpenCv which was used to manipulate the images in this project. The OpenCv data structure was limited to two-dimensional data structure (Bradski, G., 2008). Due to this, as discussed in section 3.5.4, to get the full effect of craniofacial complex, 2.5D images was used. The 2.5D image give a 3D view of the craniofacial complex to obtained measurements with high accuracy (Ozsoy et al., 2009; and Hammond et al., 2004). STASM 4.0 is the extended active shape model library and has 2 major modules, the training module known as

Training Active Shape Model (TASM) and the search module known as Search Active Shape Mode (STASM) (Milborrow & Nicolls, 2008).

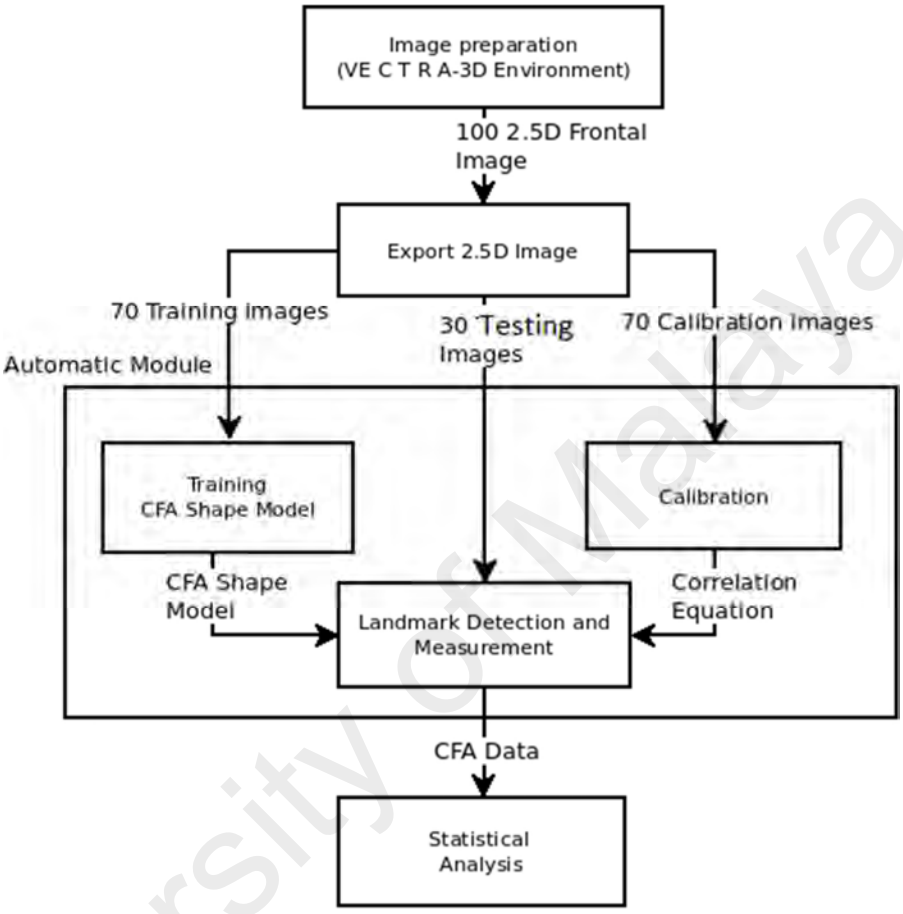


Figure 3.14: Detailed methodology process flow for the development of automatic system module: Image preparation, Exportation of 2.5D facial image, CFA Shape Model Training, Measurement calibration and CFA data acquisition on testing facial images.

### 3.5.6 Image Preparation and exportation

VECTRA-3D system is a commercial and proprietary system. In order to proceed with this project, we exported the 3D images from VECTRA 3D Stereo-photogrammetry system environment to get 3D-2D facial images which we referred to as 2.5D images in portable network photograph (.png) format. To export the images, firstly, the VECTRA-3D environment needed to be standardised by loading it with few images. It was decided that to include the biggest and the smallest face models so that the grid size was fix at one

standard environment. Then, the 3D images were saved as 2D images with the aspect ratio suggested by the VECTRA-3D System. This would ensure that the 2D images was saved at same scale and resolution. The image had the look of a 3D image but appeared as 2D image. Adjustment must be done to the face to be frontal as possible before exporting the images.

These images were referred to as 2.5D frontal images. The 2.5D images are in 2D images form with fix depth value of one. They were 2D images with the look of 3D appearance. The images are different from normal 2D images whereby the 2D images are flat and do not have the 3D appearance. The preparation of the 2.5D images was very important and must be done in a correct manner. The most important aspect to be considered when exporting the images was that all images were in a correct aspect ratio resolution and the size of all images was in correct proportion. The face must be in the most frontal position where possible. There are three types of 2.5D images that were produced: the training, the testing and the calibration images.

### 3.5.7 Training CFA Shape Model

An example of training images that were used in the training process is shown in Figure 3.15. There were 70 training shapes being used in this project. The 70 training shapes were enough to cover most typical variations of an object, however, the more the better (Milborrow, 2007). An object shape is represented by a set of labelled points or landmarks. In this project, the face shape was defined by 77 landmarks. The 23 anthropometric landmarks needed in this project were included in the 77 landmarks.

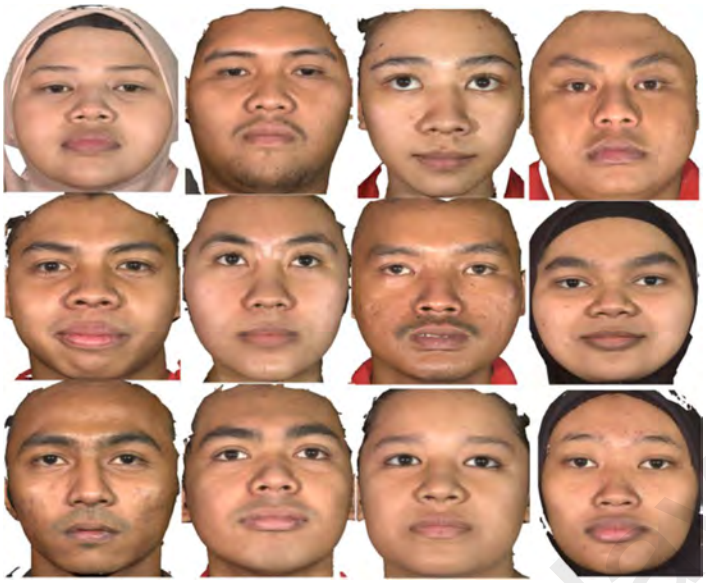

Figure 3.15: Example of 2.5-Dimensional Frontal Face Training Images.

**The shape profiles**

A shape can be represented by a set of landmarks points $\{x_i,y_i\}$, where (i=1..n), which defined the particular positions on the object of interest and were placed at consistent positions for every example in a training set. The craniofacial shape as defined by 77 landmarks included 23 craniofacial landmarks while another 54 landmarks were pseudo-landmarks interpolated between the craniofacial landmarks as shown in Figure 3.16. Only the x and y coordinate landmarks were extracted and all 70 face shapes were arranged in a shape file. To extract the landmark locations, firstly, the landmarks were annotated manually on the faces; there is a software tool available to help in marking. It was important that the landmarks must be accurately and consistently located on all faces. Then, the coordinates of the landmarks were extracted using a program written specifically for this task. It is important to extract the landmarks in sequence. Figure 3.17 is the output to check all the face shape landmarks were in correct sequence.

Figure 3.16: An example of training image that made up the shape of frontal face. These 77 landmarks include the craniofacial landmarks, used to construct the face shape for this project.

**The Training Face Shape**

All 70 face shapes were aligned into common by applying Procrustes Analysis. The process of aligning the 70 face shapes can be referred at Figure 3.1. All the shapes were aligned in vector X.

$$X = (x_1, x_2, x_3, \ldots, x_n, y_1, y_2, y_3, \ldots, y_n)^T \quad (3.1)$$

The Principal Component Analysis (PCA) was used to build a linear model of variation over the data set and generate the eigenvectors of covariance matrix. The shape model can be represented by equation 3.2, where $\bar{X}$ is the mean shape, P is a set of eigenvectors of the covariance matrix describing the modes of variation, and b is a vector of shape parameter and being constraint within a range. Statistical shape models can be used to analyse the differences in shapes between populations, or can be used to help locate structures in new images. Figure 3.18 is a mean shape aligned on a training face.

$$x = \bar{X} + Pb \quad (3.2)$$

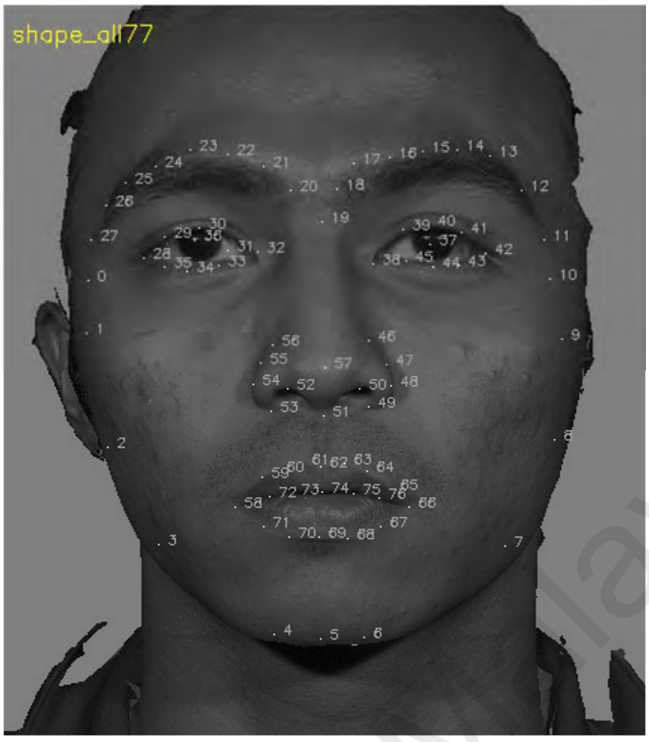


Figure 3.17: The face shape landmarks with numbering in order to check the sequence is in correct position.

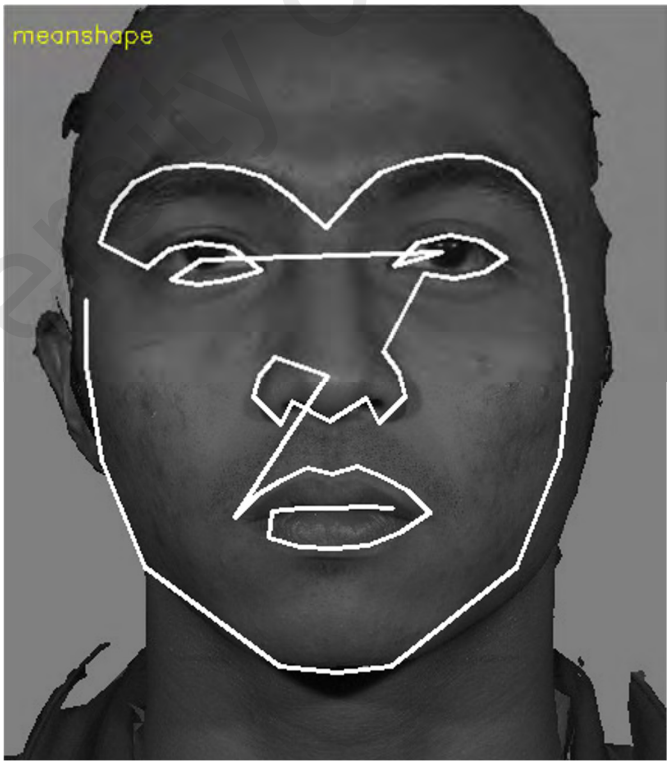


Figure 3.18 The mean shape aligned on a training image.

**Landmarks Profile Model**

The original of active shape model (ASM ) profile model used one-dimensional line along the whisker (Figure 2.2) (Cootes, Edwards & Taylor, 1998). To improved fits on each landmark STASM 4.0 uses two-dimensional profiles at each landmark, enable the system to produced better shape. In the 2D profiles, instead of sampling a one-dimensional line of pixels along the whisker (as shown in Figure 2.2), the system samples a square region around the landmarks. The 2D profile area captures more information around the landmark and this information gives better results. A 13x13 square around the landmark were best used to sample information around the landmark (Milborrow, 2013).

**Landmark Detection and Measurement**

An Active Shape Model (ASM) is a method of searching and matching a statistical shape model to a new image. The positions of the points in the image are given by the equation:

$$X = T\,\theta(\bar{X} + Pb) \tag{3.3}$$

Where $T\,\theta(X)$ is a transformation to the set of points encoded in the vector X, with parameter $\theta$ (rotation, scaling and translation). $T$ defines the mapping from the reference frame to the target image frame, giving the global pose of the object. A method of locating a good candidate position for each model point in a region is required by building a statistical model of the image patch about each point from the training set, then searching the region for the best match using this model. In this project, a 13x13 pixel around a landmark was use as a profile point.

The process of searching is described in Figure 3.1. A set of 77, x and y coordinates were retrieved which was the location of the face shape (vector X). The system then, provides

an output of 23 CFA landmarks coordinate that were extracted from the face shape. The measurement process is discussed further in the next section.

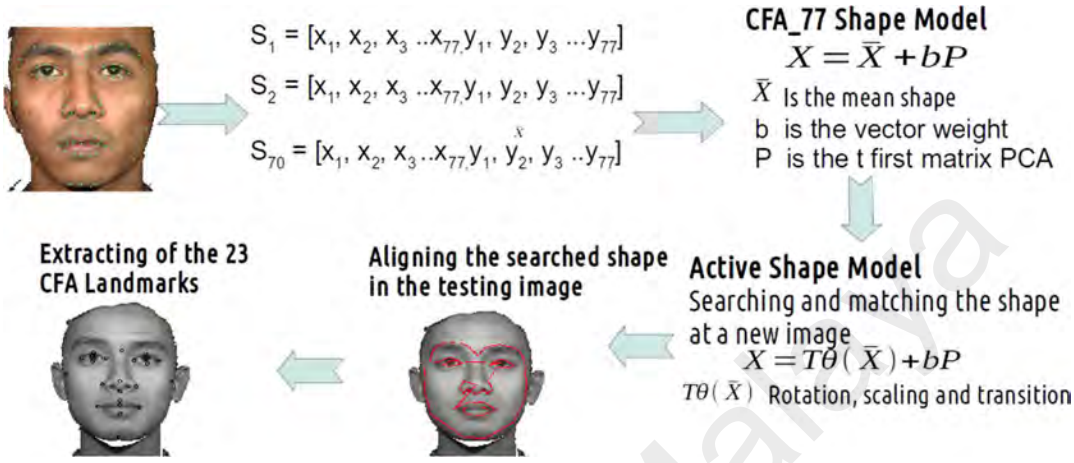


Figure 3.19: The whole process of training and detecting.

### 3.5.8 Calibration

In this project, the calibration process was done in order to have the correct conversion of the pixel distance to millimetre. The calibration images were images with few marks to get several samples of measurements. Therefore, before exporting the calibration images, the facial images were marked with seven (7) landmarks and four (4) measurements were produced from these landmarks. The images were exported into 2.5D with the landmarks on the facial images. The example of calibration image is shown in Figure 3.22.

#### *3.5.8(a) The pinhole camera model*

The pinhole camera model is the mathematical relationship between the coordinate of a 3D point and its projection onto the image plane of an ideal pinhole camera (Falk, Brill & Stork, 1986). The geometry related to the mapping of a pinhole camera is illustrated in Figure 3.20. Point *O* is the camera aperture. The three axes of the coordinate

system are referred to as X1, X2, X3 and axis X3 is optical axis which is the direction of the of the camera viewing. An *image plane* is where the 3D world is projected through the aperture of the camera. The image plane is parallel to axes X1 and X2 and is located at the focal length distance of the pinhole camera *(f)* from the origin *O* (the camera aperture) in negative direction of the X3 axis. The image plane is intersected to the X3 axis at coordinate -f where |f| > 0. A point *R* at the intersection of the optical axis and the image plane is referred to as the principal point or image plane centre.

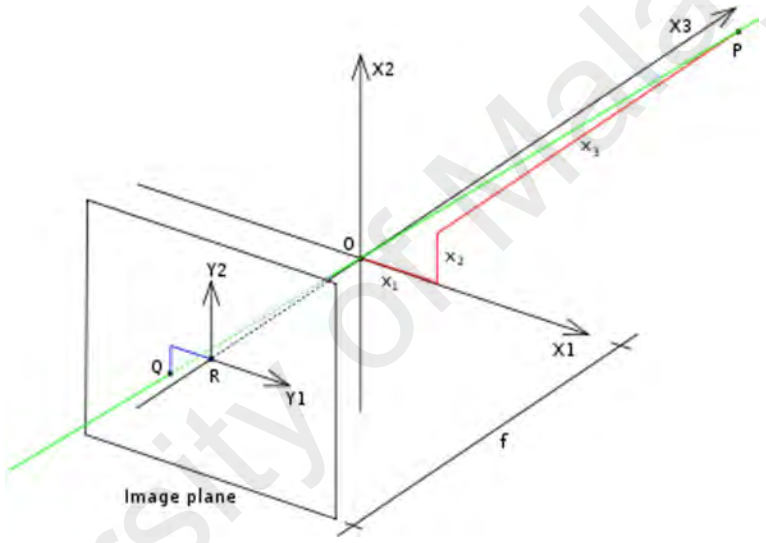


Figure 3.20 The geometry of a pinhole camera. (Image from: opticsphysics.weebly.com/pinholers)

A point *P* somewhere in the real world at coordinate (x1, x2, x3) relative to the axes X1, X2, X3. The projection line (the green line) of point P into the camera passes through point **P** and the point **O** and the projection of point **P** onto the image plane at **Q.** The distance of point P is assumed to be x3 > 0 at axis X3. The image plane is a 2-dimensional coordinate system with an origin at *R* with axes Y1 and Y2 which are parallel to X1 and X2. The coordinates of point **Q** relative to this coordinate system is (y1, y2).

The pinhole aperture of the camera, through which all projection lines must pass, is assumed to be infinitely small, as one point. This point in 3D space is referred to as the optical (or lens or camera) centre. Figure 3.21 shows the mathematical relationship of the coordinates (y1, y2) of point *Q* is the projection of 3D coordinates (x1, x2, x3) of point *P* as described in equation 3.4 to 3.7 (Falk, Brill & Falk, 1984).

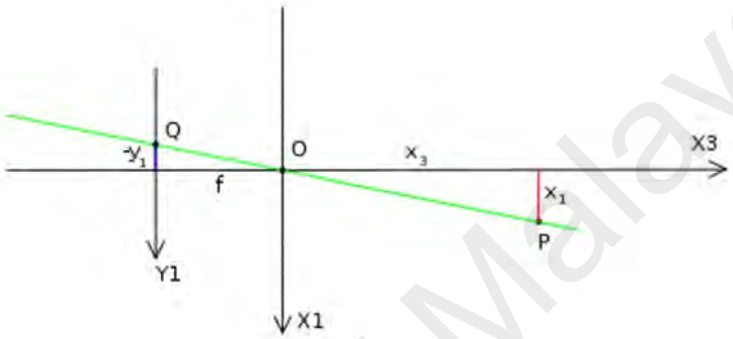


Figure 3.21: The geometry of a pinhole camera as seen from X2 axis. (Image from: opticsphysics.weebly.com/pinholers)

$$\frac{-y1}{f} = \frac{x1}{x3} \tag{3.4}$$

$$y1 = |f| * \frac{x1}{x3} \tag{3.5}$$

Similarly, when viewing from axis X1 the equations are as follow.

$$\frac{-y2}{f} = \frac{x2}{x3} \tag{3.6}$$

$$y2 = |f| * \frac{x2}{x3} \tag{3.7}$$

### *3.5.8 (b) The conversion correlation equation*

The CFA-ES environment producing the anthropometric measurements was different compared to the indirect method which used the VECTRA-3D system environment. The pixel resolution of the 2.5D is different from the pixel resolution of 3D images. In VECTRA-3D environment, all measurement outputs were in millimetre while in CFA-ES, the measurements were measured in pixels distance before they were converted into millimetres. Therefore, to get a correct measurement in millimetre, the conversion association factor between these two environments need to be defined.

First, in VECTRA-3D environment we sampled four measurements from each of 3D images before we exported them into 2.5D calibration images (calibration images that have seven (7) marks). Then we used the GNU Image Processing (GIMP) version 4.0 which is an Open Source Software (OSS) for image processing tool to sample four measurements in pixels correspondence to the four (4) sample measurements from VECTRA-3D (before the images were exported). Next, we did a reverse engineering calculation to calculate the distance in pixel of the four measurements in millimetre that were produced in VECTRA-3D system. This is because we would like to find the correlation of the pixel distance in VECTRA-3D and the pixel distance in 2.5D image. Before that we must understand the concept of the pinhole camera.

There are two problem statements to be considered when determining the correlation equation for the relationship between measurements in 3D images (VECTRA-3D) and 2.5D images (craniofacial automatic system)

The first problem question:

What is the craniofacial measurement in pixels in the VECTRA-3D (3D image) for a given craniofacial measurement in pixel in the automatic system (2.5D image).

The second problem question:

What is the distance in millimetre for a given distance in pixel unit in automatic system.

Figure 3.22: Example of Calibration Image.

The known facts gathered from the VECTRA-3D camera information and calibration are as below (Information from Vectra-3D):

1. The camera focal length (f) is 25.195 mm.
2. The pixel size on the image plane (y1 or y2) is 0.0044 mm.
3. The distance of the subject from the camera at axis X3 (x3) is 900 mm.

A correlation equation between the distance in pixel between Vectra-3D and 2.5D needs to be established. We calculated four measurements for each correspondence image of VECTRA-3D and 2.5D images as shown in Table 3.3 below.

Table 3.3: The example of calculated distances in pixel in VECTRA-3D environment

| Measurement | VECTRA-3D Distance (mm) | VECTRA-3D Distance (pixel) | 2.5D image distance (pixel) |
|---|---|---|---|
| 0001.tom-1 | 35.924 | 228.562 | 81.099 |
| 0001.tom-2 | 131.245 | 835.030 | 285.142 |
| 0001.tom-3 | 188.266 | 1197.819 | 418.059 |
| 0001.tom-4 | 92.589 | 589.083 | 207.010 |

To calculate distance in pixel of the (VECTRA-3D) we need to calculate the size of pixel in VECTRA-3D in millimetre. Either formula 3.4 and 3.6 can be used. From equation 3.6 we arrived at equation 3.8.

$$x1 = \frac{y1 * x3}{|f|} = \frac{0.0044 * 900}{25.195} \tag{3.8}$$

The diameter of pixel in VECTRA-3D (x1) = 0.157174 mm.

The distance in pixel of VECTRA-3D conversion to millimetre formula is

$$Distance\ (pixel) = \frac{Distance(mm)}{x1} \tag{3.9}$$

Pearson Correlation was used to analyse the correlation between the two variables (Vectra-3D distance pixel and 2.5D distance pixel). Results of the Pearson correlation indicated that there was a significant positive association between Vectra-3D distance pixel and 2.5D distance pixel, ($r = 0.997$, $n=120$, $p < .001$).

A linear regression analysis was done to derive a relationship between the two parameters where Vectra-3D distance pixel is the dependent variable and 2.5D distance pixel is the independent variable. The linear regression results for significant of p-value is less than 0.01 ($p<0.01$). The cutting point was forced to be 0, (Vectra-3 pixel 0 when 2.5D pixel is 0). The equation 3.10 is derived from the unstandardized coefficients independent variable (2.5D distance pixel) is 2.859.

$$f(x) = 2.859 * x \quad (3.10)$$

The equation was used to calculate the pixel distance in VECTRA-3D for a given distance in pixel in 2.5D images. The conversion of VECTRA-3D pixel distance into millimetre can be done by using the formula below:

$$\text{Distance (mm)} = \text{Distance (pixel)} * x1 \quad (3.11)$$

Where x1 is a pixel size of VECTRA-3D in millimetre = 0.157174 mm. To do the conversion, a distance for measurement obtained by CFA-ES in pixel will be converted into distance of pixel in VECTRA-3D environment by using equation 3.10. Then using equation 3.11, the distance is converted into millimetre. In summary, the measurement process went through two conversions.

### 3.6 Inter- and Intra-Examiners Assessment

Vectra-3D was used to analysed the reliability of the inter- and intra-examiner error. For intra-examiner reliability assessment, the landmarks were digitized on 30 images where 19 facial parameters were measured for each image. After the first measurement, the landmarks were not saved. After a 5-day period, the landmarks and parameters were

digitized and measured again. For inter-examiner reliability analysis, measurements obtained by SA were compared to the measurements carried out by RA.

### 3.7 Facial feature extraction using local method

During the initial stage of this project, we were trying to build classifier for each CFA landmark using Viola and Jones (2001) image detection framework. This is local technique approach of object detection process where structures such as edges or regions, are assembled into groups in an order to identify features of interest. This technique was used to define the local features of the landmarks. We intended to build the local landmark classifiers based on feature landmarks. The HAAR like features was used to build our landmarks classifier and we implemented the integral image by Viola and Jones object detection framework (Viola and Jones, 2001) to identify the landmark feature. So, we intended to build the Haar Classifiers for the 23 CFA landmarks. However, this method was not suitable and only produced *"en"* and *"ex"* HAAR classifiers that was able to measure three CFA measurements, the intercanthal *(en-en)*, biocular *(ex-ex)*, left and right eye fissure length *(en-ex)*.

The 2.5D facial images were divided into seventy (70) images for training data and thirty (30) images for testing data. For each 30 test images, four measurements were obtained: the left and right eye fissures lengths, the intercanthal width and the biocular width by using the Visualizing and Measurement Software (VAM). These are the measurements at the orbital region. To enable one to obtain these measurements automatically, both eye corners for left and right eye must be detected automatically.

### 3.7.1 The training dataset

Firstly, from 70 training facial images, the positive images were prepared by extracting the eyes from the facial image. Then, two sets of positive samples were prepared and each sample was used to train the inner *(en)* and external *(ex)* eye corner classifiers. Each set contained 300 images of size of 200 x 200 pixel size. On each positive sample we marked the corner models. The inner eye *(en)* was 3/4 of the object height and 3/4 of the object width. The external eye corner *(ex)* was 2/3 of the object height and 3/4 of the object width. An example of the datasets is shown in Figure 3.23 and the object model of en and ex eye corners are shown in Figure 3.24.

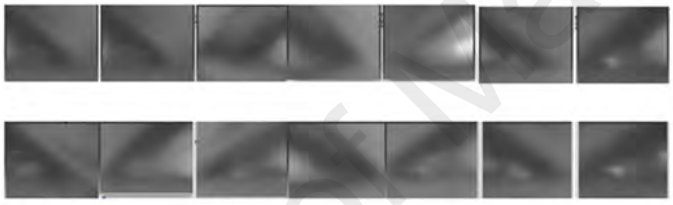

Figure 3.23: Example of training data set: above the inner eye-corner *(en)* and below the external eye-corner *(ex)*.


Figure 3.24: The object model for landmarks *(en and ex)* position in the training data set. On the left is inner eye-corner and on the right, is external eye-corner.

The negative image samples were the images that do not contain *en* and *ex* objects model. To improve the accuracy of eye corner classifiers, negative images were created by extracting any region of the size of 200 x 200 pixels at the face area which do not include the eye corners. AdaBoost was used to boost these weak classifiers consisting of selected

Haar-like features and construct the cascade classifiers. In this study the *"enHaar"* and "exHaar" cascade classifiers were constructed.

### 3.7.2 Landmark detection and auto measurement

To detect the eye-corners, firstly, the OpenCV eye classifier was applied to search and detect the eye at the face image. The eye was segmented. The *enHAAR* and *exHAAR* classifiers were applied to detect the inner and outer eye-corners. The *enHaar* classifier was applied to find inner eye corners while the *exHaar* was used to look for external.

Due to the small amount of the data used in training session, there were many false positive detected in the output results. To overcome this problem an algorithm in Figure 3.25 was prepared to predict the eye corners by eliminating the false detections.

| | |
|---|---|
| To detect inner eye (en):<br>- Get the boundry point,<br>bPoint = image width/3, height/3<br>- Eliminate detections above the bpoint<br>If right eye:<br>- Eliminate detections on the right of bPoint<br>- Get the most left point<br>Else if left eye<br>- Eliminate detections on the left of bPoint<br>- Get the most right point. | To detect outer eye (ex):<br>- Get the boundry point<br>bPoint = image width/2, height/2<br>- Eliminate detections above the bpoint<br>If right eye:<br>- Eliminate detections on the left of bPoint<br>- Get the most right point<br>Else if left eye<br>- Eliminate detections on the right of bPoint<br>- Get the most left point |

Figure 3.25: The algorithm used to remove the false positive detections

In summary, the detected landmarks were used to measure the distances between the related landmarks in pixel. Then the distances in pixel were converted into millimetre by using the correlation equation. To measure the intercanthal *(en-en)* the software calculated the distance between the inner eye-corner of left and right eyes, the biocular

*(ex-ex)* which distance was the distance between the outer corners of both eyes and the eye fissure lengths which was the distance between the inner and the outer eye-corners.

The used of local features to locate the 23 craniofacial landmarks was not suitable because the training sample must be very large to get a good classifier. The technique is exhaustive and difficult, some of craniofacial landmarks do not have distinct feature for example the gnanthion *(gn)*, zygion (zy) and nasion *(n)*. Alternatively, global method seemed to be suitable in this project. Active shape model was chosen to be used in this project.

### 3.8 Statistical Data Analysis

Statistical analysis tests were performed using SPSS version 19. To determine the accuracy of Vectra-3D stereo-photogrammetry system and the automatic system (CFA-ES), mean measurements derived from the systems were compared to mean measurements derived from the reference methods by using paired student t-test. Kolmogorov-Smirnov test for data normality was performed on mean measurements for the comparison. Following this, for normally distributed measurements, standard paired t tests were performed. The p value of 0.05 or smaller considered to be significant.

Reliability is defined as the consistency of values for repeated sets of both in Vectra- 3D and CFA-ES measurements, were assessed by test-retest reliability (Wong et al., 2008). Test-retest and inter- and intra-rater reliability is the degree of similarity and agreement between repeated measurements therefore ICC is the most ideal test to be used (Koo and Li, 2016). For this project, ICC with two-way random effect model was used to analyse the degree of correlation and agreement (Weinberg et al., 2004; Koo & Li, 2016). Below is the ICC index guideline in interpreting the reliability by Koo & Li, (2016)

Table 3.4 The ICC Index Categories (Koo & Li, 2016)

| **ICC Category** | **Range Index** |
|---|---|
| Poor reliability | Less than 0.50 |
| Moderate reliability | 0.50 – 0.75 |
| Good reliability | 0.75 – 0.90 |
| Excellent reliability | 0.90 – 1.00 |

All tests were performed on measurements obtained from 30 testing images. Figure 3.26 shows a sample of testing images. A 30 testing images ware used in this project is based on the central limit theorem which is one of the fundamental probability theorem which states that the t-distribution becomes a close fit to the normal distribution when the number of samples reach 30.

Figure 3.26: A sample of the thirty (30) testing images used for the validation of VECTRA-3D.

# CHAPTER 4: RESULT AND DISCUSSION

## 4.1 Introduction

In this chapter the results of the experiments that have been carried out are presented. The results are presented in 4 sections, 1) inter- and intra-examiners analysis. 2) validity and reliability of Vectra-3D measurements 3) reproducibility of CFA-ES landmarks localization 4) validity and reliability CFA-ES measurements

## 4.2 Inter- and Intra-examiner error assessment

In this section, the results of inter- and intra-examiner results are presented. The reliability of intra and inter-examiner were analysed using intra-class correlation coefficient (ICC). Table 4.1 shows the ICC results for inter and intra-examiner analysis. Overall, both analysis have significant measurements. For both intra-examiner and inter-examiner assessment, the reliability was good to excellent. The poorest reliability was observed in inter-examiner assessment for left eye fissure length ($r=790$, 95% CI=564-900, $p<0.001$), which nevertheless showed good reliability.

## 4.3 Validity and Reliability of VECTRA-3D against Direct Measure

The second objective of this project is to analysed the validity and reliability of CFA measurements by using VECTRA-3D and direct method. It is mandatory to evaluate the reliability and validity of a system before standard implementation. In this study, the reliability and validity of VECTRA-3D were investigated by comparing the measurements that were acquired by VECTRA-3D against measurements taken manually.

Table 4.1: ICC test result for Intra- and inter-examiner analysis

| Region | Landmarks | Intra-examiner | | | | Inter-examiner | | | |
|---|---|---|---|---|---|---|---|---|---|
| | | ICC (r) | 95% CI | | Sig | ICC (r) | 95% CI | | Sig |
| | | | Lower | Upper | | | Lower | Upper | |
| Face | zy-zy | .994 | .988 | .997 | .000 | .991 | .981 | .996 | .000 |
| | n-gn | .996 | .992 | .998 | .000 | .989 | .977 | .995 | .000 |
| | n-sto | .994 | .987 | .997 | .000 | .992 | .983 | .996 | .000 |
| | sn-gn | .972 | .941 | .987 | .000 | .934 | .863 | .969 | .000 |
| Orbital | en-en | .986 | .970 | .993 | .000 | .980 | .922 | .992 | .000 |
| | ex-ex | .972 | .942 | .987 | .000 | .945 | .885 | .974 | .000 |
| | ex-en(l) | .888 | .765 | .947 | .000 | .790 | .564 | .900 | .000 |
| | ex-en(r) | .959 | .913 | .980 | .000 | .787 | .559 | .898 | .000 |
| | ps-pi(l) | .866 | .720 | .936 | .000 | .836 | .660 | .922 | .000 |
| | ps-pi(r) | .875 | .739 | .940 | .000 | .831 | .650 | .919 | .000 |
| | ip-ip | .971 | .938 | .986 | .000 | .978 | .954 | .989 | .000 |
| Nose | n-sn | .995 | .990 | .998 | .000 | .992 | .983 | .996 | .000 |
| | al-al | .993 | .986 | .997 | .000 | .979 | .937 | .991 | .000 |
| | sn-prn | .952 | .899 | .977 | .000 | .867 | .659 | .942 | .000 |
| Orolabial | ch-ch | .955 | .905 | .978 | .000 | .884 | .757 | .945 | .000 |
| | sn-sto | .897 | .785 | .951 | .000 | .820 | .625 | .914 | .000 |
| | sn-ls | .968 | .932 | .985 | .000 | .934 | .861 | .969 | .000 |
| | ls-sto | .922 | .837 | .963 | .000 | .845 | .677 | .926 | .000 |
| | sto-li | .892 | .775 | .948 | .000 | .844 | .676 | .925 | .000 |

### 4.3.1 Accuracy of Vectra-3D

Paired t-test was performed on nineteen (19) measurements by Vectra-3D and by manually. Table 4.2 shows paired t-test results for this comparison. It shows the mean difference, the significant (p) value, and lower and upper mean difference at 95% confidence interval (CI) and the t distribution (t-dist) for each of 19 measurements. Of the 19 comparisons made, thirteen (13) parameters showed the comparisons were statistically significant and only six (6) parameters were statistically not significant. From 13 parameters that were significant, one (1) was from the face region, the face breadth *(zy-zy)*, all seven (7) orbit parameters, two (2) were from nose region, the nose width *(al-al)* and nasal protrusion *(sn-prn)* and three (3) were from orolabial region the mouth width *(ch-ch)*, subcutanous (*sn-ls)* and lower vermilion height *(sto-li)*.

Out of these, seven (7) of them have mean difference of less than 1 mm. They were, the intercanthal *(en-en)*, right eye fissure height *(ps-piR),* interpupilary *(ip-ip),* nose width *(al-al),* subcutaneous *(sn-ls) and the* lower vermillion height *(sto-li)*. Three (3) of them were less than 2 mm in difference namely, the face breadth, left eye fissure height, and the mouth width. The other three (3) measurements i.e. the biocular *(ex-ex)*, the right and left eye fissure length (Figure 4.3) the mean differences were more than 3 mm.

Therefore, a systematic bias or errors can be observed in these comparisons. The direction and magnitude of the bias are listed in column 2 in table 4.1. However, a mean different of less than 2 mm were said to be clinically not significant (Abdulkareem, 2012). Nevertheless, many researchers prefer less than 1 mm difference.

### 4.3.2 Reliability of Vectra-3D

To analyse the reliability of Vectra-3D, ICC with two-way random and absolute agreement was used. Column 8 in table 4.2 is the index coefficient of ICC test for Vectra-3D against direct method. All ICC indices were statistically significant except the linear distance for the left eye fissure height (r=0.323, 95% CI = 0.423 – 0.678, p>0.05).

An excellent degree of reliability with the indices *r* above than 0.9 were observed in all measurements in the face regions except the face height (p=0.943, 95% CI = 0.880 - 0.973, p<0.001), where the reliability was good to excellent. In the nose region, the nose height *(n-sn)* and nose width *(al-al)* had excellent degree of reliability (r=0.921 and 0.969, 95% CI =0.829 - 0.991, p<0.001) while tip of nose protrusion *(sn-prn),* the reliability was good (r=0.810, 95% CI = 0.804 – 0.992, p<0.001). Overall, the 95% of CI for this region ranged between 0.8 to 0.992. Therefore, the reliability for this region can be regarded as good to excellent.

At the orolabial region, the distance for lower and upper vermilion height, were regarded as having poor to moderate reliability. (r=0.501-0.560, 95% CI = -0.049 to 0.79, p<0.05). Other measurements were regarded as moderate to excellent (r>0.798, 95% CI =0.575 – 0.965, p<0.001). At the orbit, other than left eye fissure height, the average measure for this region, (r = 0.571 – 0.973). Two measurements have excellent reliability which were interchantal *(en-en)* and interpupilary *(ip-ip).* The left eye fissure length *(en-exL)* has moderate degree of reliability while the right eye fissure length *(en-exR)* poor to moderate reliability (r=0.968, 95% CI=365 – 0.856, p<0.05).

Table 4.2: Paired t-test and ICC results of measurements obtained by Direct Method and Vectra-3D.

| Region | Measurements | Mean Difference | p-value | 95% (CI) | | t-dist | ICC | 95% CI | | Sig |
|---|---|---|---|---|---|---|---|---|---|---|
| | | | | Lower | Upper | | | Lower | Upper | |
| Face | zy-zy | 1.303 | 0.007* | 0.391 | 2.215 | 2.923 | 0.973 | 0.942 | 0.987 | .000 |
| | n-gn | 0.131 | 0.850 ns | -1.271 | 1.533 | 0.191 | 0.943 | 0.880 | 0.973 | .000 |
| | n-sto | -0.112 | 0.714 ns | -0.729 | 0.506 | -0.370 | 0.970 | 0.938 | 0.986 | .000 |
| | sn-gn | 0.194 | 0.659 ns | -0.695 | 1.083 | 0.446 | 0.960 | 0.917 | 0.981 | .001 |
| Orbital | en-en | -0.910 | 0.000* | -1.331 | -0.488 | -4.415 | 0.973 | 0.944 | 0.987 | .000 |
| | ex-ex | 6.171 | 0.000* | 5.188 | 7.154 | 12.841 | 0.938 | 0.869 | 0.970 | .000 |
| | ex-en(l) | 3.255 | 0.000* | 2.533 | 3.978 | 9.216 | 0.698 | 0.365 | 0.856 | .001 |
| | ex-en(r) | 3.186 | 0.000* | 2.543 | 3.829 | 10.134 | 0.782 | 0.542 | 0.896 | .000 |
| | ps-pi(l) | -1.200 | 0.002* | -1.942 | -0.459 | -3.312 | 0.323 | -0.423 | 0.678 | .150* |
| | ps-pi(r) | -0.922 | 0.007* | -1.578 | -0.267 | -2.879 | 0.571 | 0.098 | 0.796 | .013 |
| | ip-ip | 0.635 | 0.003* | 0.235 | 1.034 | 3.249 | 0.981 | 0.961 | 0.991 | .000 |
| Nose | n-sn | 0.031 | 0.941 ns | -0.805 | 0.866 | 0.075 | 0.919 | 0.829 | 0.961 | .000 |
| | al-al | -0.508 | 0.002* | -0.813 | -0.202 | -3.400 | 0.967 | 0.921 | 0.991 | .000 |
| | sn-prn | 1.222 | 0.000* | 0.824 | 1.620 | 6.284 | 0.810 | 0.804 | 0.956 | .000 |
| Orolabial | ch-ch | -1.142 | 0.002* | -1.842 | -0.442 | -3.337 | 0.874 | 0.649 | 0.947 | .000 |
| | sn-sto | 0.202 | 0.557 ns | -0.493 | 0.897 | 0.594 | 0.798 | 0.575 | 0.904 | .000 |
| | sn-ls | 0.751 | 0.001* | 0.341 | 1.161 | 3.747 | 0.919 | 0.730 | 0.968 | .000 |
| | ls-sto | 0.709 | 0.052 ns | -0.006 | 1.424 | 2.027 | 0.501 | -0.049 | 0.762 | .033 |
| | sto-li | 0.524 | 0.025* | 0.074 | 1.010 | 2.368 | 0.560 | 0.075 | 0.790 | .015 |

Note: * significant $p<0.05$

To summarized, the Vectra-3D reliability were moderate to good, except for the left eye-fissure height (not significant) and the labiale superius and inferius, their reliability were poor to good. A systemic bias can be observed at seven measurements. However, only three parameters were clinically significant (biocular, left and right eye fissure length). Therefore, Vectra-3D performed poor at these measurements. This can be explained by the way it works. The software generates the 3D position of any pixel by analysing its 2D position on multiple photographs in a process called triangulation. If any pixel is missing from any photograph, the software gave us an approximated location of the missed pixel in that picture to complete the geometric 3D reconstruction. Since the geometry of eye and lips shapes are highly complex, some information might be lost during the 3D construction. The structure of the eye also might give disadvantage during the construction of the 3D image such as the eye lashes.

**Disadvantages of direct method**

To explain further for the above problems, errors might also be introduced from the direct method. During measuring process, there were landmarks that were being referred several times because they were needed in several measurements.

For example, to measure the eye fissure lengths, intercanthal and biocular measurements, the examiner needed to refer the endocanthion *(en)* and exocanthion *(ex)* twice. The measurements will not be consistently obtained if the locations for the same landmarks differed during the measuring process. But this problem did not happen in Vectra-3D, all landmarks were marked before measure. During the measuring process, examiner will always refer to the same landmarks.

Table 4.3: The mean difference from comparing between anthropometric measurement obtained by direct method and VECTRA-3D.

| Region | < 1 mm | > 1 mm < 2 mm | > 2 mm |
|---|---|---|---|
| Face | n-gn<br>n-sto<br>sn-gn | zy-zy | |
| Orbital | en-en<br>ps-pi(R)<br>ip-ip | ps-pi(L) | ex-ex<br>ex-en(L)<br>ex-en(L) |
| Nose | n-sn<br>al-al | | |
| Orolabial | sn-sto<br>ls-sto<br>sn-ls<br>ls-li | | |

It was observed that, for the intercanthal distance, measurements obtained by Vectra-3D were consistently larger than the direct method while measurements for biocular were consistently lower than Vectra-3D. Figure 4.1 is the illustration for the observation. It can be explained that, during direct measurement, examiner tend to avoid the sensitive area of the eyes. This could lead to systemic bias that was observed at the orbital region where its p values were significant in all measurements

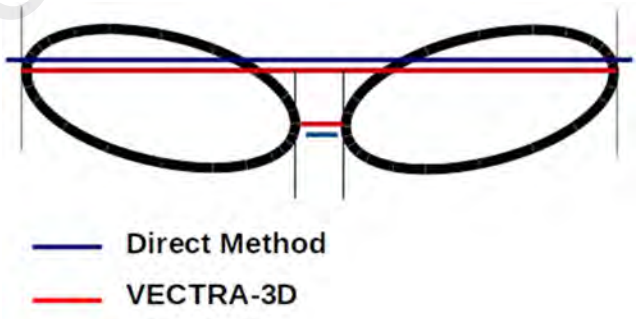


Figure 4.1: Systematic bias: for intercanthal *(en-en)* and biocular *(ex-ex)* the blue line was measurements obtained by direct method and the red lines were by Vectra-3D i.e. Vectra-3D measurement for biocular is always smaller than direct method and for intercanthal vice versa.

**Other studies**

Weinberg et al., 2006, and Wong et. al., 2008 studied the accuracy and reliability of 3dMD stereo-photography system and concluded that the 3dMD system was suitable to be used to obtain facial anthropometric measurements. Weinberg et al. (2006), evaluated the system by obtaining facial measurement from mannequin while Wong et al. use normal adults. Both observed systemic bias in measurements at orbital and orolabial regions i.e. biocular, interchantal, mouth width and labiale superius (sn-sto). Another study by Abdulkareem & Al-Mothaffar, (2012) also found measurements at orbital and orolabial to be significant. However, the mean different were less than 2 millimetres.

In conclusion, the Vectra-3D acquired anthropometric measurement data as well as direct method. However, it performed less at the eye and mouth area. Furthermore, 3 measurements were clinically not significant (biocular, left and right eye fissure length) but the reliability were relatively high. However, measurements such as left eye fissure height was not reproducible by Vectra-3D. Other measurements such as labiale superius and inferius also show poor to moderate reliability. Furthermore, VECTRA-3D provides digital data and management module could manage the image efficient.

**4.4 Reproducibility of Anthropometric landmarks localization by CFA-ES**

In CFA-ES the face shape was aligned to position itself on the facial image. Then the landmarks profile will suggest the most suitable location for various landmarks using the grey level feature to get a new suggested shape. Next the CFA landmarks position of x and y coordinates were extracted. Figure 4.2 shows the CFA mean shape that is aligned on a frontal facial image. Figure 4.3 shows twenty-three (23) craniofacial landmarks detected and localized by the automatic method. The landmarks were marked by the black circles. Figure 4.4 shows example outputs of 9 testing images with twenty-three (23) craniofacial landmarks. There were variations of the landmarks detection position. The

questions were how far the deviation landmark positions deviated from the ground truth data and how far the deviation remained valid to be regarded as reproducible or being accepted as at the same positions. To study the accuracy and reliability for these positions localization, x and y coordinates in pixel produced by CFA-ES and ground truth landmarks were transformed into Euclidean position by using formula 4.1.

$$Z = \sqrt{x^2 + y^2} \tag{4.1}$$

Figure 4.2 The CFA Mean Shape aligned and position itself on the facial image.



### 4.4.1 Reliability of landmark positions produced by CFA-ES

To analyse the test-retest reliability for CFA-ES, ICC test was performed to landmark position produced by CFA-ES and the ground truth. The ground truth landmark positions were obtained by SA using image processing tool (Gnu Image Processing, GIMP). GIMP is the same software that we use to do image pre-processing. Table 4.4 shows the ICC

results for anthropometric landmark locations that were produced by CFA-ES compared to the ground truth locations. Overall, all landmark positions produced by CFA-ES and ground truth were significant with average measure (r) that ranged from 0.751 to 0.969 which means good to excellent reliability.

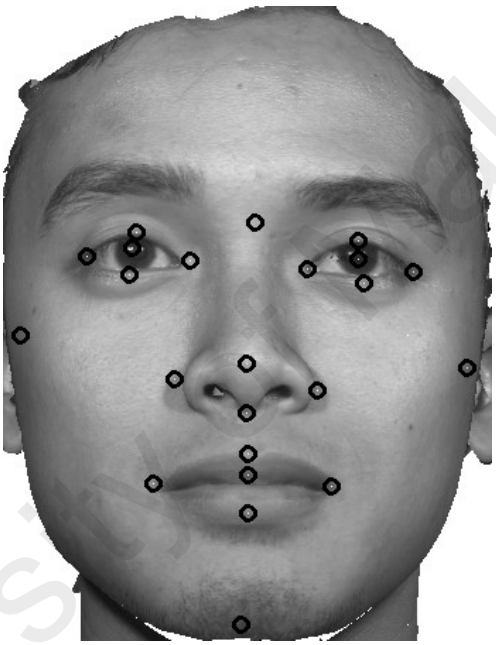

Figure 4.3: 23 CFA landmarks are extracted and localized.

At face region, all four landmarks showed moderate to excellent reliability ($r > 0.900$, 95% CI = 0.834 – 0.975, $p<0.001$). At the orbit, generally, a high degree reliability was observed between CFA-ES and manual in locating all the landmarks. All average measures of ICC were more than 0.900 except that at the left palpebrale inferius (piL) ($r=0.751$, 95% CI = 0.484 and 0.881 and $p<001$) which was a poor to good reliability. The other landmarks, right exocathion (exR), right palpebrale superius (psR), right palpebrale inferius (piR) and left pupillary (ipL) showed excellent reliability ($r > 0.900$, 95% CI >0.900, $p <0.001$). Another 5 landmarks at this region namely, left and right

endocathion (enL, enR), left exocathion (exL), left palpebrale superius (psL) and left inter-pupilary (ipL) showed good to excellent reliability (r >0.900, 95% CI = 0.842 – 0.989).

A high degree of reliability for landmarks localization at the nose region can be observed, except pronasale (prn) (r>0.90, 95% CI >0.9, p<0.001). At the orolabial region, reliability at all landmark positions produced by CFA-ES were good to excellent except for left cheilion which showed good to excellent (r=0.836, 95% CI = 0.666 – 0.923)

Table 4.4 Reliability of Ground Truth and CFA-ES anthropometric landmarks localization.

| Regions | Distance | Test-Retest (Ground truth vs CFA-ES | | | |
|---|---|---|---|---|---|
| | | R | 95% CI | | Sig |
| | | | Lower | Upper | |
| Face | ZyR | 0.922 | 0.836 | 0.963 | .000 |
| | ZyL | 0.922 | 0.834 | 0.913 | .000 |
| | N | 0.933 | 0.859 | 0.972 | .000 |
| | Gn | 0.941 | 0.872 | 0.975 | .000 |
| Orbital | enR | 0.948 | 0.892 | 0.975 | .000 |
| | enL | 0.946 | 0.887 | 0.975 | .000 |
| | exR | 0.977 | 0.951 | 0.989 | .000 |
| | exL | 0.924 | 0.842 | 0.915 | .000 |
| | psR | 0.960 | 0.915 | 0.981 | .000 |
| | psL | 0.946 | 0.886 | 0.974 | .000 |
| | piR | 0.959 | 0.913 | 0.980 | .000 |
| | piL | 0.751 | 0.484 | 0.881 | .000 |
| | ipL | 0.957 | 0.911 | 0.980 | .000 |
| | ipR | 0.933 | 0.857 | 0.969 | .000 |
| Nose | Prn | 0.947 | 0.890 | 0.975 | .000 |
| | alL | 0.969 | 0.935 | 0.985 | .000 |
| | alR | 0.954 | 0.904 | 0.978 | .000 |
| | Sn | 0.959 | 0.915 | 0.981 | .000 |
| Orolabial | chR | 0.918 | 0.829 | 0.961 | .000 |
| | chL | 0.839 | 0.666 | 0.923 | .000 |
| | Ls | 0.964 | 0.871 | 0.971 | .000 |
| | Sto | 0.958 | 0.925 | 0.983 | .000 |
| | Li | 0.958 | 0.912 | 0.980 | .000 |

### 4.4.2 Accuracy of landmark positions produced by CFA-ES

All 23 landmarks positions produced by CFA-ES and manual (ground truth) were analysed by paired t-test. All landmark positions were not significant ($p>0.05$). No systemic bias or errors were observed. Table 4.5 shows the paired t-test results for the comparison of anthropometric landmarks produced by CFA-ES and manual (ground truth) in pixel. To conclude, all 23 anthropometric landmarks localization produced by the automatic system (CFA-ES) were reproducible.

Figure 4.4: Some of the example results of landmark localization for 23 CFA landmarks on several facial images.

## 4.5. Validity and Reliability of CFA-ES against Vectra-3D

The fourth objective of this project was to investigate the validity and reliability of CFA measurements taken using CFA-ES. It is mandatory to evaluate for its reliability and

validity before standard implementation. In this study, the reliability and validity of CFA-ES were investigated by comparing the linear distance that were acquired by CFA-ES and the linear distance taken by VECTRA-3D.

### 4.5.1 Accuracy of CFA-ES

To evaluate the accuracy of CFA-ES, paired t-test was performed on 18 measurements obtained by CFA-ES and Vectra-3D. The results of paired t-test for the comparison is shown in Table 4.8. There were seven parameters that were significant. From these, 4 measurements were from the orbital region and three were from the orolabial. Systemic bias was observed in these CFA-ES measurements. The direction and the magnitude of the mean different are listed in table 4.8 at column 2.

At the orbit, four (4) measurements that were not significant were both eye fissure lengths (en-exL and en-exR) and both eye fissure heights (ps-piL and ps-piR). The mean different for both eye fissure heights were less than 1 mm. It can be regarded as clinically not significant and Vectra-3D measurements always smaller than CFA-ES. The mean different for both eye fissure lengths were less than 2 mm. It can be regarded as clinically not significant. However, some researchers would prefer less than 1 mm to be clinically not significant. For these parameters, Vectra-3D measurements were always larger than CFA-ES measurements.

The other three (3) significant measurements were at the orolabial region. They were upper and lower lips, and subcutaneous distances. The systematic bias could be observed in these measurements. However, the mean different for these measurements were less than 1 mm. Therefore, it can be regarded as clinically not significant. For these parameters, measurements obtained by Vectra-3D were always larger than CFA-ES.

Table 4.5: Paired t-test: Accuracy of anthropometric landmark produced by CFA-ES against ground truth marking

| Landmark | Mean diff | 5% CI | | t-dist | Sig |
|---|---|---|---|---|---|
| | | Lower | Upper | | |
| zyR | 3.711 | -6.377 | 13.801 | .752 | .458 |
| zyL | 12.211 | -2.239 | 26.662 | 1.728 | .095 |
| N | -2.885 | -14.849 | 9.078 | -.493 | .626 |
| Gn | 2.187 | -9.935 | 14.310 | .369 | .715 |
| EnR | 4.556 | -5.347 | 14.461 | .941 | .354 |
| EnL | -.784 | -11.594 | 10.025 | -.148 | .883 |
| ExR | -1.195 | -7.535 | 5.144 | -.386 | .703 |
| ExL | 9.138 | -4.750 | 23.028 | 1.346 | .189 |
| PsR | 1.298 | -7.067 | 9.664 | .317 | .753 |
| PsL | -1.346 | -13.015 | 10.322 | -.236 | .815 |
| PiR | -1.372 | -9.801 | 7.056 | -.333 | .741 |
| PiL | -14.872 | -41.105 | 11.360 | -1.159 | .256 |
| IpR | -1.118 | -9.809 | 7.573 | -.263 | .794 |
| IpL | 11.912 | -1.174 | 24.999 | 1.862 | .073 |
| Prn | 6.558 | -3.647 | 16.764 | 1.314 | .199 |
| AlR | .063 | -7.817 | 7.944 | .016 | .987 |
| AlL | 3.587 | -6.932 | 14.106 | .697 | .491 |
| SnD | 13.720 | -7.149 | 34.590 | 1.345 | .189 |
| ChR | 1.936 | -6.728 | 10.602 | .457 | .651 |
| ChL | 7.236 | -7.441 | 21.913 | 1.008 | .322 |
| Ls | -2.657 | -15.453 | 10.139 | -.425 | .674 |
| Sto | -.396 | -9.472 | 8.678 | -.089 | .929 |
| Li | -.529 | -10.805 | 9.747 | -.105 | .917 |

### 4.5.2 Reliability of CFA-ES

Overall, there were three (3) measurements of the comparisons that were not statistically significant ($p>0.05$). They were the right eye fissure length (en-exR) and both eye fissure height (ps-piL and ps-piR) These measurements have the average of ICC indices less than 0.500 and are regarded to have poor reliability. The right eye fissure length has the average measure ICC was 0.294, 95% CI = (-0.214) – 0.710 and $p<0.05$. The left eye fissure height has the average measure ICC of 0.324, the 95% CI ranged from (-0.243) to 0.654 while ICC indices for right eye fissure length was 0.277 with 95% CI ranged between -0.334 and 0.631.

Other measurements were significant, the ICC indices ranged between 0.51 and 0.950. At the face region, facial height (n-gn) and upper facial height (n-sto), their reliability can be regarded as excellent where facial height, r= 0.950, 95% CI = 0.899 – 0.977, p<0.001 and upper face height, r = 0.949, 95% CI = 0.893 – 0.976 and p<0.001. The reliability for other two measurements were moderate to excellent where face breadth; r=0.780, 95% CI = 0.743 – 0.941, p < 0.001 and lower face height: r = 0.843, 95% CI = 0.671 and 0,925, p<0.001.

At the orbit, the reliability for inter-pupilary *(ip-ip)* can be regarded as good to excellent (r= 0.900, 95% CI = 0.789 – 0.952, p<0.001). Two measurements at this region were moderate to good, intercanthal (en-en) (r=0.774, 95% CI = 0.511 – 0.889, p< 0.001) and the biocular (r=0840, 95% CI = 0.666 – 0.924, p<0.001). For left eye fissure length, the reliability was poor (r=0.494, 95% CI =(-0.120) – 0.770, p<0.05).

Measurements at nose region, the reliability was good for nose height, r = 0.877, 95% CI = 0.744 – 0.941, p<0.001. For nose width (al-al), r = 0.793, 95% CI = 0.570 – 0.901, p<0.001) regarded as moderate to good. At the orolabial region, the reliability were ranged from poor to good. For the upper lip (sn-sto), average measure ICC was 0.510, 95% CI ranged from -0.011 to 0,765, p<0,05. The average ICC measure for other measurements at this region, were moderate with ICC indices ranged between 0.663 and 0.700. However, the 95% CI ranged between 0.293 and 0.857and p< 0.05.

In summary, systematic bias or errors in CFA-ES were observed at the orbit and orolabial region.

Table 4.6: Paired t-test and ICC results for validity and reliability CFA-ES against Vectra-3D.

| Region | Measurement | Mean Difference | p-value | 95% CI | | t-dist | ICC | 95% CI | | Sig |
|---|---|---|---|---|---|---|---|---|---|---|
| | | | | Lower | Upper | | | Lower | Upper | |
| Face | zy-zy | -1.281 | 0.202 | -3.287 | 0.725 | -1.306 | 0.780 | 0.743 | 0.941 | .000 |
| | n-gn | -0.660 | 0.302 | -1.944 | 0.624 | -1.052 | 0.950 | 0.899 | 0.977 | .000 |
| | n-sto | -0.574 | 0.146 | -1.359 | 0.211 | -1.495 | 0.949 | 0.893 | 0.976 | .000 |
| | sn-gn | -0.583 | 0.492 | -2.118 | 1.042 | -0.696 | 0.843 | 0.671 | 0.925 | .000 |
| Orbital | en-en | 0.357 | 0.471 | -0.643 | 1.356 | 0.730 | 0.767 | 0.511 | 0.889 | .000 |
| | ex-ex | -1.104 | 0.116 | -2.497 | 0.289 | -1.621 | 0.840 | 0.666 | 0.927 | .000 |
| | ex-en(l) | -1.720 | 0.000* | -2.422 | -1.018 | -5.009 | 0.494 | -0.120 | 0.770 | .004 |
| | ex-en(r) | -1.991 | 0.000* | -2.785 | -1.197 | -5.129 | 0.294 | -0.214 | 0.710 | .065* |
| | ps-pi(l) | 0.956 | 0.005* | 0.306 | 1.606 | 3.008 | 0.324 | -0.243 | 0.654 | .104* |
| | ps-pi(r) | 0.902 | 0.012* | 0.218 | 1.586 | 2.698 | 0.277 | -0.334 | 0.631 | .156* |
| | ip-ip | -0.121 | 0.791 | -1.049 | 0.807 | -0.267 | 0.900 | 0.789 | 0.952 | .000 |
| Nose | n-sn | 1.665 | 0.669 | 0.171 | 0.107 | 0.749 | 0.877 | 0.744 | 0.941 | .000 |
| | al-al | -1.318 | 0.356 | -1.649 | 0.198 | -0.646 | 0.793 | 0.570 | 0.901 | .000 |
| | sn-prn | NA | NA | NA | NA | NA | NA | NA | NA | NA |
| Orolabial | ch-ch | 0.684 | 0.250 | -0.507 | 1.874 | 1.174 | 0.668 | 0.311 | 0.841 | .002 |
| | sn-sto | -0.578 | 0.228 | -0.381 | 1.537 | 1.232 | 0.510 | -0.011 | 0.765 | .028 |
| | sn-ls | -0.735 | 0.040* | -1.434 | -0.035 | -2.149 | 0.637 | 0.258 | 0.825 | .002 |
| | ls-sto | -0.827 | 0.003* | -1.350 | -0.304 | -3.235 | 0.640 | 0.207 | 0.833 | .001 |
| | sto-li | -0.597 | 0.003* | -0.976 | -0.217 | -3.215 | 0.608 | 0.158 | 0.816 | .002 |

Note: * significant $p < 0.05$

**Discussion**

From the result presented, CFA-ES can work as good as Vectra-3D. However, its reliability to reproduce measurements at orbital region was not significant. Systematic bias was observed but the measurements mean different were less than 2 mm.

There were several studies that focused on the shape profile of ASM. The shape profile is the intelligent module that is able to suggest better landmarks. This is where the expert knowledge was embedded. Hsu et al., (2010) has developed an Adaboosting based algorithm ASM and the result were out performed at the eye-brow landmark detection. There were also study that uses genetic algorithm (GA) in ASM and the used of hybrid algorithm which combined the 2 or more algorithms in the searching module of ASM have provided better results (Hsu et al., 2010). Improvement can be implemented in the CFA-ES by adopting the hybrid algorithm in its searching module. The use of better expert knowledge by the medical profession who had been well-trained with craniofacial anthropometry can be replaced to get better landmarks detection.

One important advantages that can be highlighted is the framework can be used for generating, for example a cleft-palate face shape. Therefore, a set of cleft-palate data can be trained.

**Other related studies**

There are few similar systems have been developed for facial landmarking. They automatically detected facial landmarks for different purposes. Liang et al., (2003) developed an improved method to automatically detect landmarks from 3D human facial data. A geometric information was used to locate 17 prominent points. Following this, a deformable transformation between target mesh and data mesh determined 20 established

landmarks and located them more accurately than with the geometric method alone. The method produced an average error of 2.64 mm over a sample of 115 heads.

Creusot et al., (2010), provided a proof-of-concept for a face labelling system. A set of anthropometric points containing hand- placed landmarks was used as input data. The aim was to retrieve the landmark's labels when some part of the face is missing. They used graph matching techniques to reduce the number of candidates, translation and unit-quaternion clustering to determine a final correspondence. Their method was suitable to be used in the situation that involved a large set of anthropometric landmarks involve.

Another study by Gupta et. al., (2010) detected several prominent anthropometric landmarks automatically, but they used it in the face detection and recognition application.

### 4.6 Local landmarks detection using Haar Cascade Classifier and Viola and Jones object detection Framework

Early in our study, we concentrated on analysing the local features to filter facial features or facial landmarks. We started with the prominent facial features and that were the inner and outer eye corners. We used Viola and Jones (2001) object detection framework to start with, to build our own classifiers that are able to detect the anthropometric landmarks. However, it was very difficult to implement the local filter as we observed so many outliers which resulted in large number of false positives. We considered training other type of local operator such as the Gabor filter but the need to build the Gabor bank and match them, involved too much work and was almost impossible because this project had twenty-three (23) landmarks. In addition, the craniofacial landmarks used in this study were a mix of landmarks with prominent features and landmarks with no features such as nasion, gnathion, zygions and subnasal. Furthermore, the data sample in this project were

100 frontal images, therefore it was not suitable implementing the local operator filter. Different quality of image will give different results. However, we developed the HAAR cascade classifier to detect the (inner eye corner) and ex (external eye corner) and we called them enHAAR and exHAAR.

With the framework and our HAAR classifier we detected and located the en and ex on the face image. Following this, we calculated the four distances related to these landmarks in millimetre. The measurements calculated were the intercanthal length, the biocular, the left eye fissure length and the right eye fissure length. We performed paired t-test to compare the mean difference between the measurements obtained with the measurements Vectra-3D.

### 4.6.1 Haar Cascade Classifier

The detection can be observed as the red spot. There were many red spot detection and many of them were false positive detections except the two red spots. We excluded the false positive by using the algorithm in Figure 3.26. Figure 4.5 shows the detection of inner and outer eye corners for the left eye. The detection was very good and very specific as what we define as endocathion (en) and exocathion (ex). 59 out of 60 ex and en landmarks were detected. There was one (1) case of miss detection (Figure 4.7) of en for the right eye. Therefore, we can only measure 29 pairs of the testing data.

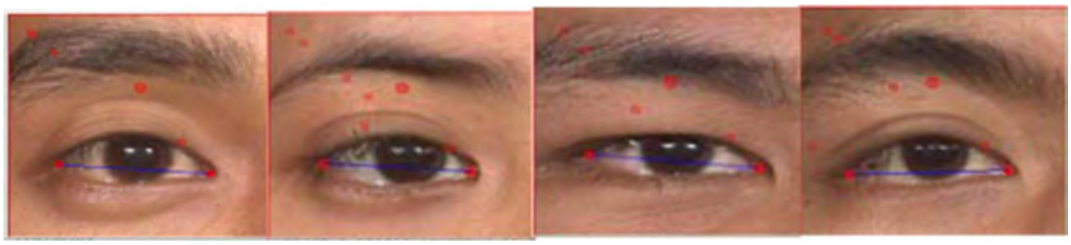

Figure 4.5: Samples of successful cases in obtaining the eye fissure length for right eye

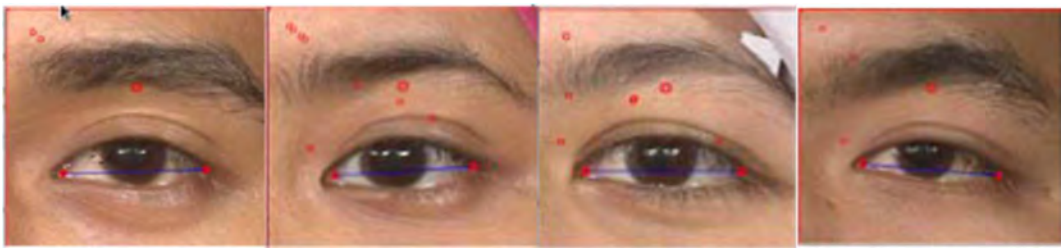

Figure 4.6: Samples of successful cases in obtaining the eye fissure length for left eye

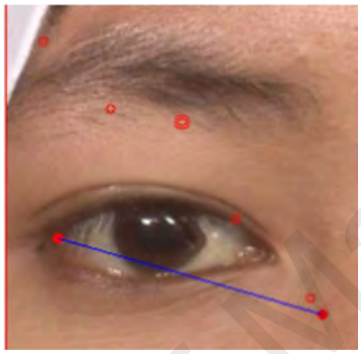

Figure 4.7: A miss detection of endocathion (en)

Table 4.7 shows accuracy for the measurements by HAAR classifier and Vectra-3D. All measurements were significant ($p>0.05$). There was no systemic bias observed. Two measurements were poor reliability (right and right eye fissure length), moderate reliability for biocular and good reliability for intercanthal distance.

Table 4.7: Results of paired t-test and ICC between measurement by HAAR classifier and byVectra-3D

| Measurement | Mean Diff | p-value | ICC |
|---|---|---|---|
| Right Eye Fissure (ex-en(R)) | 0.89 | 0.11 | 0.40 |
| Left Eye Fissure (ex-ex(L)) | 0.71 | 0.20 | 0.40 |
| Intercanthal (en-en) | 0.57 | 0.35 | 0.78 |
| Biocular (ex-ex) | 1.16 | 0.37 | 0.55 |

# CHAPTER 5: CONCLUSION

## 5.1 Research Summary

Errors during CFA measurements acquisition cannot be compromised due to the highly accurate requirement needed in some application, such as in determining the phenotype and genotype relationship (Farkas, 1996, Sforza et al., 2013). To be able to identify the anthropometric landmarks correctly is the most important requirement in craniofacial anthropometry (Hrdlička, 1920).

Many studies worked on evaluating various techniques or method on craniofacial anthropometric data acquisition. The most frequently used technique to perform indirect anthropometry of the facial surface is the 3D stereo-photogrammetry. The system enables us to overcome the limitation of direct anthropometry where engagement of the examiner and patient are totally removed, by offering a 3D facial image for the examiners to acquire anthropometric measurements. This method is suitable for use to acquire measurements from children and patients with involuntary movement. In direct method, this will be difficult to have children sitting still for a long duration, while movement by patient would make it difficult for the examiner to determine the landmarks. In long hours session, patient and examiner would be very tired and this will affect the quality of the measurement process. Many studies had been carried out to evaluate the accuracy of this indirect technique (Ayoub et al., 2003; Wong et al., 2008, Weinberg et al., 2006, Metzler et al., 2013, Aynechi et al., 2011).

In indirect method, only well-trained examiners are taking measurements. In case, where the expert is not available, the task would be pending. In screening program especially when the experts are needed more they would imposed high cost (Meintjes et al., 2002).

Studies done by Fagertun, (2014) in interoperability accuracy, suggested that in indirect method, there were landmarks that were difficult to locate. These landmarks were those associated with the bony feature underneath. The detection for these landmarks were highly variable. In addition, Toma, (2009) and Metzler, (2003) reported the existence of inter- and intra-examiner errors during the measurement process in indirect method. They also suggest that the 3 axes in a 3-dimension environment would affect the reproducibility of the landmarks localization.

To overcome the problem faced by the indirect method, a new alternative method to perform craniofacial anthropometry have been suggested. Douglas, (2003) designed an automatic system to measure, eye fissure height and eye fissure length in FAS patients. This system was able to segment the eye by applying genetic algorithm and eye template. However, this method only dedicated to the FAS problem and does not cater to landmarks which have high variability. Fagertun, (2014) designed an automatic system to help in annotating a large amount of facial landmark. He used ASM technique to automatically locate the landmarks, but did not expect high accuracy out of it, as errors in determining landmarks will be corrected by human. This would relief the burden of examiner who need to do landmark annotation in large amount. However, the system still requires human effort and furthermore the measurements were not generated automatically. Liang et al., (2013) designed a system that was able to improve facial landmark detection automatically. He used deformable technique and geometry landmarks of eyes, nose and mouth to improve the detection. The deformable technique was not able to capture the knowledge of an expert into the system. The deformable technique was not smart enough to suggest a good anthropometric landmark position.

This project tried to develop a craniofacial anthropometry expert system (CFA-ES). The system uses expert knowledge to research the initial landmark position and the system suggests a better position of landmark on a new image. This system used ASM with a 2D landmark profile. The 2D landmark profile was able to suggest better new shape for the new image. The expert knowledge of the craniofacial anthropometry was captured in the CFA shape model that were constructed in this study. The ASM technique shall be better than the deformable template used by Liang et al., (2013) and Hsu et al., (2013), as the deformable template does not have smart knowledge on craniofacial anthropometry.

The CFA-ES detect twenty-three (23) landmarks and produces eighteen (18) measurements, compared with Douglas's technique which detected landmarks around the eyes only. Classical ASM method used 1-dimensional (1D) profile landmarks. The 1D profile landmarks was not able to suggest a better new shape as good as those obtained by 2D landmark profile (Milborrow & Nicolls, 2008). Furthermore, all systems discussed were not able to produce anthropometric measurements. In comparison, this CFA-ES was able to produce 18 anthropometric landmarks that were good enough for facial evaluation or assessment.

There were other systems that can detect CFA landmarks for face recognition. For example, Gupta, (2010) designed *anthroface3D* to be able to recognize a face. She used CFA landmarks and indices in her system.

### 5.2 Research Finding

To the best of our knowledge, this is the wholesome expert system being proposed in the craniofacial anthropometry. All CFA-ES landmarks are reproducible ($p<0.001$). The reliability of CFA-ES landmarks localization was good to excellent. There was no

systemic bias observed in all detected landmarks. From 18 measurements produced by CFA-ES, 7 measurements were significant. They were obtained from the orbital and orolabial regions. Even though, systemic bias was observed at these region, the mean different were less than 2 mm. Therefore, all eighteen measurements were clinically not significant. For the reliability of CFA-ES, 3 of the measurements from orbital region were not reproducible ($p>0.05$). Overall, the reliability of other measurements was moderate to excellent with the face region having reliability that is good to excellent. In conclusion, measurements produced by CFA-ES are as good as Vectra-3D.

The system is able to solve problems posted by the research question and achieve objectives of improving the reliability of the CFA data acquisition methods. Errors and biasness in human were removed.

Less performance at the orbital area might be due to improper construction of the 3D geometry at the eye. This is due to the convex shape of the eye ball and dark colour of the pupils (Hajeer, 2002). The eye lashes would also contribute to poor 3D construction of the eye. This is also the same at the mouth region where the shape of the lips is complex and have many valleys.

### 5.2 Future enhancement

A complete framework for automatic craniofacial anthropometry for frontal face 3D-like image has been described. The framework is able to detect twenty-three craniofacial landmarks and produced eighteen craniofacial measurements without human intervention.

There are few things that we can possibly do to enhance the CFA Expert System. First is to train shape model that consists of more points, for example a shape described by 100

points of landmarks. This is because more landmarks would define better shape (Cootes, Edwards & Taylor, 1998).

Secondly, the CFA shape model can be trained with more CFA landmarks so that more measurements can be produced by the system. The knowledge base of CFA-ES can be extended with the cleft face shape model or other facial syndrome.

It is also possible to enhance the performance of the system by introducing advance local feature classifiers such as HAAR and Gabor and the used of smart algorithm such as genetic algorithm in the landmark profile.

Lastly, we may able to include more data in the training the shape model by including many more facial shapes to generate better mean shape. Consideration should be given to incorporate the texture and local features of the shape point so that the shape is able to adjust itself to better positions and produce accurate measurements.

In conclusion, the proposed method has been validated against VECTRA-3D, where VECTRA-3D had been validated with direct method before it was used to build the automatic system. We believed that we have achieved our objective and answer all our research questions. CFA-ES can be used as an alternative method in obtaining the anthropometric data. This new method is able to perform 3D craniofacial anthropometry as good as VECTRA-3D and is better than direct method. The system has shown consistency in producing measurements. It produces measurements faster than manual and Vectra-3D.

## REFERENCES


Abu-gharbieh, R., Hamarneh, G., & Gustavsson, T. (1998). Review Active Shape Models - Part II: Image Search and Classification. In *Proceedings of the Swedish Symposium on Image Analysis, SSAB* (pp. 1–4).

Abdulkareem, S. E., & Al-Mothaffar, N. (2012). Accuracy and precision of a photographic system for the three-dimensional study of facial morphology. *Orthodontics, Pedodontics, and Preventive Dentistry, 24(1):138-145.*

Abdullah, N., Naing, L., Ismail, N. M., & Ismail, A. R. (2006). A Cross-Sectional Study of Soft Tissue Facial Morphometry in Children and Adolescent. *Malaysian Journal of Medical Sciences, 13(1), 25–29.*

Aksu, M., Kaya, D., & Kocadereli, I. (2010). Reliability of reference distances used in photogrammetry. *The Angle Orthodontist, 80, 482-489.*

Aldridge, K., Boyadjiev, S. A., Capone, G. T., DeLeon, V. B., & Richtsmeier, J. T. (2005). Precision and error of three-dimensional phenotypic measures acquired from 3dMD photogrammetric images. *American journal of medical genetics Part A, 138A (3), 247-253.*

Aldridge, K., George, I. D., Cole, K. K., Austin, J. R., Takahashi, T. N., Duan, Y., & Miles, J. H. (2011, Oct). Facial phenotypes in subgroups of prepubertal boys with autism spectrum disorders are correlated with clinical phenotypes. *Molecular Autism, 2(15).*

Aldridge, K., Boyadjiev, S. A., Capone, G. T. ., DeLeon, V. B. ., & Richtsmeier, J. T. . (2005). Precision and error of three-dimensional phenotypic measures acquired from 3dMD photogrammetric images. *American Journal of Medical Genetics Part A*, *138A*(3), 247–253.

Al-Khatib, A. R. (2010). Facial three-dimensional surface imaging: an overview. *Archives of Orofacial Sciences, 5, 1-8.*

Arslan, S. G., Genc, C., Odaba, B., & Kama, J. D. (2008). Comparison of facial proportions and anthropometric norms among Turkish young adults with different face types. *Aesthetic Plastic Surgery, 32, 234–242.*

Asha, K. R., Lakshmiprabha, S., Nanjaiah, C. M., & Prashanth, S. N. (2011). Craniofacial anthropometric analysis in down syndrome. *Indian journal of pediatrics, 78, 1091–1095.*

Asi, S. M., Ismail, N. H., H, R. N., Ramlan, E. I., & Rahman, Z. A. A. (2014). Automatic Craniofacial Anthropometry Landmarks Detection and Measurements for the Orbital Region. *Procedia Computer Science, 42, 372–377.*

Asi, S. M., Ismail, N. H., & Rahman, Z. A. A. (2012, December). Validity and reliability evaluation of data acquisition using Vectra 3D compare to direct method. *In Biomedical engineering and sciences (IECBES), 2012 IEEE EMBS conference on (p. 883-887).*

Aynechi, N., Larson, B. E., Leon-Salazar, V., & Beiraghi, S. (2011). Accuracy and precision of a 3D anthropometric facial analysis with and without landmark labelling before image acquisition. *The Angle orthodontist, 81(2), 245-252.*

Ayoub, A. F., Garrahy, A., Hood, C., White, J., Bock, M., Siebert, J. P., Spencer R., Ray, A. (2003). Validation of a vision-based, three-dimensional facial imaging system. *Cleft Palate-Craniofacial Journal, 40(5), 523-529.*

Bagi´c, I., & Verzak, Z. (2003). Craniofacial anthropometric analysis in Down's syndrome patients. *Collegium antropologicum, 27 Suppl 2,* 23–30.

Bradski, G., & Kaehler, A. (2008). *Learning OpenCV*. Sebastopol, CA: O'Reilly Media.

Budai, M., Farkas, L. G., Tompson, B., Katic, M., & Forrest, C. R. (2003). Relation between anthropometric and cephalometric measurements and proportions of the face of healthy young white adult men and women. *The Journal of Craniofacial Surgery*, *14*(2), 154-61; discussion 162-3.

Caterson, E.J., Diaz-Siso, J. R., Shetye, P., Junker, J. P. E., Bueno, E. M., Soga,S., et al., (2012). Craniofacial Principles in Face Transplantation, *Journal of Craniofacial Surgery*, *23,* 1234-1238.

Cevidanes, L. H. C., Tucker, S., Styner, M., Kim, H., Chapuis, J., Reyes, M., et al., (2010). Three-dimensional surgical simulation. *American Journal of Orthodontics and Dentofacial Orthopedics, 138*, 361–371.

Cheung, L. K., Chan, Y. M., Jayaratne, Y. S. N., Lo, J. (2011). Three-dimensional cephalometric norms of Chinese adults in Hong Kong with balanced facial profile. *Oral Surgery, Oral Medicine, Oral Pathology, Oral Radiology and Endodontology, 112(2), e56-e73.*

Claes, P., Vandermeulen, D., De Greef, S., Willems, G., Clement, J. G., & Suetens, P. (2010). Computerized craniofacial reconstruction: Conceptual framework and review. *Forensic Science International, 201(1-3), 138–145.*

Cootes, T., Hill, A., Taylor, C., & Haslam, J. (1994). Use of active shape models for locating structures in medical images. *Image and Vision Computing*, *12*(6), 355–365.

Cootes, T. F., Taylor, C. J., Cooper, D. H., & Graham, J. (1995). Active Shape Models-Their Training and Application. *Computer Vision and Image Understanding*, *61*(1), 38–59.

Cootes, T. F., Edwards, G. J., & Taylor, C. J. (1998). Active appearance models. In *Proceedings european vonference on computer vision* (pp. 484–498).

Cootes, T. (2000). Model-Based Methods in Analysis of Biomedical Images. In R. Baldock an J. Graham (Ed.), *Image processing and analysis (pp. 223–248).* Oxford University Press.

Cootes, T. F., & Taylor, C. J. (2001). Statistical models of appearance for medical image analysis and computer vision. In M. Sonka & K. M. Hanson (Eds.), *Proceedings of SPIE* (Vol. 4322, pp. 236–248).

Cootes, T. F. (2011). Deformable Object Modelling and Matching. In *Lecture Notes in Computer Science (including subseries Lecture Notes in Artificial Intelligence and Lecture Notes in Bioinformatics)* (Vol. 6492 LNCS, pp. 1–10).

Creusot, C., Pears, N., & Austin, J. (2010). 3D face landmark labelling. In *Proceedings of the ACM workshop on 3D object retrieval - 3DOR '10* (p. 27). New York, New York, USA: ACM Press.

Cristinacce, D., Cootes, T., & Scott, I. (2004). A Multi-Stage Approach to Facial Feature Detection. In *Procedings of the British Machine Vision Conference 2004* (p. 30.1-30.10). British Machine Vision Association.

Cristinacce, D., & Cootes, T. F. (2006). Feature Detection and Tracking with Constrained Local Models. In *Procedings of the British Machine Vision Conference 2006* (p. 95.1-95.10). British Machine Vision Association.

Cristinacce, D., & Cootes, T. F. (2007). Boosted Regression Active Shape Models. In *Procedings of the British Machine Vision Conference 2007* (p. 79.1-79.10). British Machine Vision Association.

Cristinacce, D., & Cootes, T. (2008). Automatic feature localisation with constrained local models. *Pattern Recognition*, *41*(10), 3054–3067.

DeCarlo, D., Metaxas, D., & Stone, M. (1998). An anthropometric face model using variational techniques. In *Proceedings of the 25th annual conference on Computer graphics and interactive techniques - SIGGRAPH '98* (pp. 67–74). New York, New York, USA: ACM Press.

Dellavia, C., Catti, F., Sforza, C., Tommasi, D. G., & Ferrario, V. F. (2010). Craniofacial growth in ectodermal dysplasia. *The Angle Orthodontist*, *80*(4), 733–739.

Dias, P. E. M., Beaini, T. L., & Melani, R. F. H. (2013). Evaluation of osifix software with craniofacial anthropometric purposes. *JRD-Journal of Research in Dentistry, Tubarão, v. 1, n. 4, Nov/Dec. 2013*, *1*(4).

Djordjevic, J., Lawlor, D. a, Zhurov, A. I., Toma, A. M., Playle, R., & Richmond, S. (2013). A population-based cross-sectional study of the association between facial morphology and cardiometabolic risk factors in adolescence. *BMJ Open*, *3*(5), e002910.

Douglas, T. S., Martinez, F., Meintjes, E. M., Vaughan, C. L., & Viljoen, D. L. (2003). Eye feature extraction for diagnosing the facial phenotype associated with fetal alcohol syndrome. *Medical & Biological Engineering & Computing*, *41*(1), 101–106.

Douglas, T. S. (2004). Image processing for craniofacial landmark identification and measurement: a review of photogrammetry and cephalometry. *Computerized Medical Imaging and Graphics*, *28*(7), 401–409.

Douglas,T.S. (2011). Facial image analysis to detect gestational alcohol exposure. CME,29 (3), 108–110.

El-Hakim, H., Crysdale, W. S., Abdollel, M., & Farkas, L. G. (2001). A study of anthropometric measures before and after external septoplasty in children: a preliminary study. *Archives of Otolaryngology--Head & Neck Surgery*, *127*(11), 1362–1366.

Enciso, R., Shaw, A., Neumann, U., & Mah, J. (2003). 3D Head Anthropometric Analysis. *Proceedings of the International Society for Optical Engineering SPIE Medical Imaging*, *5029*, 590–597

Erkan, M., Gurel, H. G., Nur, M., & Demirel, B. (2012). Reliability of four different computerized cephalometric analysis programs. *European Journal of Orthodontics*, *34*(3), 318–321.

Fagertun, J., Harder, S., Rosengren, A., Moeller, C., Werge, T., Paulsen, R. R., & Hansen, T. F. (2014). 3D facial landmarks: Inter-operator variability of manual annotation. *BMC Medical Imaging*, *14*(1), 35.

Falk, D. R., Brill, D. R., & Stork, D. G. (1986). *Seeing the Light: Optics in Nature, Photography color, vision and holography*. John Wiley & Sons, Inc.

Farkas, L. G. (1994). *Anthropometry of the head and face* (2nd ed.). New York, USA: Raven Press.

Farkas, L. G., & James, J. S. (1977). Anthropometry of the face in Lateral Facial Dysplasia: The Unilateral Form. *Cleft Palate Journal*, *14*(3), 193–199.

Farkas, L. G., Posnick, J. C., & Hreczko, T. (1991). Anthropometry of the head and face in 95 Down syndrome patients. *Progress in Clinical and Biological Research*, *373*, 53–97.

Farkas, L. G. (1996). Accuracy of anthropometric measurements: past, present, and future. *The Cleft Palate-Craniofacial Journal: Official Publication of the American Cleft Palate-Craniofacial Association*, *33*(1), 10-8; discussion 19-22.

Farkas, L. G., Forrest, C. R., & Phillips, J. H. (2000). Comparison of the morphology of the "cleft face" and the normal face: defining the anthropometric differences. *The Journal of Craniofacial Surgery*, *11*(2), 76–82.

Farkas, L. G., Katic, M. J., Forrest, C. R., Alt, K. W., Bagic, I., Baltadjiev, G., et al. (2005). International anthropometric study of facial morphology in various ethnic groups/races. *The Journal of Craniofacial Surgery*, *16*(4), 615–646.

Farkas, L. G., Katic, M. J., & Forrest, C. R. (2007). Comparison of craniofacial measurements of young adult African-American and North American white males and females. *Annals of Plastic Surgery*, *59*(6), 692–698.

Ferrario, V. F., Sforza, C., Dellavia, C., Tartaglia, G. M., Colombo, A., & Carù, A. (2003). A quantitative three-dimensional assessment of soft tissue facial asymmetry of cleft lip and palate adult patients. *The Journal of Craniofacial Surgery*, *14*(5), 739–746.

Ferrario, V. F., Sforza, C., Miani, A., & Tartaglia, G. (1993). Craniofacial morphometry by photographic evaluations. *American Journal of Orthodontics and Dentofacial Orthopedics: Official Publication of the American Association of Orthodontists, Its Constituent Societies, and the American Board of Orthodontics*, *103*(4), 327–337.

Ferrario, V. F., Sforza, C., Poggio, C. E., Cova, M., & Tartaglia, G. (1998). Preliminary evaluation of an electromagnetic three-dimensional digitizer in facial anthropometry. *The Cleft Palate-Craniofacial Journal: Official Publication of the American Cleft Palate-Craniofacial Association*, *35*(1), 9–15.

Ferrario, V. F., Sforza, C., Schmitz, J. H., & Santoro, F. (1999). Three-dimensional facial morphometric assessment of soft tissue changes after orthognathic surgery. *Oral Surgery, Oral Medicine, Oral Pathology, Oral Radiology, and Endodontics*, *88*(5), 549–556.

Ferrario, V. F., Sforza, C., Dellavia, C., Tartaglia, G. M., Colombo, A., & Carù, A. (2003). A quantitative three-dimensional assessment of soft tissue facial asymmetry of cleft lip and palate adult patients. *The Journal of Craniofacial Surgery*, *14*(5), 739–746.

Finlay, L. M. (1980). Craniometry and Cephalometry: A history Prior to Advent of Radiography. *Craniometry*, *50*(4), 312–322.

Fourie, Z., Damstra, J., Gerrits, P. O., & Ren, Y. (2011). Accuracy and repeatability of anthropometric facial measurements using cone beam computed tomography. *The Cleft Palate-Craniofacial Journal: Official Publication of the American Cleft Palate-Craniofacial Association*, *48*(5), 623–630.

Fukuda, H., & Ohashi, Y. (1997). A guideline for reporting results of statistical analysis in Japanese Journal of Clinical Oncology. *Japanese Journal of Clinical Oncology*, *27*(3), 121–127.

Gupta, S., Markey, M. K., & Bovik, A. C. (2010). Anthropometric 3D Face Recognition. *International Journal of Computer Vision*, *90*(3), 331–349.

Gupta, S., Castleman, K. R., Markey, M. K., & Bovik, A. C. (2010). Texas 3D Face Recognition Database. In *IEEE Southwest Symposium on Image Analysis and Interpretation* (pp. 97–100). Austin Texas.

Guyot, L., Dubuc, M., Pujol, J., Dutour, O., & Philip, N. (2001). Craniofacial anthropometric analysis in patients with 22q11 microdeletion. *American Journal of Medical Genetics*, *100*(1), 1–8.

L Guyot, M Dubuc, O Richard, N Philip, O Dutour, O. (2003). Comparison between direct clinical and digital photogrammetric measurements in patients with 22q11 microdeletion. *Journal of Oral and Maxillofacial Surgery*, *32*(3), 246–252.

Hajeer, M. Y., Ayoub, A. F., & Millett, D. T. (2002). Three-dimensional imaging in orthognathic surgery: the clinical application of a new method. *International Journal of Adult Orthod Orthognath Sur*, *17*(4), 1–13.

Hammond, P., Hutton, T. J., Allanson, J. E., Campbell, L. E., Hennekam, R. C. M., Holden, S., … Winter, R. M. (2004). 3D analysis of facial morphology. *American Journal of Medical Genetics*, *126A*(4), 339–348.

Hammond, P., & Suttie, M. (2012). Large-scale objective phenotyping of 3D facial morphology. *Human Mutation*, *33*(5), 817–825.

Hashim, H., & Iqbal, S. (2011). Motorcycle accident is the main cause of maxillofacial injuries in the Penang Mainland, Malaysia. Dental Traumatology, 27(1), 19–22.

Hashim, H., & Iqbal, S. (2011). Motorcycle accident is the main cause of maxillofacial injuries in the Penang Mainland, Malaysia. *Dental Traumatology*, *27*(1), 19–22.

Heike, C. L., Cunningham, M. L., Hing, A. V, Stuhaug, E., & Starr, J. R. (2009). Picture Perfect? Reliability of Craniofacial Anthropometry Using Three-Dimensional Digital Stereophotogrammetry. *Plastic and Reconstructive Surgery*, *124*(4), 1261–1272.

Huang, Y.-S., Hsu, T.-C., & Cheng, F.-H. (2010). Facial landmark detection by combining object detection and active shape model. In *2010 Third International Symposium on Electronic Commerce and Security* (pp. 381–386). IEEE.

Hrdlička, A. (1920). Anthropometry. Wistar Institute of Anatomy and Biology.

Hsu, T.-C., Huang, Y.-S., & Cheng, F.-H. (2010). A Novel ASM-Based Two-Stage Facial Landmark Detection Method. In *Lecture Notes in Computer Science (including subseries Lecture Notes in Artificial Intelligence and Lecture Notes in Bioinformatics)* (Vol. 6298 LNCS, pp. 526–537).

Hussaini, H. M., Rahman, N. A., Rahman, R. A., Nor, G. M., AI Idrus, S. M., & Ramli, R. (2007). Maxillofacial trauma with emphasis on soft-tissue injuries in Malaysia. *International Journal of Oral and Maxillofacial Surgery*, *36*(9), 797–801.

Jain, A. K., Zhong, Y., & Dubuisson-Jolly, M.-P. (1998). Deformable template models: A review. *Signal Processing*, *71*(2), 109–129.

Jain, P., & Kalra, J. P. S. (2011). Soft tissue cephalometric norms for a North Indian population group using Legan and Burstone analysis. *International Journal of Oral and Maxillofacial Surgery*, *40*, 255–259.

Jamison, P. L., & Ward, R. E. (1993). Brief communication: measurement size, precision, and reliability in craniofacial anthropometry: bigger is better. *American Journal of Physical Anthropology*, *90*(4), 495–500.

Jiao, F., Li, S., Shum, H.-Y., & Schuurmans, D. (2003). Face alignment using statistical models and wavelet features. *2003 IEEE Computer Society Conference on Computer Vision and Pattern Recognition*, *1*, 321–327.

Kau, C. H., Cronin, A., Durning, P., Zhurov, A. I., Sandham, A., & Richmond, S. (2006). A new method for the 3D measurement of postoperative swelling following orthognathic surgery. *Orthodontics & Craniofacial Research*, *9*, 31–37.

Kohno, Y., Yahara, H., Fukui, Y., Mochimaru, M., & Kouchi, M. (2005). *Automatic landmarking in 3D human head scans*. *Science*.

Koo, T. K., & Li, M. Y. (2016). A Guideline of Selecting and Reporting Intraclass Correlation Coefficients for Reliability Research. *Journal of Chiropractic Medicine*, *15*(2), 155–163.

Kolar, J. C., Farkas, L. G., & Munro, I. R. (1985). Surface morphology in Treacher Collins syndrome: an anthropometric study. *The Cleft Palate Journal*, *22*(4), 266–274.

Kolar, J. C., & Salter, E. M. (1997). *Craniofacial Anthropometry: Practical Measurement of the head and face for Clinical, surgical and research use.* United States of America: Charles C Thomas Publisher LTD.

Koo, T. K., & Li, M. Y. (2016). A Guideline of Selecting and Reporting Intraclass Correlation Coefficients for Reliability Research. *Journal of Chiropractic Medicine*, *15*(2), 155–163.

Kuijpers, M. A. R., Chiu, Y.-T., Nada, R. M., Carels, C. E. L., & Fudalej, P. S. (2014). Three-dimensional imaging methods for quantitative analysis of facial soft tissues and skeletal morphology in patients with orofacial clefts: a systematic review. *PloS One*, *9*(4), e93442.

Li, G., Wei, J., Wang, X., Wu, G., Ma, D., Wang, B., et al. (2013). Three-dimensional facial anthropometry of unilateral cleft lip infants with a structured light scanning system. *Journal of Plastic, Reconstructive & Aesthetic Surgery: JPRAS*, *66*(8), 1109–1116.

Liang, S., Wu, J., Weinberg, S. M., & Shapiro, L. G. (2013). Improved detection of landmarks on 3D human face data. *Conference Proceedings: ... Annual International Conference of the IEEE Engineering in Medicine and Biology Society. IEEE Engineering in Medicine and Biology Society. Annual Conference*, *2013*, 6482–6485.

Lienhart, R., & Maydt, J. (2002). An extended set of Haar-like features for rapid object detection. *Proceedings. International Conference on Image Processing*, *1*.

Mahdi, E. (2012). Assessment of Facial and Cranial Development and Comparison of Anthropometric Ratios. *Journal of Craniofacial Surgery*, *23*(2), e75–e83.

Majid, Z., Chong, A., & Setan, H. (2006). Natural features technique for non-contact three dimensional craniofacial anthropometry using stereophotogrammetry. *Archives of Orofacial Sciences*, *1*, 42–50.

Marchetti, C., Bianchi, A., Muyldermans, L., Di Martino, M., Lancellotti, L., & Sarti, A. (2011). Validation of new soft tissue software in orthognathic surgery planning. *International Journal of Oral and Maxillofacial Surgery*, *40*(1), 26–32.

Meintjes, E. M., Douglas, T. S., Martinez, F., Vaughan, C. L., Adams, L. P., Stekhoven, A., & Viljoen, D. (2002). A stereo-photogrammetric method to measure the facial dysmorphology of children in the diagnosis of fetal alcohol syndrome. *Medical Engineering & Physics*, *24*(10), 683–689.

Mercan, E., Shapiro, L. G., Weinberg, S. M., & Lee, S. I. (2013). The use of pseudo-landmarks for craniofacial analysis: A comparative study with L1-regularized logistic regression. In *Proceedings of the Annual International Conference of the IEEE Engineering in Medicine and Biology Society, EMBS* (pp. 6083–6086).

Metzler, P., Bruegger, L. S., Kruse Gujer, A. L., Matthews, F., Zemann, W., Graetz, K. W., & Luebbers, H.-T. (2012). Craniofacial landmarks in young children: how reliable are measurements based on 3-dimensional imaging? *The Journal of Craniofacial Surgery*, *23*(6), 1790–1795.

Metzler, P., Sun, Y., Zemann, W., Bartella, A., Lehner, M., Obwegeser, J. A., et al., (2014). Validity of the 3D VECTRA photogrammetric surface imaging system for cranio-maxillofacial anthropometric measurements. *Oral and Maxillofacial Surgery*, *18*(3), 297–304.

Milborrow, S. (2007). *Locating Facial Features with Active Shape Models*. (Unpublished doctoral dissertation). University of Cape Town.

Milborrow, S., & Nicolls, F. (2008). Locating Facial Features with an Extended Active Shape Model. In *Computer Vision – ECCV 2008* (Vol. 5305 LNCS, pp. 504–513). Berlin, Heidelberg: Springer Berlin Heidelberg.

Milborrow, S. (2013). *STASM 4.0 User Manual*. Cape Town.

Moore, E. S., & Ward, R. E. (2012). Use of Computerized Anthropometry and Morphometrics to Identify Fetal Alcohol Syndrome. In V. Preedy (Ed.), *Handbook of Anthropometry: Physical Measures of Human Form in Health and Disease* (pp. 1049–1065). Springer.

Moore, E. S., Ward, R. E., Jamison, P. L., Morris, C. A., Bader, P. I., & Hall, B. D. (2002). New perspectives on the face in fetal alcohol syndrome: What anthropometry tells us. *American Journal of Medical Genetics*, *109*(4), 249–260.

Mutsvangwa, T., & Douglas, T. S. (2007). Morphometric analysis of facial landmark data to characterize the facial phenotype associated with fetal alcohol syndrome. *Journal of Anatomy*, *210*(2), 209–220.

Mutsvangwa, T. E. M., Meintjes, E. M., Viljoen, D. L., & Douglas, T. S. (2010). Morphometric analysis and classification of the facial phenotype associated with fetal alcohol syndrome in 5- and 12-year-old children. *American Journal of Medical Genetics Part A*, *152A*(1), 32–41.

Nagle, E., Teibe, U., & Kapoka, D. (2005). Craniofacial anthropometry in a group of healthy Latvian residents. *Acta Medica Lituanica*, *12*(1), 47–53.

Ngeow, W. C., & Aljunid, S. T. (2009a). Craniofacial anthropometric norms of Malays. *Singapore Medical Journal*, *50*(5), 525–528.

Ngeow, W. C., & Aljunid, S. T. (2009b). Craniofacial anthropometric norms of Malaysian Indians. *Indian Journal of Dental Research: Official Publication of Indian Society for Dental Research*, *20*(3), 313–319.

Ni, K., Sun, Z., Bliss, N., & Snavely, N. (2010). Construction and exploitation of a 3D model from 2D image features. In C. A. Bouman, I. Pollak, & P. J. Wolfe (Eds.), *Proc. SPIE* (Vol. 7533, p. 75330J).

Nordin, R., Rahman, N. A., Rashdi, M. F., Yusoff, A., Rahman, R. A., Sulong, S., et al. (2014). Oral and maxillofacial trauma caused by road traffic accident in two university hospitals in Malaysia: A cross-sectional study. *Journal of Oral and Maxillofacial Surgery, Medicine, and Pathology*, *27*(2), 166–171.

Othman, S. A., Ahmad, R., Asi, S. M., Ismail, N. H., & Rahman, Z. A. A. (2013). Three-dimensional quantitative evaluation of facial morphology in adults with unilateral cleft lip and palate, and patients without clefts. *Br J Oral Maxillofac Surg*, *52*, 208–213.

Ozsoy, U., Demirel, B. M., Yildirim, F. B., Tosun, O., & Sarikcioglu, L. (2009). Method selection in craniofacial measurements: advantages and disadvantages of 3D digitization method. *Journal of Cranio-Maxillo-Facial Surgery: Official Publication of the European Association for Cranio-Maxillo-Facial Surgery*, *37*(5), 285–290.

Papadopoulos, M. A., Christou, P. K., Christou, P. K., Athanasiou, A. E., Boettcher, P., Zeilhofer, H. F., … Papadopulos, N. A. (2002). Three-dimensional craniofacial reconstruction imaging. *Oral Surgery, Oral Medicine, Oral Pathology, Oral Radiology, and Endodontics*, *93*(4), 382–393.

Plooij, J. M., Maal, T. J. J., Haers, P., Borstlap, W. A., Kuijpers-Jagtman, A. M., & Bergé, S. J. (2011). Digital three-dimensional image fusion processes for planning and evaluating orthodontics and orthognathic surgery. A systematic review. *International Journal of Oral and Maxillofacial Surgery*, *40*(4), 341–352.

Popat, H., Richmond, S., & Drage, N. A. (2010). New developments in: three-dimensional planning for orthognathic surgery. *Journal of Orthodontics*, *37*(1), 62–71.

Popat, H., Richmond, S., Marshall, D., & Rosin, P. L. (2012). Three-dimensional assessment of functional change following Class 3 orthognathic correction--a preliminary report. *Journal of Cranio-Maxillo-Facial Surgery: Official Publication of the European Association for Cranio-Maxillo-Facial Surgery*, *40*(1), 36–42.

Posnick, J. C., & Farkas, L. G. (1994). The Application of Anthropometric Surface Measurement in Craniofacial Surgery. In L. G. Farkas (Ed.), *Antropometry of the head and face* (2nd ed., pp. 125– 150). Raven Press.

Purmal, K., & Alam, M. K. (2013). Cephalometric Norms of Malaysian Adult Indian Cephalometric Norms of Malaysian Adult Indian. *Internation Medical Journal*, *20*(August 2015), 192–196.

Richtsmeier, J. T., & Lele, S. (1990). Analysis of craniofacial growth in Crouzon syndrome using landmark data. *Journal of Craniofacial Genetics and Developmental Biology*, *10*(1), 39–62.

Ruiz, M. C., & Illingworth, J. (2008). Automatic landmarking of faces in 3D-ALF. In *5th International Conference on Visual Information Engineering (VIE 2008)* (pp. 41–46).

Samad, R., & Sawada, H. (2011). Edge-Based Facial Feature Extraction Using Gabor Wavelet and Convolution Filters. In *IAPR Conference on Machine Vision Applications on Machine Vision Applications*.

Schaaf, H., Wilbrand, J.-F., Boedeker, R.-H., & Howaldt, H.-P. (2010). Accuracy of photographic assessment compared with standard anthropometric measurements in nonsynostotic cranial deformities. *The Cleft Palate-Craniofacial Journal : Official Publication of the American Cleft Palate-Craniofacial Association*, *47*(5), 447–453.

Sforza, C., Laino, A., Grandi, G., Pisoni, L., & Ferrario, V. F. (2010). Three-Dimensional Facial Asymmetry in Attractive and Normal People from Childhood to Young Adulthood. *Symmetry*, *2*(4), 1925–1944.

Sforza, C., & Ferrario, V. (2006). Soft-tissue facial anthropometry in three dimensions: from anatomical landmarks to digital morphology in research, clinics and forensic anthropology. J Anthropol Sci, 84, 97–124.

Sforza, C., & Ferrario, V. F. (2010). Three-dimensional analysis of facial morphology: growth, development and aging of the orolabial region. *Italian Journal of Anatomy and Embryology*, *115*(1/2), 141–145.

Shaheera, N., Aziz, A., Talib, M. A., Alam, M. K., Basri, R., Purmal, K., & Rahman, S. A. (2014). Linear and Angular Cephalometric Lip Morphology in Malaysian Chinese Population Linear and Angular Cephalometric Lip Morphology in Malaysian Chinese Population. *Internationl Medical Journal*, *21*(August 2015), 45–48.

Swennen, G. R. J., Mollemans, W., & Schutyser, F. (2009). Three-Dimensional Treatment Planning of Orthognathic Surgery in the Era of Virtual Imaging. *Journal of Oral and Maxillofacial Surgery*, *67*, 2080–2092.

Toma, A. M. (2014). *Characterization of normal facial features and their association with genes.* University of Cardiff.

Toma, A. M., Zhurov, A., Playle, R., Ong, E., & Richmond, S. (2009). Reproducibility of facial soft tissue landmarks on 3D laser-scanned facial images. *Orthodontics & Craniofacial Research*, *12*(1), 33–42.

van den Elzen, M. E. P., Twigg, S. R. F., Goos, J. A. C., Hoogeboom, A. J. M., van den Ouweland, A. M. W., Wilkie, A. O. M., & Mathijssen, I. M. J. (2014). Phenotypes of craniofrontonasal syndrome in patients with a pathogenic mutation in EFNB1. *Eur J Hum Genet*, *22*(8), 995–1001.

Vegter, F., & Hage, J. (2000). Special Topic Clinical Anthropometry and Canons of the Face in Historical Perspective. *Plastic and Reconstructive Surgery*, *106*(5), 1090–1096.

Vegter, F., & Hage, J. J. (2001). Facial anthropometry in cleft patients: a historical appraisal. *The Cleft Palate-Craniofacial Journal: Official Publication of the American Cleft Palate-Craniofacial Association*, *38*(6), 577–581.

Viola, P., & Jones, M. (2001). Rapid object detection using a boosted cascade of simple features. *Proceedings of the 2001 IEEE Computer Society Conference on Computer Vision and Pattern Recognition. CVPR 2001*, *1*.

Vukadinovic, D., & Pantic, M. (2005). Fully Automatic Facial Feature Point Detection Using Gabor Feature Based Boosted Classifiers. In *2005 IEEE International Conference on Systems, Man and Cybernetics* (Vol. 2, pp. 1692–1698). IEEE.

Wagenmakers, M. A. E. M., Roerink, S. H. P. P., Maal, T. J. J., Pelleboer, R. H., Smit, J. W. A., Hermus, A. R. M. M., et al. (2014). Three-dimensional facial analysis in acromegaly: a novel tool to quantify craniofacial characteristics after long-term remission. *Pituitary*.

Ward, R. E., Jamison, P. L., & Allanson, J. E. (2000). Quantitative approach to identifying abnormal variation in the human face exemplified by a study of 278 individuals with five craniofacial syndromes. *American Journal of Medical Genetics*, *91*(1), 8–17.

Weinberg, S. M., Raffensperger, Z. D., Kesterke, M. J., Heike, C. L., Cunningham, M. L., Hecht, J. T., et al. (2016). The 3D Facial Norms Database: Part 1. A Web-Based Craniofacial Anthropometric and Image Repository for the Clinical and Research Community. *The Cleft Palate–Craniofacial Journal*, *53*(6), e185–e197.

Weinberg, S. M. (2007). *Three-Dimensional Morphometric Analysis Of The Craniofacial Complex In the Unaffected Relatives Of Individuals With Nonsyndromic Orofacial Clefts*. University of Pittsburg.

Weinberg, S. M., Naidoo, S., Govier, D. P., Martin, R. A., Kane, A. A., & Marazita, M. L. (2006). Anthropometric precision and accuracy of digital three-dimensional photogrammetry: comparing the Genex and 3dMD imaging systems with one another and with direct anthropometry. *The Journal of Craniofacial Surgery*, *17*(3), 477–483.

Weinberg, S. M., Scott, N. M., Neiswanger, K., Brandon, C. A., & Marazita, M. L. (2004). Digital three-dimensional photogrammetry: evaluation of anthropometric precision and accuracy using a Genex 3D camera system. *The Cleft Palate-Craniofacial Journal: Official Publication of the American Cleft Palate-Craniofacial Association*, *41*(5), 507–518.

Wiskott, L., Fellous, J.-M., Kruger, N., & von der Malsburg, C. (1997). Face recognition by elastic bunch graph matching. In *Proceedings of International Conference on Image Processing* (Vol. 1, pp. 129–132). IEEE Comput. Soc.

Wong, R. W. K., Chau, A. C. M., & H??gg, U. (2011). 3D CBCT McNamara's cephalometric analysis in an adult southern Chinese population. *International Journal of Oral and Maxillofacial Surgery*, *40*, 920–925.

Wong, J. Y., Oh, A. K., Ohta, E., Hunt, A. T., Rogers, G. F., Mulliken, J. B., & Deutsch, C. K. (2008). Validity and reliability of craniofacial anthropometric measurement of 3D digital photogrammetric images. *Cleft Palate-Craniofacial Journal*, *45*(3), 232–239.

Yasir, S. (2014). FACIAL TRAUMA AMONG PATIENTS WITH HEAD INJURIES. *Journal of IMAB - Annual Proceeding (Scientific Papers)*, *20*(6), 535–538.

Zuo, F., & de With, P. H. N. (2004). Real-time facial feature extraction using statistical shape model and Haar-wavelet based feature search. In *2004 IEEE International Conference on Multimedia and Expo (ICME) (IEEE Cat. No.04TH8763)* (pp. 1443–1446). IEEE.